BULLETIN OF RUSSIAN STATE MEDICAL UNIVERSITY

BIOMEDICAL JOURNAL OF PIROGOV RUSSIAN NATIONAL RESEARCH MEDICAL UNIVERSITY

SUBMISSION http://vestnikrgmu.ru/login?lang=en
CORRESPONDENCE editor@vestnikrgmu.ru
COLLABORATION manager@vestnikrgmu.ru
ADDRESS ul. Ostrovityanova, d. 1, Moscow, Russia, 117997

Indexed in Scopus. CiteScore 2022: 0.6

Indexed in WoS. JCR 2021: 0.5

Five-year h-index is 8

SCImago Journal & Country Rank 2020: 0.14

Listed in HAC 31.01.2020 (№ 507)

Open access to archive

Issue DOI: 10.24075/brsmu.2024-02
The mass media registration certificate № 012769 issued on July 29, 1994
Founder and publisher is Pirogov Russian National Research Medical University (Moscow, Russia)

Approved for print 30.04.2024
Circulation: 100 copies. Printed by Print.Formula
www.print-formula.ru

ВЕСТНИК РОССИЙСКОГО ГОСУДАРСТВЕННОГО МЕДИЦИНСКОГО УНИВЕРСИТЕТА

НАУЧНЫЙ МЕДИЦИНСКИЙ ЖУРНАЛ РНИМУ ИМ. Н. И. ПИРОГОВА

ПОДАЧА РУКОПИСЕЙ http://vestnikrgmu.ru/login
ПЕРЕПИСКА С РЕДАКЦИЕЙ editor@vestnikrgmu.ru
СОТРУДНИЧЕСТВО manager@vestnikrgmu.ru
АДРЕС РЕДАКЦИИ ул. Островитянова, д. 1, г. Москва, 117997

Журнал включен в Scopus. CiteScore 2022: 0,6

Журнал включен в WoS. JCR 2021: 0,5

Индекс Хирша (h^5) журнала по оценке Google Scholar: 8

SCImago Journal & Country Rank 2020: 0,14

Журнал включен в Перечень 31.01.2020 (№ 507)

Здесь находится открытый архив журнала

DOI выпуска: 10.24075/vrgmu.2024-02
Свидетельство о регистрации средства массовой информации № 012769 от 29 июля 1994 г.
Учредитель и издатель — Российский национальный исследовательский медицинский университет имени Н. И. Пирогова (Москва, Россия)

Подписано в печать 30.04.2024
Тираж 100 экз. Отпечатано в типографии Print.Formula
www.print-formula.ru

BULLETIN OF RSMU **2, 2024**
ВЕСТНИК РГМУ

Contents
Содержание

GENOTYPIC CHARACTERISTICS OF BORDETELLA PERTUSSIS, CANDIDATE STRAINS FOR PRODUCTION OF PERTUSSIS COMPONENT OF VACCINES (STATEMENT I)

Borisova OYu[1,3]✉, Andrievskaya IYu[1], Pimenova AS[1], Gadua NT[1], Chagina IA[1], Borisova AB[1], Chaplin AV[1,3], Alekseeva IA[2], Kafarskaya LI[3]

[1] Gabrichevsky Research Institute for Epidemiology and Microbiology, Moscow, Russia

[2] Scientific Centre for Expert Evaluation of Medicinal Products, Ministry of Health of the Russian Federation, Moscow, Russia

[3] Pirogov Russian National Research Medical University, Moscow, Russia

Vaccination is an effective means of preventing pertussis infection. The purpose of this work was to improve vaccines available in the Russian Federation in general and actualize vaccine strains used for the production thereof in particular. We studied *B. pertussis* strains isolated in Moscow, Voronezh, Novosibirsk, Ulyanovsk and Chelyabinsk regions, and eight production strains part of the adsorbed diphtheria-pertussis-tetanus (DPT) vaccine. Multilocus antigenic sequence typing (MAST) and whole genome multilocus sequence typing (wgMLST) were used for genotyping. We studied cultural morphological, enzymatic, serological, and genotypic properties of the candidate *B. pertussis* strains, and compared their genotypic properties to those of B. pertussis vaccine strains from the current composition of the DPT vaccine. Candidate strains belong to four genotypes: *ptxA1/ptxB2/ptxC2/ptxP3/fim2-2/fim3-2/prn2*, *ptxA1/ptxB2/ptxC2/ptxP3/fim2-2/fim3-2/prn9, ptxA1/ptxB2/ptxC2/ptxP3/fim2-1/fim3-1/prn1* and *ptxA1/ptxB2/ptxC2/ptxP3/fim2-2/fim3-1/prn2*. Current vaccine strains were from other six genotypes: *ptxA2/ptxB1/ptxC1/ptxP1/fim2-1/fim3-1/prn1, ptxA2/ptxB2/ptxC1/ptxP2/fim2-1/fim3-1/prn1, ptxA4/ptxB1/ptxC1/ptxP2/fim2-1/fim3-1/prn1, ptxA2/ptxB2/ptxC1/ptxP1/fim2-1/fim3-1/prn1, ptxA4/ptxB2/ptxC1/ptxP2/fim2-1/fim3-1/prn1* and *ptxA1/ptxB2/ptxC1/ptxP1/fim2-1/fim3-1/prn1*. With the help of wgMLST, we established affiliation of all candidate strains of *B. pertussis* to ST2.

Keywords: *Bordetella pertussis*, vaccines, genotyping, multilocus antigenic sequence typing

Author contribution: Borisova OY — molecular genetic research, data analysis, literature analysis, manuscript authoring; Andrievskaya IY — molecular genetic research, data analysis, manuscript authoring; Pimenova AS, Gadua NT, Chagina IA, Alekseeva IA — microbiological research, manuscript authoring; Borisova AB, Kafarskaya LI — literature analysis, data analysis, manuscript authoring; Chaplin AV — bioinformatic and phylogenetic analysis, manuscript authoring.

✉ **Correspondence should be addressed:** Olga Yu. Borisova
Admirala Makarova, 10, 125212, Moscow, Russia; olgborisova@mail.ru

Received: 09.04.2024 **Accepted:** 24.04.2024 **Published online:** 30.04.2024

DOI: 10.24075/brsmu.2024.017

ГЕНОТИПИЧЕСКАЯ ХАРАКТЕРИСТИКА ШТАММОВ *BORDETELLA PERTUSSIS* — КАНДИДАТОВ ДЛЯ ПОЛУЧЕНИЯ КОКЛЮШНОГО КОМПОНЕНТА ВАКЦИННЫХ ПРЕПАРАТОВ (СООБЩЕНИЕ I)

О. Ю. Борисова[1,3]✉, И. Ю. Андриевская[1], А. С. Пименова[1], Н. Т. Гадуа[1], И. А. Чагина[1], А. Б. Борисова[1], А. В. Чаплин[1,3], И. А. Алексеева[2], Л. И. Кафарская[3]

[1] Московский научно-исследовательский институт эпидемиологии и микробиологии имени Г. Н. Габричевского, Москва, Россия

[2] Научный центр экспертизы средств медицинского применения Минздрава России, Москва, Россия

[3] Российский национальный исследовательский медицинский университет имени Н. И. Пирогова, Москва, Россия

Вакцинация является эффективным средством предупреждения заболевания коклюшной инфекцией. Целью работы было усовершенствование вакцинных препаратов в РФ, в том числе актуализация производственных вакцинных штаммов. Изучали штаммы *B. pertussis*, выделенные в г. Москве, Воронежской, Новосибирской, Ульяновской и Челябинской областях, и восемь производственных штаммов для адсорбированной коклюшно-дифтерийно-столбнячной (АКДС) вакцины. Для генотипирования использовали мультилокусное антигенное сиквенс-типирование (MAST) и полногеномное мультилокусное сиквенс-типирование (wgMLST). Изучены культурально-морфологические, ферментантивные, серологические и генотипические свойства штаммов *B. pertussis* — кандидатов в производственные вакцинные штаммы и проведен сравнительный анализ генотипических свойств этих штаммов и производственных вакцинных штаммов *B. pertussis* для вакцины АКДС. Кандидатные штаммы являются представителями четырех генотипов — *ptxA1/ptxB2/ptxC2/ptxP3/fim2-2/fim3-2/prn2, ptxA1/ptxB2/ptxC2/ptxP3/fim2-2/fim3-2/prn9*, *ptxA1/ptxB2/ptxC2/ptxP3/fim2-1/fim3-1/prn1* и *ptxA1/ptxB2/ptxC2/ptxP3/fim2-2/fim3-1/prn2*. Производственные вакцинные штаммы принадлежали к другим шести генотипам: *ptxA2/ptxB1/ptxC1/ptxP1/fim2-1/fim3-1/prn1, ptxA2/ptxB2/ptxC1/ptxP2/fim2-1/fim3-1/prn1, ptxA4/ptxB1/ptxC1/ptxP2/fim2-1/fim3-1/prn1, ptxA2/ptxB2/ptxC1/ptxP1/fim2-1/fim3-1/prn1, ptxA4/ptxB2/ptxC1/ptxP2/fim2-1/fim3-1/prn1* и *ptxA1/ptxB2/ptxC1/ptxP1/fim2-1/fim3-1/prn1*. С помощью wgMLST установлена принадлежность всех кандидатных штаммов *B. pertussis* к ST2.

Ключевые слова: *Bordetella pertussis*, вакцинные препараты, генотипирование, мультилокусное антигенное сиквенс-типирование

Вклад авторов: О. Ю. Борисова — молекулярно-генетические исследования, анализ данных, анализ литературы, подготовка рукописи; И. Ю. Андриевская — молекулярно-генетические исследования, анализ данных, подготовка рукописи; А. С. Пименова, Н. Т. Гадуа, И. А. Чагина, И. А. Алексеева — микробиологические исследования, подготовка рукописи; А. Б. Борисова, Л. И. Кафарская — анализ литературы, анализ данных, подготовка рукописи; А. В. Чаплин — биоинформатический и филогенетический анализ, подготовка рукописи.

✉ **Для корреспонденции:** Ольга Юрьевна Борисова
ул. Адмирала Макарова, д. 10, 125212, г. Москва, Россия; olgborisova@mail.ru

Статья получена: 09.04.2024 **Статья принята к печати:** 24.04.2024 **Опубликована онлайн:** 30.04.2024

DOI: 10.24075/vrgmu.2024.017

Pertussis is a dangerous disease that may end in a fatality, especially among newborns and infants [1-3]. Growing prevalence of pertussis, spread of its severe forms among babies below 1 year of age, and lethal outcomes underpin relevance of the study. In 2023, there were 52,727 pertussis cases registered in the Russian Federation, yielding the incidence rate of 36.2 per 100,000 population), which is 16.4 times more than in 2022 (2.2 per 100,000 population) and 7.5 times higher than the average long-term incidence rate (4.8 per 100,000 population). Over 80% of the patients were children under 14 years of age, according to the Pertussis and Diphtheria Monitoring Reference Center of G.N Gabrichevsky

Research Institute for Epidemiology and Microbiology (based on the analysis of form No. 2 "Information on infectious and parasitic diseases") [4–6].

Routine vaccination against pertussis in the first year of life triggers development of immunity and resistance to infection [1, 3]. By the age of 6–7, this post-vaccination immunity weakens. Starting school, children enter new groups, some members of which may be infected. In such groups, unvaccinated and those who have lost their post-vaccination immunity contract the disease most often, with the latter having it in a light form with atypical cough [7–9]. Previously, 7 to 17% of prolonged cough in adolescents have been shown to be associated with *B. pertussis*. Various authors estimate that in 75% of cases, infants under 1 year of age catch this infection from school-age children [9, 10]. Therefore, vaccination is an effective means of preventing pertussis in youngest populations.

With the incidence of pertussis on the rise, medical professionals and researchers have expressed their concerns about efficacy of the currently applied prevention strategy [11, 12]. The reasons that, most likely, underpin the said rise, are as follows: large number of parents refusing vaccination of their infants under the age of 1, which delays the entire vaccination schedule [2, 6]; growing number of non-immune individuals among older children; deterioration of specific immunity in adults [10, 13]; genotypic variability of the pathogen under selective action of the vaccines [14–23]; spread of *B. pertussis* by asymptomatic carriers [24]. In addition, wide adoption of PCR tests has significantly increased the number of detected cases of pertussis, which now includes mild, subclinical courses of the disease, as well as cases registered when investigating group infections (unpublished data from the Pertussis and Diphtheria Monitoring Reference Center).

For more than 60 years, DPT vaccine includes a whole-cell pertussis component. Though highly effective, such component is reactogenic, which necessitated development of cell-free vaccines that have been widely used throughout the world since the second half of the 1990s. These vaccines contain from 1 to 5 purified pertussis antigens (pertussis toxin (PT), filamentous hemaglutinin (FHA), pertactin *(PRN*), type 2 and type 3 fimbriae (*Fim2* and *Fim3*)). Nevertheless, vaccination of the population cannot fully prevent the spread of pertussis, the incidence of which is nowadays growing in many countries of the world. Since the 2000s, against the background of widespread use of cell-free pertussis vaccine in Europe, Japan, the USA, and Australia, the prevalence of this disease has been growing, in some cases — to the point of epidemic outbreaks [https://www.who.int/health-topics/pertussis#tab=tab_1]. According to several researchers, there is a correlation between preference for such vaccines and the increasing incidence of pertussis, which raises a number of questions about the their efficacy and ability to control the disease [11, 12, 22, 23].

Numerous monitoring studies investigating emergence of the new strains of *B. pertussis* have shown that some of them acquire genetic mutations affecting the structure of protective antigens, thus granting ability to evade the immune response [14–23]. Multilocus antigenic sequence typing (MAST) focuses on changes in the population of *B. pertussis*. In particular, genotyping studies gene sequences encoding protective antigens, including those part of the currently common cell-free vaccines: *ptxA* (encodes the S1 subunit of pertussis toxin), *ptxB* (encodes the S2 subunit of pertussis toxin), *ptxC* (encodes the S3 subunit of pertussis toxin), *prn* (encodes pertactin, the adhesive protein), *fim2* and *fim3* (encode the fimbrial proteins *Fim2* and *Fim3*, respectively). Pertussis toxin's promoter, *ptxP*, is also part of typing isolates, since it has been established that the *ptxP3* allele enhances toxin production [25].

In the Russian Federation, both whole-cell and cell-free pertussis vaccines (as a component of combined preparations) are common. Thus, the purpose of this work was to study the biological and genotypic properties of the vaccine candidate *B. pertussis* strains.

METHODS

Under regulations of the Russian Federation, Pertussis and Diphtheria Monitoring Reference Center of G.N Gabrichevsky Research Institute for Epidemiology and Microbiology receives bacterial strains of *Bordetella* and clinical samples obtained from pertussis patients for the purposes of *B. pertussis* verification and genotyping. We selected eight verified strains of *B. pertussis* (smooth form phase of development) with good growth potential, and, as prescribed by the applicable regulations, studied their morphological, cultural, enzymatic, serological, and genotypic properties in order to select candidates to design a pertussis vaccine on. The origin of the strains was one of the inclusion criteria: they were supposed to be from various regions of the Russian Federation.

The selected *B. pertussis* strains were isolated from samples donated by patients of different ages in 2016 through 2020 in Moscow, Voronezh, Novosibirsk, Ulyanovsk, and Chelyabinsk regions. For comparison, we used eight vaccine strains from the collection of Scientific Centre for Expert Evaluation of Medicinal Products that are in production of the pertussis component of DPT vaccine (Table 1).

The strains were cultured on Bordetelagar (State Research Center for Applied Biotechnology and Microbiology, Obolensk, Russia), a dense nutrient medium, for 72 hours at +36–37 °C. The identification of microorganisms relied on their cultural morphological, tinctorial and biochemical properties. The cultural and morphological properties of the resulting colonies were uncovered using a SteREO Discovery V12 stereoscopic microscope (Carl Zeiss; Germany) with a PlanApo S 1.0 × FWD 60 mm lens objective and a PI 10 × 23 Br foc eyepiece. Gram staining (ECOlab; Russia) allowed gauging the tinctorial properties. The stained smears were examined through an Axio Scope A1 light microscope with EC Plan-NEOFLUAR 100 × 1.3 lens and PI 10 × 23 Br foc eyepiece (Carl Zeiss; Germany).

The identification of *B. pertussis* strains by biochemical properties was carried out in accordance with the applicable regulations [26].

To learn the antigenic structure (serotypes) of the strains, we staged an extended agglutination reaction using pertussis sera to agglutinogens 1,2,3 dry adsorbed (NPO Microgen; Russia).

We carried out a whole genome sequencing of the eight strains of *B. pertussis* currently used for the pertussis component of DPT vaccine and eight strains of *B. pertussis* selected as candidates to design such component on based on their microbiological and growth characteristics. For this task, we employed MAST, which enabled analysis of the sequence of genes encoding protective antigens of the pathogen (*ptxA*, *ptxB*, *ptxC*, *ptxP*, *prn*, *fim2* and *fim3*), as recommended in [27] and relying on the data from GenBank and BIGSdb databases, and whole genome multilocus sequence typing (wgMLST).

Genomic DNA was isolated from bacterial culture using the ExtractDNA Blood&Cells kit (Eurogen, Russia). For whole genome sequencing, we used the GenoLab platform (GeneMind Biosciences; China) and SG GM kits (Raissol; Russia), as recommended by the manufacturer. The data were assembled in SPAdes-3.15.4, the quality of the array was verified with

Table 1. Genotypic characteristics, vaccine production *B. pertussis* strains

№	№ Piece	Isolation year, location	Year introduced to production	Serovar	*ptxA*	*ptxB*	*ptxC*	*ptxP*	*prn*	*fim2*	*fim3*
1	305	Russia, 1957	1958	1.2.0	2	1	1	1	1	1	1
2	312	Russia, 1959	1962	1.2.3	2	2	1	2	1	1	1
3	475	Russia, 1966	1967	1.2.3	4	1	1	2	1	1	1
4	267	Russia, 1967	1968	1.0.3	2	1	1	1	1	1	1
5	38	Russia, 1966	1967	1.2.0	2	2	1	1	1	1	1
6	39	Russia, 1970	1980	1.2.3	2	2	1	1	1	1	1
7	345	Russia, 1959	1962	1.2.3	4	2	1	2	1	1	1
8	703	Russia, 1970	1976	1.0.3	1	2	1	1	1	1	1

the help of QUAST 5.2.0 (https://github.com/ablab/quast; Russia). We employed the BIGSdb server to identify alleles of the genes of interest. For the purpose of comparison of the nucleotide sequences yielded by MAST, we used the following reference gene numbers: ptxA gene (*ptxA1* (AJ245366), *ptxA2* (AJ245367), *ptxA4* (AJ245368)); *ptxA4* gene (HM185483.1) (*ptxA41*, *ptxA42*); *ptxC* gene (AJ420987) (*ptxC1* (M13223), *ptxC2* (AJ420987)); *ptxP*, pertussis toxin promoter (*ptxP1* (FN252323.1), *ptxP2* (FN252322.1), *ptxP3* (FN252324.1)); *fim2* gene (*fim2-1* (KT194049), *fim2-2* (AJ420988)); *fim3* gene (*fim3-1* (X51543.1) and *fim3-2* (AY464180.1)); *prn* gene (*prn1* (AJ011091.1), *prn2* (AJ011092.1), *prn9* (AJ315611.1)). To find the alleles needed to build the tree based on wgMLST, we used pyMLST 2.1.65 (https://github.com/bvalot/pyMLST /; France). All complete ST2 genomes available in the NCBI Refseq public database, as well as the ST1 Tohama as an external representative, were used for the purpose of comparison. Based on the sequences of 2974 genes, we compiled the allele profile of each strain, then calculated the distance matrix reflecting the number of mismatched alleles between the strains. Using the distance matrix and the rapidNJ 2.3.2 software (https://github.com/somme89/rapidNJ; Denmark), we then built the employing the Neighbor-Joining algorithm.

Two clades were taken from the said tree, one of which consisted entirely of the candidate strains, while the other included strain 3–20 and five comparison strains. For these strains (as well as for Tohama I), we took sequences of all 2974 studied genes, concatenated and used them to build a tree applying the Neighbor-Joining algorithm and the Kimura distance model. This approach was applied to evaluate bootstrap support levels in the above-described clades of the previous tree.

RESULTS

Cultured on Bordetelagar for 72 hours, all eight studied strains of *B. pertussis* developed convex round shiny smooth surface colonies of grayish-white color, up to 1.5 mm in size, with oily consistency, which could be easily removed by a loop. Observing the colonies through a SteREO Discovery V12 stereoscopic microscope with a PlanApo S 1.0 × FWD 60 mm lens and a PI 10 × 23 Br foc eyepiece (Carl Zeiss; Germany), we noted a narrow beam of light ("tail") radiating from their centers. Microscopy also revealed small randomly arranged gram-negative rods. All studied strains of *B. pertussis* exhibited catalase and oxidase activity, did not grow on blood and meat-peptone agar, did not produce enzymes tyrosinase and urease, did not grow on Simmons' citrate agar, did not reduce nitrates to nitrites, and were immobile. Considering the antigenic structure, all studied strains of *B. pertussis* had agglutinogen 1 (species feature), and agglutinated with adsorbed type-specific sera to agglutinogens 1,2,3 not lower than 1 : 280. The production vaccine strains belonged to three different serotypes: 1.2.0, 1.0.3 and 1.2.3; candidate strains to two serotypes: 1.0.3 and 1.2.0 (Tables 1, 2).

By the sequence of the *ptxA* gene, which encodes S1 subunit of pertussis toxin, most of the production strains of *B. pertussis* correspond to the two alleles of *ptxA*, *ptxA4* and *ptxA2*, and only one production strain has the *ptxA1* allele, like all current candidate strains. The *ptxA1* allele differs from other alleles by significant mutational changes with amino acid substitution in the T-epitope of pertussis toxin's S1 subunit (nucleotide positions 204, 586, 668 and 96), which has a continuous immunodominant structure recognized by monoclonal protective m-antibodies (mAT). The *ptxA1* allele differs from the *ptxA4* allele at positions D68E, I228M and I232V, and differs from the *ptxA2* allele at position I228M [12, 27].

By the sequence of the *ptxB* gene, which encodes pertussis toxin's S2 subunit, three production strains of *B. pertussis* correspond to the *ptxB1* allele of the gene, and most production strains (five) and all current candidate strains have the *ptxB2* allele. The *ptxB1* allele differs from the *ptxB2* allele by the changed G18S in the S2 subunit of pertussis toxin.

Studying the *ptxC* gene, which encodes S3 subunit of the pertussis toxin B complex, we found strains of two nucleotide sequence variants, *ptxC1* and *ptxC2*. All production vaccine

Table 2. Genotypic characteristics, candidate *B. pertussis* strains

№	№ Piece	Year of isolation	Serotype	*ptxA*	*ptxB*	*ptxC*	*ptxP*	*prn*	*fim2*	*fim3*
1	16–16	2016	1.0.3	1	2	2	3	2	2	2
2	31–2–17	2017	1.0.3	1	2	2	3	9	2	2
3	25–16	2016	1.0.3	1	2	2	3	2	2	2
4	37–18	2018	1.2.0	1	2	2	3	2	2	1
5	30–18	2018	1.0.3	1	2	2	3	2	2	2
6	1–20	2020	1.0.3	1	2	2	3	2	2	2
7	2–20	2020	1.0.3	1	2	2	3	2	2	2
8	3–20	2020	1.2.0	1	2	2	3	2	2	1

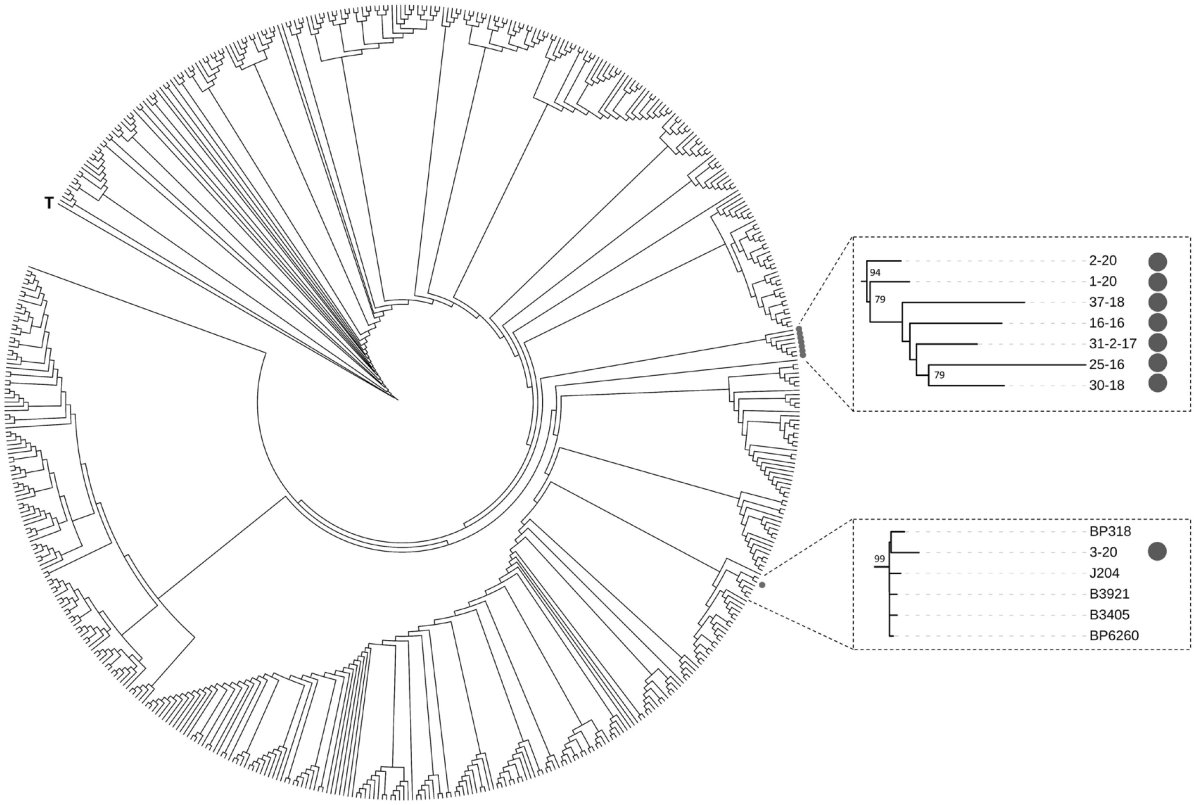

Fig. Phylogenetic tree of bacteria of ST2 type based on wgMLST. Vaccine candidate strains are *gray dots*. Sections of the tree containing these strains are presented magnified on the right, with bootstrap support levels marked in the nodes (only values above 70). The ring diagram does not show lengths of branches because some strains have abnormally long branches. Letter T denotes the Tohama I strain used as an external representative

strains of *B. pertussis* carry the *ptxC1* allele, while all current candidate strains have the *ptxC2* allele, which differs from the *ptxC1* allele by a replaced nucleotide at position C681T, this replacement entailing no changes at the amino acid level.

Although *ptxP,* pertussis toxin's promoter, is not part of the cell-free vaccine, it is usually used in strain typing as a marker of the emerging genetic lineage that has spread throughout the world [14–23, 27]. Analysis of the *ptxP* region's sequence has shown that the studied strains have three *ptxP* alleles: *ptxP1*, *ptxP2*, and *ptxP3*. Five *B. pertussis* vaccine production strains carried the *ptxP1* allele, three — *ptxP2* allele, and all candidate strains carried the *ptxP3* allele. This allele differs from *ptxP1* and *ptxP2* by a mutation at position –65, which reinforces binding to the BvgA dimer and thus increases production of the pertussis toxin [25].

Sequencing of the *fim3* gene, which encodes fimbrial protein Fim3, revealed two variants of the nucleotide sequence, *fim3-1* and *fim3-2*. All vaccine production strains were found to carry a similar *fim3-1* allele, six candidate strain — *fim3-2*, and two remaining candidate strains — *fim3-1*. The nucleotide sequence of *fim3-2* differs from that of *fim3-1* allele by a significant mutation, which entails changes at A87E in the Fim3 protein molecule.

Sequencing of the *fim2* gene, which encodes fimbrial protein *Fim2*, revealed two variants of the nucleotide sequence, *fim2-1* and *fim2-2*. All production strains had a similar allele, *fim2-1*, and all candidate strains of *B. pertussis* — *fim2-2*. The identified allelic variants of *fim2-1* and *fim2-2* differed in R174K of Fim2 protein molecule.

The *prn* gene contains about 2800 bases that encode a large adhesive precursor protein: the 5' gene end encodes a part of the pertactin precursor that is exported from the cell, while the 3' end encodes the integral outer membrane protein that enables the export. Sequencing of the pertactin (*prn*) gene in the studied *B. pertussis* strains revealed three variants of its alleles, *prn1*, *prn2* and *prn9*, with *prn1* identified in the vaccine production strains, and *prn2* and *prn9* — in 7 and 1 candidate strains, respectively. The nucleotide sequences of the *prn2* and *prn9* alleles differ from that of the *prn1* allele: the former contain significant mutational changes in six positions (828, 831, 832, 833, 834 and 836), which entail V279G and A278F substitutions on the amino acid level. The *prn2* allele's nucleotide sequence has an insert in the 15 bp, GGCGGCCTCGGTCC in the gene's 1st region (positions 841-855), and the gene's prn9 allele has an extra fragment in the 30 bp, GGCGGCCTCGGTCCTCGGTCC (1st region, positions 841–871). All changes in the *prn2* and *prn9* alleles are in the *Prn* protein's 1st and 2nd regions, which are immunogenic and participate in the development of the B-cell immune response.

This study has shown that all vaccine production strains belong to six genotypes: *ptxA2/ptxB1/ptxC1/ptxP1/fim2-1/fim3-1/prn1, ptxA2/ptxB2/ptxC1/ptxP2/fim2-1/fim3-1/prn1, ptxA4/ptxB1/ptxC1/ptxP2/fim2-1/fim3-1/prn1, ptxA2/ptxB2/ptxC1/ptxP1/fim2-1/fim3-1/prn1, ptxA4/ptxB2/ptxC1/ptxP2/fim2-1/fim3-1/prn1 and ptxA1/ptxB2/ptxC1/ptxP1/fim2-1/fim3-1/prn1* (Table 1). Candidate strains belong to four genotypes: *ptxA1/ptxB2/ptxC2/ptxP3/fim2-2/fim3-2/prn2, ptxA1/ptxB2/ptxC2/ptxP3/fim2-2/fim3-2/prn9, ptxA1/ptxB2/ptxC2/ptxP3/fim2-1/fim3-1/prn1* and *ptxA1/ptxB2/ptxC2/ptxP3/fim2-2/fim3-1/prn2* (Table 2).

Based on the candidate strains' complete genome sequences, we have built a phylogenetic tree that shows the evolutionary position of these strains among all the representatives of the ST2 sequence type (Figure). It was established that all of them, except one, form a single cluster, apparently inherent in the Russian Federation.

DISCUSSION

All the *B. pertussis* genome sequences learned in the context of this study were added to the National Catalog kept by the State Research Center for Applied Biotechnology and Microbiology as part of the Federal Project "Sanitary Shield of the Country — Health Safety (Prevention, Detection, Response)."

Long-term monitoring of the genotypic properties of B. pertussis has shown that more than 60 years of routine immunization of children triggered spread of pertussis pathogens with new genotypes (allelic profiles) [14–16], which is consistent with the changes in the genetic structure of *B. pertussis* protective antigens registered worldwide [18–23]. Studies conducted in different countries of the world have also revealed genotypic differences between vaccine production strains and circulating pertussis pathogens [11, 18–23, 28, 29].

This study describes and suggests as candidates eight strains of *B. pertussis* that belong to four different genotypes different from the currently used DPT vaccine production strains. Graduation of these candidates to vaccine production strains requires animal studies designed to investigate their immunobiological, hemagglutinating, hemolytic and leukocytosis-stimulating properties, virulence and toxicity, as well as deposition in the National Collection of Pathogenic Microorganisms (NCPM-Obolensk).

Circulating strains of *B. pertussis* change continuously, which necessitates ceaseless monitoring of the strains' genetic properties that would allow assessing the effect of the said changes on the efficacy of the vaccine. Reasoned assessment of the adequacy of the currently common whole-cell and cell-free pertussis vaccines as means of preventing the respective infection requires further research of the circulating *B. pertussis* strains' genotype and specifics of development of post-infection and post-vaccination immunity. Evaluation of protective properties of the produced vaccines also calls for animal model experiments that involve strains of *B. pertussis* with modern genotypes.

CONCLUSIONS

This study yielded *B. pertussis* strains suggested as candidates for pertussis vaccines, and presents assessment of their growth, cultural, morphological, and genotypic properties.

References

1. Petrova MS, Popova OP, Borisova OYu, Abramova EN, Vartanjan RV, Kelli EI. Kokljush u detej rannego vozrasta. Jepidemiologija i infekcionnye bolezni. 2012; 6: 19–24. DOI: 10.17816/EID40704. Russian.
2. Babachenko IV, Nesterova YuV, Chernyshova YuYu, Karasev VV, Pochinjaeva LM, Kalisnikova EL. Kliniko-jepidemiologicheskie aspekty kokljusha u detej v uslovijah massovoj vakcinoprofilaktiki. Zhurnal infektologii. 2019; 11 (2): 88–96. DOI: 10.22625/2072-6732-2019-11-2-88-96. Russian.
3. Krasnov VV, Iljanenkov KF, Pavlovich LR, Kuzmicheva MV. Kokljush u detej pervogo goda zhizni. Detskie infekcii. 2018; 1 (1): 12–17. DOI: 10.22627/2072-8107-2018-17-1-12-17. Russian.
4. Ob organizacii provedenija vneshnego kontrolja kachestva issledovanij po diagnostike difterii i kokljusha v 2024 godu v Dal'nevostochnom i Ural'skom federal'nyh okrugah. Informacionnoe pis'mo # 02/1860-2024-27 ot 06.02.2024. Federal'naja sluzhba po nadzoru v sfere zashhity prav potrebitelej i blagopoluchija cheloveka (Rospotrebnadzor). Russian.
5. Basov AA, Vysochanskaja SO, Cvirkun OV, Belova TR, Adugjuzelov SYe, i dr. Kriterii ocenki jepidemiologicheskoj situacii po kokljushu v Rossijskoj Federacii. Jepidemiologija i vakcinoprofilaktika. 2024; 23 (2): 4–13. DOI: 10.31631/2073-3046-2024-23-1-4-13. Russian.
6. O sostojanii sanitarno-jepidemiologicheskogo blagopoluchija naselenija v Rossijskoj Federacii v 2021 godu: Gosudarstvennyj doklad. M.: Federal'naja sluzhba po nadzoru v sfere zashhity prav potrebitelej i blagopoluchija cheloveka, 2022; 340 s. Russian.
7. Nesterova YuV, Medkova AYu, Babachenko IV, Semin EG, Kalisnikova EL, Sinjashina LN. Kliniko-diagnosticheskoe znachenie geneticheskih markerov Bordetella pertussis u kontaktnyh lic v semejnyh ochagah. Zhurnal infektologii. 2019; 11 (1): 17–24. DOI: 10.22625/2072-6732-2019-11-1-17-24. Russian.
8. Philipson K, Goodyear-Smith F, Grant CC, Chong A, Turner N, Stewart J. When is acute persistent cough in school-age children and adults whooping cough? British Journal of General Practice. 2013; 63 (613): 573–9. DOI: 10.3399/bjgp13X670705.
9. Pimenova AS, Borisova OYu, Cvirkun OV, Basov AA, Aleshkin VA, Afanasev SS, i dr. Jeffektivnost' primenenija molekuljarno-geneticheskoj diagnostiki pri obsledovanii ochagov kokljushnoj infekcii. Infekcija i immunitet. 2017; 7 (2): 162–70. DOI: 10.15789/2220-7619-2017-2-162-170. Russian.
10. Skirda TA, Borisova OYu, Petrova MS, Borisova AB. Serologicheskaja diagnostika kokljusha u lic starshego vozrasta. Klinicheskaja laboratornaja diagnostika. 2020; 65 (8): 492–5. DOI: 10.18821/0869-2084-2020-65-8-492-495. Russian.
11. Esposito S, Stefanelli P, Fry NK, Fedele G, He Q, Paterson P, et al. Pertussis prevention: reasons for resurgence, and differences in the current acellular pertussis vaccines. Frontiers in Immunology. 2019; 10: 1344. DOI: 10.3389/fimmu.2019.01344.
12. Mooi FR, Van Der Maas NA, De Melker HE. Pertussis resurgence: waning immunity and pathogen adaptation — two sides of the same coin. Epidemiol Infect. 2014; 142 (4): 685–94. DOI: 10.1017/S0950268813000071.
13. Skirda TA, Borisova OJu, Borisova AB, Kombarova SJu, Pimenova AS, Gadua NT, i dr. Opredelenie protivokokljushnyh antitel u shkol'nikov s dlitel'nym kashlem. Zhurnal infektologii. 2023; 15 (1): 93–100. DOI: 10.22625/2072-6732-2023-15-1-93-100. Russian.
14. Borisova OYu, Gadua NT, Pimenova AS, Petrova MS, Popova OP, Aleshkin VA, i dr. Struktura populjacii shtammov vozbuditelja kokljusha na territorii Rossii. Jepidemiologija i vakcinoprofilaktika. 2016; 4: 22–28. DOI: 10.31631/2073-3046-2016-15-4-22-28. Russian.
15. Andrievskaja IYu, Borisova OYu, Pimenova AS, Borisova AB, Gadua NT, Chagina IA. Genotipirovanie vozbuditelja kokljusha iz klinicheskih obrazcov. Materialy XVI Ezhegodnogo Vserossijskogo kongressa po infekcionnym boleznjam imeni akademika V.I. Pokrovskogo k 300-letiju Rossijskoj akademii nauk, Moskva, 25–27 marta 2024 g. M.: Medicinskoe Marketingovoe agentstvo, 2024; 250 s: 19–20. ISBN 978-5-6048391-2-6. Russian.
16. Andrievskaja IYu, Pimenova AS, Gadua NT, Chagina IA, Borisova OYu. Allel'noe tipirovanie ptxP Bordetella pertussis v klinicheskih obrazcah. Materialy kongressa s mezhdunarodnym uchastiem «Molekuljarnaja diagnostika i biobezopasnost' — 2024», Moskva, 16–17 aprelja 2024 g. M.: FBUN CNII Jepidemiologii Rospotrebnadzora, 2024; 266 s.: 36. DOI: 10.36233/978-5-6048873-9-4. Russian.
17. Kentaro K, ShuMan Y, Chuen-Sheue C, Phung TBT, Do TTN, et al. Genotyping and macrolide-resistant mutation of Bordetella pertussis in East and South-East Asia. J Glob Antimicrob Resist. 2022; 31: 263–9. DOI: 10.1016/j.jgar.2022.10.007.
18. Barkoff AM, Mertsola J, Pierard D, Dalby T, Hoegh SV, Guillot S, et al. Surveillance of Circulating Bordetella pertussis Strains in Europe during 1998 to 2015. J Clin Microbiol. 2018; 56 (5): e01998-17. DOI: 10.1128/JCM.01998-17.
19. Moosa F, du Plessis M, Weigand MR, Peng Y, Mogale D, de Gouveia L, et al. Genomic characterization of Bordetella pertussis in South Africa, 2015–2019. Microb Genom. 2023; 9 (12):

001162. DOI: 10.1099/mgen.0.001162.
20. Fu P, Zhou J, Yang C, Nijiati Y, Zhou L, Yan G, et al. Molecular Evolution and Increasing Macrolide Resistance of Bordetella pertussis, Shanghai, China, 2016–2022. Emerg Infect Dis. 2023; 30 (1): 29–38. DOI: 10.3201/eid3001.221588.
21. Weigand MR, Williams MM, Peng Y, Kania D, Pawloski LC, Tondella ML. Genomic Survey of Bordetella pertussis Diversity, United States, 2000–2013. Emerg Infect Dis. 2019; 25 (4): 780–3. DOI: 10.3201/eid2504.180812.
22. Zomer A, Otsuka N, Hiramatsu Y, Kamachi K, Nishimura N, Ozaki T, et al. Bordetella pertussis population dynamics and phylogeny in Japan after adoption of acellular pertussis vaccines. Microb Genom. 2018; 4 (5): 000180. DOI: 10.1099/mgen.0.000180
23. Mir-Cros A, Moreno-Mingorance A, Martín-Gómez MT, Codina G, Cornejo-Sánchez T, Rajadell M, et al. Population dynamics and antigenic drift of Bordetella pertussis following whole cell vaccine replacement, Barcelona, Spain, 1986–2015. Emerg Microbes Infect. 2019; 8 (1): 1711–20. DOI: 10.1080/22221751.2019.1694395.
24. Althouse BM, Scarpino SV. Asymptomatic transmission and the resurgence of Bordetella pertussis. BMC Med. 2015; 13: 146. DOI: 10.1186/s12916-015-0382-8.
25. Mooi FR, van Loo IH, van Gent M, He Q, Bart MJ, Heuvelman KJ, et al. Bordetella pertussis strains with increased toxin production associated with pertussis resurgence. Emerg Infect Dis. 2009; 15 (8): 1206–13. DOI: 10.3201/eid1508.081511.
26. Metodicheskie ukazanija «Laboratornaja diagnostika kokljusha i zabolevanij, obuslovlennyh drugimi bordetellami». MUK 4.2.3701-21. M.: Federal'naja sluzhba po nadzoru v sfere zashhity prav potrebitelej i blagopoluchija cheloveka. 2021. Russian.
27. Mooi FR, Hallander H, Wirsing von König CH, Hoet B, Guiso N. Epidemiological Typing of Bordetella pertussis Isolates: Recommendations for a Standard Methodology. Eur J Clin Microbiol Infect Dis. 2000; 19: 174–81.
28. Gordana D, Teemu K, Annika E, Pljesa T, Vignjevic-Krastavcevic M, He Q. Bordetella pertussis vaccine strains and circulating isolates in Serbia Vaccine. 2010; 28 (5): 1188–92. DOI: 10.1016/j.vaccine.2009.11.036.
29. Alai S, Ghattargi VC, Gautam M, Patel K, Pawar SP, Dhotre DP, et al. Comparative genomics of whole-cell pertussis vaccine strains from India. BMC Genomics. 2020; 21 (1): 345. DOI: 10.1186/s12864-020-6724-8.

Литература

1. Петрова М. С., Попова О. П., Борисова О. Ю., Абрамова Е. Н., Вартанян Р. В., Келли Е. И. Коклюш у детей раннего возраста. Эпидемиология и инфекционные болезни. 2012; 6: 19–24. DOI: 10.17816/EID40704.
2. Бабаченко И. В., Нестерова Ю. В., Чернышова Ю. Ю., Карасев В. В., Починяева Л. М., Калисникова Е. Л. Клинико-эпидемиологические аспекты коклюша у детей в условиях массовой вакцинопрофилактики. Журнал инфектологии. 2019; 11 (2): 88–96. DOI: 10.22625/2072-6732-2019-11-2-88-96.
3. Краснов В. В., Ильяненков К. Ф., Павлович Л. Р., Кузмичева М. В. Коклюш у детей первого года жизни. Детские инфекции. 2018; 1 (1): 12–17. DOI: 10.22627/2072-8107-2018-17-1-12-17.
4. Об организации проведения внешнего контроля качества исследований по диагностике дифтерии и коклюша в 2024 году в Дальневосточном и Уральском федеральных округах. Информационное письмо № 02/1860-2024-27 от 06.02.2024. Федеральная служба по надзору в сфере защиты прав потребителей и благополучия человека (Роспотребнадзор).
5. Басов А. А., Высочанская С. О., Цвиркун О. В., Белова Т. Р., Адугюзелов С. Э., и др. Критерии оценки эпидемиологической ситуации по коклюшу в Российской Федерации. Эпидемиология и вакцинопрофилактика. 2024; 23 (2): 4–13. DOI: 10.31631/2073-3046-2024-23-1-4-13.
6. О состоянии санитарно-эпидемиологического благополучия населения в Российской Федерации в 2021 году: Государственный доклад. М.: Федеральная служба по надзору в сфере защиты прав потребителей и благополучия человека, 2022; 340 с.
7. Нестерова Ю. В., Медкова А. Ю., Бабаченко И. В., Семин Е. Г., Калисникова Е. Л., Синяшина Л. Н. Клинико-диагностическое значение генетических маркеров Bordetella pertussis у контактных лиц в семейных очагах. Журнал инфектологии. 2019; 11 (1): 17–24. DOI: 10.22625/2072-6732-2019-11-1-17-24.
8. Philipson K, Goodyear-Smith F, Grant CC, Chong A, Turner N, Stewart J. When is acute persistent cough in school-age children and adults whooping cough? British Journal of General Practice. 2013; 63 (613): 573–9. DOI: 10.3399/bjgp13X670705.
9. Пименова А. С., Борисова О. Ю., Цвиркун О. В., Басов А. А., Алешкин В. А., Афанасьев С. С., и др. Эффективность применения молекулярно-генетической диагностики при обследовании очагов коклюшной инфекции. Инфекция и иммунитет. 2017; 7 (2): 162–70. DOI: 10.15789/2220-7619-2017-2-162-170.
10. Скирда Т. А., Борисова О. Ю., Петрова М. С., Борисова А. Б. Серологическая диагностика коклюша у лиц старшего возраста. Клиническая лабораторная диагностика. 2020; 65 (8): 492–5. DOI: 10.18821/0869-2084-2020-65-8-492-495.
11. Esposito S, Stefanelli P, Fry NK, Fedele G, He Q, Paterson P, et al. Pertussis prevention: reasons for resurgence, and differences in the current acellular pertussis vaccines. Frontiers in Immunology. 2019; 10: 1344. DOI: 10.3389/fimmu.2019.01344.
12. Mooi FR, Van Der Maas NA, De Melker HE. Pertussis resurgence: waning immunity and pathogen adaptation — two sides of the same coin. Epidemiol Infect. 2014; 142 (4): 685–94. DOI: 10.1017/S0950268813000071.
13. Скирда Т. А., Борисова О. Ю., Борисова А. Б., Комбарова С. Ю., Пименова А. С., Гадуа Н. Т., и др. Определение противококлюшных антител у школьников с длительным кашлем. Журнал инфектологии. 2023; 15 (1): 93–100. DOI: 10.22625/2072-6732-2023-15-1-93-100.
14. Борисова О. Ю., Гадуа Н. Т., Пименова А. С., Петрова М. С., Попова О. П., Алешкин В. А., и др. Структура популяции штаммов возбудителя коклюша на территории России. Эпидемиология и вакцинопрофилактика. 2016; 4: 22–28. DOI: 10.31631/2073-3046-2016-15-4-22-28.
15. Андриевская И. Ю., Борисова О. Ю., Пименова А. С., Борисова А. Б., Гадуа Н. Т., Чагина И. А. Генотипирование возбудителя коклюша из клинических образцов. Материалы XVI Ежегодного Всероссийского конгресса по инфекционным болезням имени академика В.И. Покровского к 300-летию Российской академии наук, Москва, 25–27 марта 2024 г. М.: Медицинское маркетинговое агентство, 2024; 250 с: 19–20. ISBN 978-5-6048391-2-6.
16. Андриевская И. Ю., Пименова А. С., Гадуа Н. Т., Чагина И. А., Борисова О. Ю. Аллельное типирование ptxP Bordetella pertussis в клинических образцах. Материалы конгресса с международным участием «Молекулярная диагностика и биобезопасность – 2024», Москва, 16 – 17 апреля 2024 г. М.: ФБУН ЦНИИ Эпидемиологии Роспотребнадзора, 2024; 266 с.: 36. DOI: 10.36233/978-5-6048873-9-4.
17. Kentaro K, ShuMan Y, Chuen-Sheue C, Phung TBT, Do TTN, et al. Genotyping and macrolide-resistant mutation of Bordetella pertussis in East and South-East Asia. J Glob Antimicrob Resist. 2022; 31: 263–9. DOI: 10.1016/j.jgar.2022.10.007.
18. Barkoff AM, Mertsola J, Pierard D, Dalby T, Hoegh SV, Guillot S, et al. Surveillance of Circulating Bordetella pertussis Strains in Europe during 1998 to 2015. J Clin Microbiol. 2018; 56 (5): e01998-17. DOI: 10.1128/JCM.01998-17.
19. Moosa F, du Plessis M, Weigand MR, Peng Y, Mogale D, de Gouveia L, et al. Genomic characterization of Bordetella pertussis in South Africa, 2015–2019. Microb Genom. 2023; 9 (12): 001162. DOI: 10.1099/mgen.0.001162.
20. Fu P, Zhou J, Yang C, Nijiati Y, Zhou L, Yan G, et al. Molecular Evolution and Increasing Macrolide Resistance of Bordetella pertussis, Shanghai, China, 2016–2022. Emerg Infect Dis. 2023; 30 (1): 29–38. DOI: 10.3201/eid3001.221588.
21. Weigand MR, Williams MM, Peng Y, Kania D, Pawloski LC,

Tondella ML. Genomic Survey of Bordetella pertussis Diversity, United States, 2000–2013. Emerg Infect Dis. 2019; 25 (4): 780–3. DOI: 10.3201/eid2504.180812.
22. Zomer A, Otsuka N, Hiramatsu Y, Kamachi K, Nishimura N, Ozaki T, et al. Bordetella pertussis population dynamics and phylogeny in Japan after adoption of acellular pertussis vaccines. Microb Genom. 2018; 4 (5): 000180. DOI: 10.1099/mgen.0.000180
23. Mir-Cros A, Moreno-Mingorance A, Martín-Gómez MT, Codina G, Cornejo-Sánchez T, Rajadell M, et al. Population dynamics and antigenic drift of Bordetella pertussis following whole cell vaccine replacement, Barcelona, Spain, 1986–2015. Emerg Microbes Infect. 2019; 8 (1): 1711–20. DOI: 10.1080/22221751.2019.1694395.
24. Althouse BM, Scarpino SV. Asymptomatic transmission and the resurgence of Bordetella pertussis. BMC Med. 2015; 13: 146. DOI: 10.1186/s12916-015-0382-8.
25. Mooi FR, van Loo IH, van Gent M, He Q, Bart MJ, Heuvelman KJ, et al. Bordetella pertussis strains with increased toxin production associated with pertussis resurgence. Emerg Infect Dis. 2009; 15 (8): 1206–13. DOI: 10.3201/eid1508.081511.
26. Методические указания «Лабораторная диагностика коклюша и заболеваний, обусловленных другими бордетеллами». МУК 4.2.3701-21. М.: Федеральная служба по надзору в сфере защиты прав потребителей и благополучия человека. 2021.
27. Mooi FR, Hallander H, Wirsing von König CH, Hoet B, Guiso N. Epidemiological Typing of Bordetella pertussis Isolates: Recommendations for a Standard Methodology. Eur J Clin Microbiol Infect Dis. 2000; 19: 174–81.
28. Gordana D, Teemu K, Annika E, Pljesa T, Vignjevic-Krastavcevic M, He Q. Bordetella pertussis vaccine strains and circulating isolates in Serbia Vaccine. 2010; 28 (5): 1188–92. DOI: 10.1016/j.vaccine.2009.11.036.
29. Alai S, Ghattargi VC, Gautam M, Patel K, Pawar SP, Dhotre DP, et al. Comparative genomics of whole-cell pertussis vaccine strains from India. BMC Genomics. 2020; 21 (1): 345. DOI: 10.1186/s12864-020-6724-8.

DETERMINING OPTIMAL AMBIENT IONIZATION MASS SPECTROMETRY DATA PRE-PROCESSING PARAMETERS IN NEUROSURGERY

Zavorotnyuk DS[1] ✉, Sorokin AA[1], Bormotov DS[1], Eliferov VA[1], Bocharov KV[2], Pekov SI[1,3,4], Popov IA[1,4]

[1] Moscow Institute of Physics and Technology, Moscow, Russia
[2] Semenov Federal Research Center for Chemical Physics of the Russian Academy of Sciences, Moscow, Russia
[3] Skolkovo Institute of Science and Technology, Moscow, Russia
[4] Siberian State Medical University, Tomsk, Russia

Radical tumor resection is still the most effective treatment method for brain tumors. The problems of intraoperative monitoring are currently solved using positron emission tomography, magnetic resonance imaging, and histochemical analysis, however, these require using expensive equipment by highly qualified personnel and are therefore still not widely available. As an alternative, it is possible to use mass spectrometry methods without sample preparation and then the analysis of mass spectrometry data involving the use of machine learning methods. The spectra that are more rich and diverse in terms of peak number are typical for mass spectrometry without sample preparation, therefore the use of this method requires specific pre-processing of experimental data. The study was aimed to develop the methods to determine the optimal parameter values for pre-processing of the data acquired by ambient ionization mass spectrometry. The paper presents two such methods and provides specific parameter values for the data acquired using the Thermo LTQ XL Orbitrap ETD mass spectrometer.

Keywords: mass spectrometry, ambient ionization, data analysis, data preprocessing

Funding: the study was performed within the framework of the state assignment of the Ministry of Science and Higher Education of the Russian Federation (agreement № 075-03-2022-107, project № 0714-2020-0006). The study involved the use of equipment of the Semenov Federal Research Center for Chemical Physics RAS.

Author contribution: Zavorotnyuk DS — data acquisition and interpretation, software development, manuscript writing and editing; Sorokin AA — study planning, data analysis and interpretation, manuscript editing; Bormotov DS — data acquisition and interpretation, manuscript writing; Eliferov VA — financial support of the experiment; Bocharov KV — data acquisition; Pekov SI — study planning, data analysis and interpretation, manuscript draft writing and manuscript text finalization; Popov IA — project management, financial support.

Compliance with ethical standards: the study was approved by the Ethics Committee of the Burdenko Research Institute of Neurosurgery (protocols № 40 dated 12 April 2016 and № 131 dated 17 July 2018) and conducted in accordance with the principles of the Declaration of Helsinki (2000) and its subsequent revisions. All patients submitted the informed consent to study participation and the use of biomaterial for scientific purposes.

✉ **Correspondence should be addressed:** Denis S. Zavorotnyuk
Institutskiy per., 9, str. 7, Dolgoprudny, Moscow Region, 141701; denis.zavorotnyuk@gmail.com

Received: 19.12.2023 **Accepted:** 03.03.2024 **Published online:** 27.04.2024

DOI: 10.24075/brsmu.2024.013

ОПРЕДЕЛЕНИЕ ОПТИМАЛЬНЫХ ПАРАМЕТРОВ ПРЕДВАРИТЕЛЬНОЙ ОБРАБОТКИ ДАННЫХ МАСС-СПЕКТРОМЕТРИИ С ПРЯМОЙ ИОНИЗАЦИЕЙ В НЕЙРОХИРУРГИИ

Д. С. Заворотнюк[1] ✉, А. А. Сорокин[1], Д. С. Бормотов[1], В. А. Елиферов[1], К. В. Бочаров[2], С. И. Пеков[1,3,4], И. А. Попов[1,4]

[1] Московский физико-технический институт, Москва, Россия
[2] Федеральный исследовательский центр химической физики имени Н. Н. Семенова Российской академии наук, Москва, Россия
[3] Сколковский институт науки и технологий, Москва, Россия
[4] Сибирский государственный медицинский университет, Томск, Россия

Радикальное удаление опухоли до сих пор остается наиболее эффективным методом лечения онкологических заболеваний головного мозга. Задачи интраоперационного мониторинга на сегодняшний день решают с помощью позитронно-эмиссионной томографии, магнитно-резонансной томографии и гистохимического анализа, однако они требуют применения дорогостоящего оборудования высококвалифицированным персоналом, поэтому до сих пор не получили широкого распространения. В качестве альтернативы возможно применение методов масс-спектрометрии без пробоподготовки с последующим анализом масс-спектрометрических данных методами машинного обучения. Так как для масс-спектрометрии без пробоподготовки характерны более богатые и разнообразные по количеству пиков спектры, ее применение требует специальной предварительной обработки экспериментальных данных. Целью исследования было разработать методы определения оптимальных значений параметров предварительной обработки данных масс-спектрометрии без пробоподготовки. В работе представлены два таких метода, а также приведены конкретные значения параметров для данных, полученных с помощью масс-спектрометра Thermo LTQ XL Orbitrap ETD.

Ключевые слова: масс-спектрометрия, прямая ионизация, анализ данных, предварительная обработка данных

Финансирование: работа выполнена в рамках государственного задания Министерства науки и высшего образования (соглашение № 075-03-2022-107, проект № 0714-2020-0006). Исследование выполнено с использованием оборудования ЦКП ФИЦ ХФ им. Н. Н. Семенова РАН.

Вклад авторов: Д. С. Заворотнюк — анализ и интерпретация данных, создание программного обеспечения, написание и редактирование рукописи; А. А. Сорокин — планирование исследования, анализ и интерпретация данных, редактирование рукописи; Д. С. Бормотов — сбор и интерпретация данных, написание рукописи; В. А. Елиферов — финансовое обеспечение эксперимента; К. В. Бочаров — сбор данных; С. И. Пеков — планирование исследования, анализ и интерпретация данных, редактирование рукописи. И. А. Попов — руководство проектом, обеспечение финансирования.

Соблюдение этических стандартов: исследование одобрено этическим комитетом НМИЦН имени Н. Н. Бурденко (протоколы № 40 от 12 апреля 2016 г. и № 131 от 17 июля 2018 г.), проведено в соответствии с принципами Хельсинкской декларации (2000 г.) и ее последующих пересмотров. Все пациенты подписали добровольное информированное согласие на участие в исследовании и использование биоматериалов в исследовательских целях.

✉ **Для корреспонденции:** Денис Сергеевич Заворотнюк
Институтский переулок, д. 9, 141701, г. Долгопрудный, Московская область; denis.zavorotnyuk@gmail.com

Статья получена: 19.12.2023 **Статья принята к печати:** 03.03.2024 **Опубликована онлайн:** 27.04.2024

DOI: 10.24075/vrgmu.2024.013

Ambient ionization mass spectrometry represents one of the promising methods to improve accuracy and completeness of the glial tumor resection, since radical tumor removal is currently the most effective treatment method for brain tumors [1]. However, there is a problem of identifying the tumor margins in order to ensure resection completeness for relapse prevention on the one hand and prevention of excessive resection and development of neuropathological sequelae on the other hand [2]. The main universal methods to ensure intraoperative control of the resected tumor margins still include positron emission tomography–computed tomography (PET-CT), magnetic resonance imaging (MRI), and histochemical analysis, since other methods, such as fluorescence staining, can turn out to be non-specific for certain diagnoses. However, these methods are time-consuming, and tomography is also expensive due to the need to equip the specialized surgical units [3].

Ambient ionization mass spectrometry (MS) makes it possible to quickly acquire the data on the molecular structure of the sample [4–6]. However, today, the vast majority of computational tools to deal with mass spectrometry data involve working with the spectra acquired by tandem MS coupled with gas/liquid chromatography. These data are distinguished by the fact that the number of peaks per scan of such a spectrum is much less than the number per scan obtained by ambient ionization MS [7, 8]. When using ambient ionization MS, the sample preparation simplicity and analysis speed make it possible to acquire far more complex mass spectra, i.e., large amounts of data within minutes. At the same time, the analysis of such data requires the use of automated processing methods and complex analysis algorithms [9–11], therefore, great attention should be paid to the data quality control and pre-processing [12].

Mass spectrometry data are the time-ordered sets of scans. Each scan represents the profile of the ion current intensities accumulated by the instrument over a certain time that is ordered on the mass-to-charge ratio (m/z) scale. In the pre-processing phase, it is necessary to transform this scan into the set consisting of intensities and m/z values of the detected peaks. Usually, this is achieved through implementation of such steps as normalization of intensity values, noise determination and elimination, peak position determination and alignment [13–15]. The great diversity of approaches to MS data processing suggests that the above steps should be implemented with various parameters depending on the nature of samples used in the study, mass spectrometer construction, ion acquisition mode, and the type of further analysis.

The paper describes the method to determine the mass spectra pre-processing parameters in order to ensure unification of mass spectrometry data for further automated analysis on the example of the experimental data obtained by mass spectrometry without sample preparation when assessing human brain tumor tissue samples.

METHODS

The study involved mass spectrometry data acquired when processing brain tissue samples of the individual diagnosed with glioblastoma and grade IV astrocytoma (according to the 2021 WHO classification [16]) and non-neoplastic samples obtained during surgical treatment of drug-resistant epilepsy. A total of 307 tissue samples obtained from 74 patients were assessed. The data were acquired using the Thermo LTQ XL Orbitrap ETD mass spectrometer (Thermo Fisher Scientific; USA) with an inline cartridge extraction [3, 17]. Each sample was separated into two parts. The first part was sent for standard histochemical analysis to obtain a medical record on the sample, while the remaining part was used to extract three fragments, about 1 mm^3 each, to be subjected to mass spectrometry analysis. The mass spectrometry protocol involved the analysis and detection of ions in eight different modes, each of which was characterized by the ions' polarity, detector resolution and bandwidth of the registered ions' m/z. Ion acquisition was performed twice in each mode.

The experimental data acquired were pre-processed using different values of the parameters described in the Results section. The pre-processing procedure involved peak intensity calibration, peak alignment relative to the scan showing maximum total ion current (TIC), reciprocal alignment of peaks among scans performed in the same mode of ion detection and filtration of rare and low-intensity peaks. Distinct scan sets were obtained for each ion detection mode. Each set of scans was transformed into the matrix of peak intensities used to train a classification model. When training the models, the matrix columns containing distributions of peak intensities across all scans of the appropriate mode were used as predictors, while the patients' histological diagnoses were used as response. The mass spectrometry data acquired for brain tissue samples of 33 patients diagnosed with glioblastoma and seven patients diagnosed with non-neoplastic disorders were used to train and validate the models. The dataset available for each mode was divided into the training and validating groups in a ratio of 3 : 1, respectively; division was implemented in such a way that different scans of the same sample were present in both groups, to reduce model overfitting.

The data were analyzed using the computer running Ubuntu 16.04 with the installed R package v. 3.4.4 and R packages MALDIquant [18], caret [19], glmnet [20], ggplot2 [21]. For that the data received from the mass spectrometer were converted from the source Thermo Finnigan format to the open NetCDF format [22] using the in-lab developed software tool [23].

RESULTS

In 2012, it was shown that the differences between mass spectra of tumors and non-neoplastic brain tissues could be used for construction of the classifiers for automatic recognition of cancerous tissues in biopsy samples [24]. Fig. 1 demonstrates peaks of two mass scans of the tissue samples obtained from the patients diagnosed with glioblastoma and non-neoplastic disorders.

The mass spectrometry data pre-processing procedure consists of several phases. In the first phase, noise is assessed and the signal-to-noise ratios are determined for all scans:

$$SNR = \frac{I_s}{I_n},$$

where I_s is signal intensity, I_n is noise intensity. There are several methods to determine the digital data noise intensity, for example, using mean absolute deviation (MAD) or regression with adaptive bandwidths (Super Smoother) [25]. In the subsequent phases, the low-intensity peaks with the signal-to-noise ratios lower than the specified SNR value are excluded from the spectrum. Positions of maxima within the scan may vary slightly under exposure to variable environmental factors and occasional fluctuation. In the next phase, alignment of profiles in different scans is performed to compensate for such changes. The scan showing maximum TIC is used as a reference one, since it is assumed that this scan has the largest number of reported ions, and its profile comprises the largest number of various ion peaks. Here every profile is

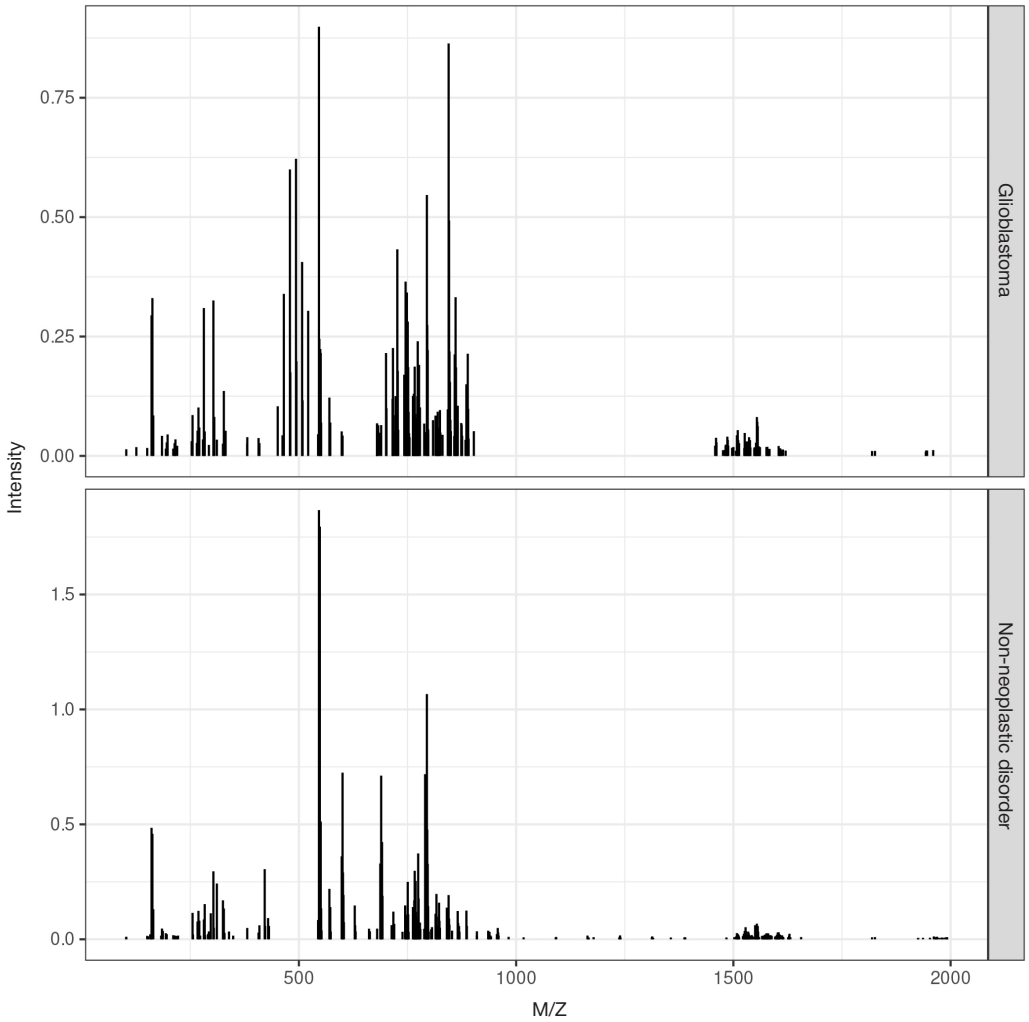

Fig. 1. Comparison of peaks in mass scans of neoplastic tumors and non-neoplastic specimens samples

subjected to alignment along the m/z axis to become as similar to the reference profile as possible. The maximum permissible value of such alignment is specified using the alignment tolerance (TA). Then peaks are detected: the scan profile is converted into the set of individual peaks. For that the entire profile is divided into several parts. The size of each part is determined by the half window size (HWS) representing the range of m/z points, within which the search for a point with the maximum intensity value is carried out. This point is designated as a peak in this part of the profile. Then positions of identical peaks are aligned across the entire set of scans. Here, peaks, the differences in m/z between which do not exceed the tolerance specified when detecting peaks (TBP), are considered to be identical. In the final phase, rare peaks are removed, and peaks of all scans are combined into the common matrix of intensities.

Thus, as a result of mass spectrometry data pre-processing, the matrix is produced [26], the number of rows in which is determined by the number of scans obtained during the experiment, while the number of rows represents the combined number of peaks from all scans. It is clear that the above parameters (SNR, TA, HWS, and TBP) have a significant impact on the number of peaks in the matrix of intensities and the question, which values these parameters should take in each particular ion acquisition mode, is not trivial.

In the classic tasks to determine the model that best describes experimental data [27, 28], the information criteria [29] are used and the extreme values of this criteria correspond to optimal values of the set of model construction criteria obtained with the regularization method. In our study, the minimum value of the classic Akaike information criterion (AIC) [30] was used to determine the optimal SNR value. Optimality of other parameters (HWS, TA and TBP) was determined based on the manual evaluation of spectra processing quality.

SNR parameter

The optimal SNR value was determined using the Akaike criterion of the LASSO classification models. For that we made a combination of SNR, TA and TBP values, pre-processed the mass spectra, constructed the matrix of intensities, and then trained the LASSO model using the matrix and the patient's diagnosis as the training data. Training of models involved 5/10-fold cross-validation, and the best model was selected based on the Accuracy metric. The parameter combinations were made of value sets:

SNR:={1.5, 2}
TA = TBP:= {20, 200, 2000}

The combination of parameters, with which the resulting model had the lowest AIC value, was named optimal. The optimal parameter values are provided in Table 1.

To prevent the emergence of negative noise intensities in the scan, 100 nulls were added to the set of points (M/Z, Intensity) on the left and on the right. As a result, the noise signal was evaluated in the broader range of M/Z values with a constant number of significant peaks in the spectrum.

Table 1. Optimal SNR values, which correspond to the LASSO models with minimal AIC values

Scanning mode	SNR	TA = TBP, ppm
Negative, High, 120–2000	1.5	20
Negative, High, 500–1000	2	2000
Negative, Low, 120–2000	1.5	20
Negative, Low, 500–1000	2	2000
Positive, High, 120–2000	1.5	2000
Positive, High, 500–1000	2	2000
Positive, Low, 120–2000	1.5	20
Positive, Low, 500–1000	2	2000

HWS, TA, TBP parameters

Optimality of the HWS, TA and TBP parameters was determined by manual evaluation of spectra processing quality. The interactive Shiny application Mass-Spectrum Observer allowing one to explore, how the spectrum shape, peak positions and characteristics of the intensity matrix of certain mass scan change with changing values of these parameters, was developed for this purpose. The application source code is available from GitHub repository [31], and the application demo version is available from the open access library of Shiny applications [32]. The screen-captured images of the application are provided in Fig. 2 and 3.

The lists of possible HWS, TA and TBP values were determined, and the mass spectrometry data pre-processing procedures were applied to each combination of these values in order to obtain separate matrices of intensities for each ion acquisition mode. The TBP parameter was proportional to the TA parameter with three possible proportionality coefficient values. The lists of parameter values are provided in Table 2.

The number of columns corresponding to the total number of peaks obtained from the mass scan profiles was determined for each matrix of intensities. Furthermore, when constructing the intensity matrix, we determined the number of peaks located close to each other in the resulting spectra. When the distance between peaks was smaller than two instrument resolutions during detection of ions in this mode, the peaks were considered as probably duplicate. Such peaks can emerge during conversion of the scan profiles into the sets of individual peaks, for example, within the same scan at too low HWS values, with the result that the intensity spike that is relatively broad on the m/z scale is represented by several spectral peaks, or in the scans of the same file at low TBP values, due to which the algorithm cannot compile the list of identical peaks from different scans. The duplicate peaks were determined within the same scan, in all scans of the same tissue specimen sample used for mass spectrometry analysis, and among all peaks of the intensity matrix. Peak duplication was defined based on the mass spectrometer resolution in this ion acquisition mode; the value of 800 at m/z = 400 was selected for the low-resolution mode, the value of 30,000 at m/z = 400 was selected for the high-resolution mode.

The reference HWS, TA and TBP values that were later subjected to manual evaluation performed using Mass-Spectrum Observer were determined based on the changes

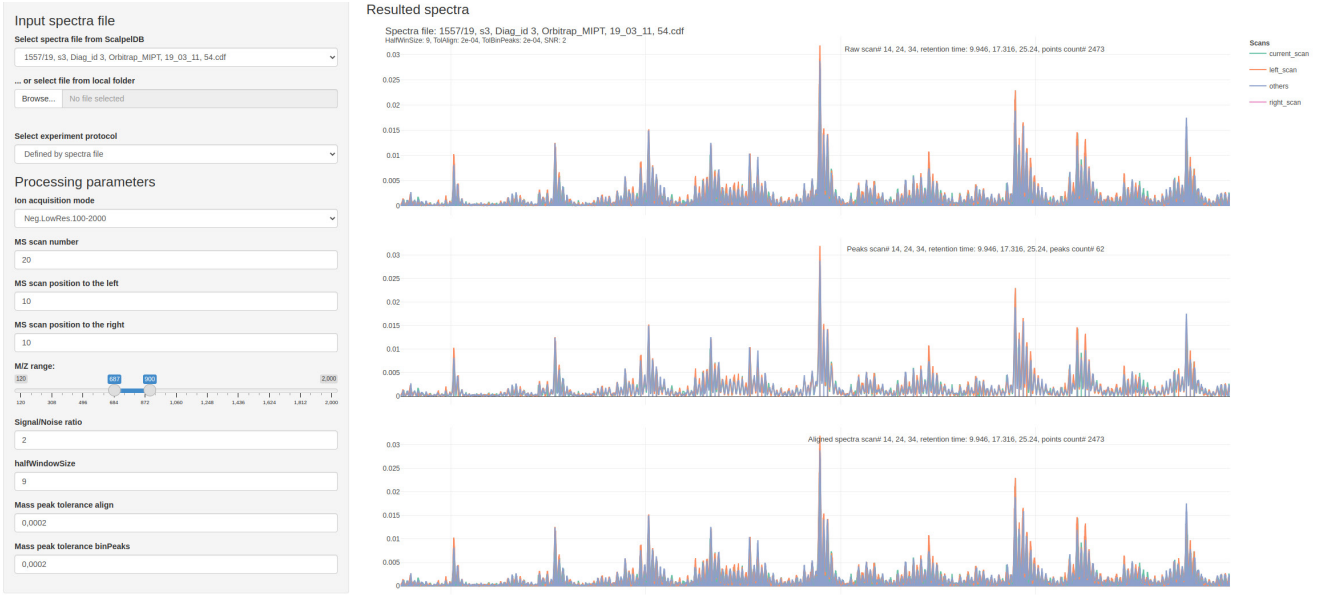

Fig. 2. Screen-captured image of the Mass-Spectrum Observer application window with the spectrum pre-processing parameter control panel

Table 2. Possible HWS, TA, and TBP values

Parameter	Values for high resolution	Values for low resolution
HWS	{3, 5, 7}	{7, 9, 11, 13, 15, 17, 19}
TA, ppm	{1, 20.8, 40.6, 60.4, 80.2, 100, 208, 406, 604, 802, $1 \cdot 10^3$}	{100, 325, 550, 775, $1 \cdot 10^3$}
TBP = m·TA	m := {0.1, 1, 10}	

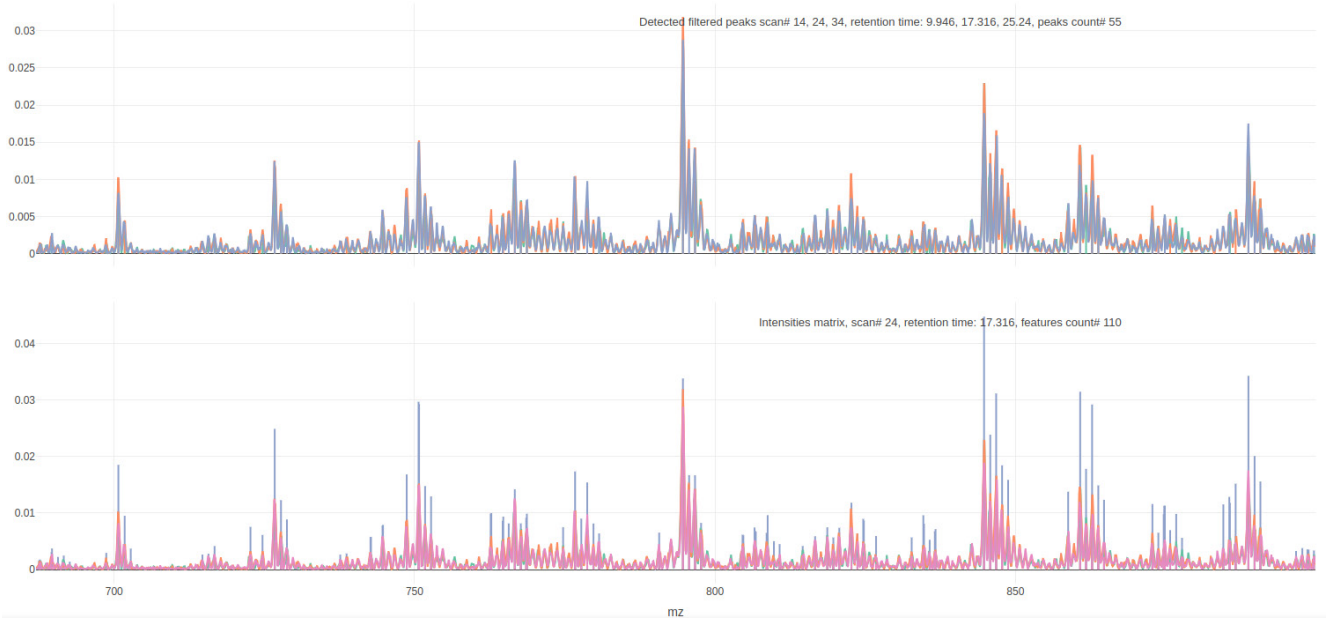

Fig. 3. Screen-captured of the Mass-Spectrum Observer application window with the plots corresponding to the spectra yielded after applying the pre-processing procedure

in these four indicators in accordance with the processing parameters. The manual evaluation results are provided in Table 3.

DISCUSSION

The findings show a close relationship between the ambient ionization mass spectrometry data pre-processing parameters and the quality of acquired spectra. The SNR parameter makes it possible to reduce the number of peaks in the resulting spectrum. However, attention should be paid to the presence of the negative estimate of noise signal values that may occur in the border spectral regions as an artifact. When detecting peaks in the profile, the noise estimate is used to determine peak intensity in this region of the profile, so negative noise can result in the emergence of the excessive number of peaks in the spectrum. This may not matter much in case of ion detection in the broad M/Z range (for example, 120–2000), but may be significant for the narrow range of 500–1000. In some cases, it is possible to eliminate such artifacts by fine-tuning the Super Smoother method (for example, by changing the smoothness degree during approximation or by narrowing the profile region, for which noise estimation is performed). However, these methods can yield different results for each particular mass scan, therefore the method of false dataset expansion was selected as a more sustainable method to eliminate negative values.

The HWS, TA and TBP values should be selected based primarily on the instrument resolution. The increase in half window size during the profile conversion into the intensity matrix enables elimination of artifact and duplicate peaks on the one hand (Fig. 4), but on the other hand the too high values of this parameter lead to exclusion of significant peaks from the subsequent analysis (Fig. 5). The values of peak position tolerance at alignment and detection are also closely related to the half window size and, therefore, to resolution, as well as to other mass spectrometer features resulting from the mass drift and the signal digitization methods. Furthermore, the TBP value should not be less than the TA value, since such configuration of values always results in the increase in the average number of possible duplicate peaks. This is due to the fact that the algorithm does not have enough tolerance for shift of identical peaks in different scans to eliminate duplicate peaks even after alignment of all scans relative to the scan with the highest ion current. It should be also noted that changing the width of the range without changing resolution and polarity of the detected ions has no significant effect on the parameter values, which is considered the expected result.

CONCLUSIONS

We developed a universal approach to determining the optimal parameter values for pre-processing of the data acquired by ambient ionization MS. The use of this approach was demonstrated on the data acquired by assessing human brain tissue samples using the Thermo LTQ XL Orbitrap ETD mass spectrometer. The approach developed can be used to determine the optimal parameter values for pre-processing

Table 3. Optimal HWS, TA and TBP values acquired by manual evaluation

Ion asquisition mode	TA, ppm	TBP, ppm	HWS
Negative, High, 120–2000	40.6	40.6	3
Negative, High, 500–1000	60.4	60.4	3
Negative, Low, 120–2000	775	7.75×10^3	13
Negative, Low, 500–1000	1×10^3	1×10^3	13
Positive, High, 120–2000	60.4	60.4	3
Positive, High, 500–1000	60.4	60.4	3
Positive, Low, 120–2000	1×10^3	1×10^4	13
Positive, Low, 500–1000	1×10^3	1×10^4	13

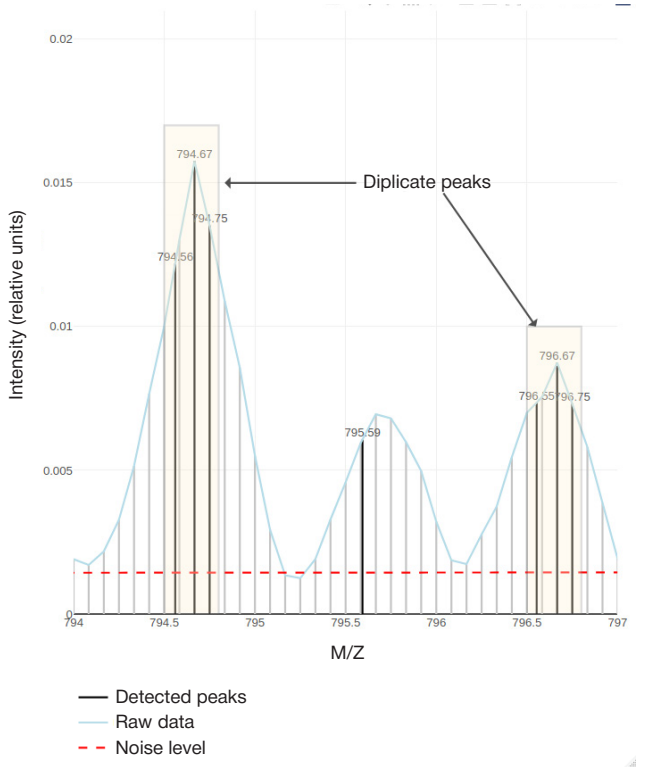

Fig. 4. Determining peak positions. The emergence of peaks, the distance between which in the wide-range low-resolution mass scan of negative ions obtained at suboptimal processing parameter values is less than two resolutions of the instrument in this ion detection mode (duplicate peaks)

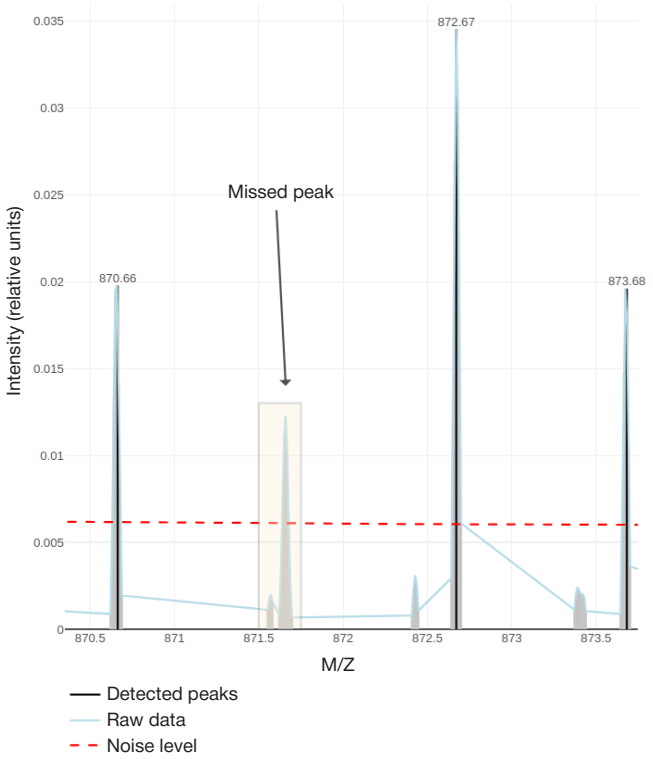

Fig. 5. Determining peak positions. A missed significant peak in the narrow-range high-resolution mass scan of negative ions obtained at suboptimal processing parameter values

of the data acquired when assessing samples of other types using other mass spectrometry equipment. The findings show that it is necessary to thoroughly adjust the mass spectrometry data processing parameters when using ambient ionization MS in the clinics as the faster and more affordable alternative to conventional intraoperative monitoring methods. Parameters have to be determined considering the mass spectrometer and research conditions. In particular, the SNR parameter determining the number of peaks in the resulting spectra should be selected based on the assessed tissue type and ionization method, while the value of 1.5–2 can be considered the lower limit. When performing scan profile alignment and peak detection, the half window size (HWS) and scan modification tolerance (TA) should be selected in accordance with the resolution of the mass spectrometer used, and the tolerance for spectra peak alignment (TBP) should not be lower than the TA value. Both machine learning methods and manual evaluation of the quality of acquired spectra can be used to choose optimal values of these parameters from several options.

References

1. Young RM, Jamshidi A, Davis G, Sherman JH. Current trends in the surgical management and treatment of adult glioblastoma. Ann Transl Med 2015: 1–15. https://doi.org/10.3978/j.issn.2305-5839.2015.05.10.
2. Chanbour H, Chotai S. Review of intraoperative adjuncts for maximal safe resection of gliomas and its impact on outcomes. Cancers. 2022; 14: 5705. Available from: https://doi.org/10.3390/cancers14225705.
3. Pekov SI, Bormotov DS, Nikitin PV, Sorokin AA, Shurkhay VA, Eliferov VA, et al. Rapid estimation of tumor cell percentage in brain tissue biopsy samples using inline cartridge extraction mass spectrometry. Anal Bioanal Chem. 2021; 413: 2913–22. Available from: https://doi.org/10.1007/s00216-021-03220-y.
4. Eberlin LS, Norton I, Orringer D, Dunn IF, Liu X, Ide JL, et al. Ambient mass spectrometry for the intraoperative molecular diagnosis of human brain tumors. Proc Natl Acad Sci. 2013; 110: 1611–6. Available from: https://doi.org/10.1073/pnas.1215687110.
5. Hänel L, Kwiatkowski M, Heikaus L, Schlüter H. Mass spectrometry-based intraoperative tumor diagnostics. Future Sci OA. 2019; 5: FSO373. Available from: https://doi.org/10.4155/fsoa-2018-0087.
6. Li L-H, Hsieh H-Y, Hsu C-C. Clinical application of ambient ionization mass spectrometry. Mass Spectrom. 2017; 6: S0060–S0060. Available from: https://doi.org/10.5702/massspectrometry.S0060.
7. Huang M-Z, Yuan C-H, Cheng S-C, Cho Y-T, Shiea J. Ambient ionization mass spectrometry. Annu Rev Anal Chem. 2010; 3: 43–65. Available from: https://doi.org/10.1146/annurev.anchem.111808.073702.
8. Shi L, Habib A, Bi L, Hong H, Begum R, Wen L. Ambient Ionization Mass Spectrometry: Application and Prospective. Crit Rev Anal Chem. 2022: 1–50. Available from: https://doi.org/10.1080/10408347.2022.2124840.
9. Boiko DA, Kozlov KS, Burykina JV, Ilyushenkova VV, Ananikov VP. Fully automated unconstrained analysis of high-pesolution mass spectrometry data with nachine learning. J Am Chem Soc. 2022; 144: 14590–606. Available from: https://doi.org/10.1021/jacs.2c03631.
10. Liebal UW, Phan ANT, Sudhakar M, Raman K, Blank LM. Machine learning applications for mass spectrometry-based metabolomics. Metabolites. 2020; 10: 1–23. Available from: https://doi.org/10.3390/metabo10060243.
11. Piras C, Hale OJ, Reynolds CK, Jones AK (Barney), Taylor N, Morris M, et al. LAP-MALDI MS coupled with machine learning: an ambient mass spectrometry approach for high-throughput diagnostics. Chem Sci. 2022; 13: 1746–58. Available from: https://doi.org/10.1039/D1SC05171G.
12. Seddiki K, Saudemont P, Precioso F, Ogrinc N, Wisztorski M, Salzet M, et al. Cumulative learning enables convolutional neural network representations for small mass spectrometry

data classification. Nat Commun. 2020; 11. Available from: https://doi.org/10.1038/s41467-020-19354-z.
13. Huang YC, Chung HH, Dutkiewicz EP, Chen CL, Hsieh HY, Chen BR, et al. Predicting breast cancer by paper spray ion mobility spectrometry mass spectrometry and machine learning. Anal Chem. 2020; 92: 1653–7. Available from: https://doi.org/10.1021/acs.analchem.9b03966.
14. Iwano T, Yoshimura K, Inoue S, Odate T, Ogata K, Funatsu S, et al. Breast cancer diagnosis based on lipid profiling by probe electrospray ionization mass spectrometry. Br J Surg. 2020; 107: 632–5. Available from: https://doi.org/10.1002/bjs.11613.
15. Zhou M, Guan W, Walker LDE, Mezencev R, Benigno BB, Gray A, et al. Rapid mass spectrometric metabolic profiling of blood sera detects ovarian cancer with high accuracy. Cancer Epidemiol Biomarkers Prev. 2010; 19: 2262–71. Available from: https://doi.org/10.1158/1055-9965.EPI-10-0126.
16. Torp SH, Solheim O, Skjulsvik AJ. The WHO 2021 Classification of central nervous system tumours: a practical update on what neurosurgeons need to know — a minireview. Acta Neurochir (Wien). 2022; 164: 2453–64. Available from: https://doi.org/10.1007/s00701-022-05301-y.
17. Bormotov DS, Eliferov VA, Peregudova OV, Zavorotnyuk DS, Bocharov KV, Pekov SI, et al. Incorporation of a disposable ESI emitter into inline cartridge extraction mass spectrometry improves throughput and spectra stability. J Am Soc Mass Spectrom. 2023; 34: 119–22. Available from: https://doi.org/10.1021/jasms.2c00207.
18. Gibb S, Strimmer K. Maldiquant: A versatile R package for the analysis of mass spectrometry data. Bioinformatics. 2012; 28. Available from: https://doi.org/10.1093/bioinformatics/bts447.
19. Kuhn M. Building predictive models in R using the caret package. J Stat Softw. 2008; 28: 1–26. Available from: https://doi.org/10.18637/jss.v028.i05.
20. Friedman JH, Hastie T, Tibshirani R. Regularization paths for generalized linear models via coordinate descent. J Stat Softw. 2010; 33: 1–22. Available from: https://doi.org/10.18637/jss.v033.i01.
21. Wickham H. ggplot2: Elegant graphics for data analysis. Springer-Verlag, New York; 2016.
22. Rew R, Davis G, Emmerson S, Cormack C, Caron J, Pincus R, et al. Unidata NetCDF 1989. Available from: https://doi.org/10.5065/D6H70CW6.
23. Zavorotnyuk DS, Pekov SI, Sorokin AA, Bormotov DS, Levin N, Zhvansky E, et al. Lipid profiles of human brain tumors obtained by high-resolution negative mode ambient mass spectrometry. Data. 2021; 6: 1–7. Available from: https://doi.org/10.3390/data6120132.
24. Eberlin LS, Norton I, Dill AL, Golby AJ, Ligon KL, Santagata S, et al. Classifying human brain tumors by lipid imaging with mass spectrometry. Cancer Research. 2012; 72 (3): 645–54. Available from: https://doi.org/10.1158/0008-5472.can-11-2465.
25. Friedman JH. Smart user's guide. Stanford Univ CA, Laboratory for Computational Statistics; 1984.
26. Morris JS, Coombes KR, Koomen J, Baggerly KA, Kobayashi R. Feature extraction and quantification for mass spectrometry in biomedical applications using the mean spectrum. Bioinformatics. 2005; 21: 1764–75. Available from: https://doi.org/10.1093/bioinformatics/bti254.
27. Burnham KP, Anderson DR, editors. Model Selection and Multimodel Inference. New York, NY: Springer New York, 2004. Available from: https://doi.org/10.1007/b97636.
28. Gustafsson F, Hjalmarsson H. Twenty-one ML estimators for model selection. Automatica. 1995; 31: 1377–92. Available from: https://doi.org/10.1016/0005-1098(95)00058-5.
29. Shitikov VK, Mastitsky SE. Klassifikacija, regressija i drugie algoritmy Data Mining s ispol'zovaniem R. 2017. Dostupna po ssylke: https://github.com/ranalytics/data-mining. Russian.
30. Akaike H. A new look at the statistical model identification. IEEE Trans Autom Control. 1974; 19: 716–23. Available from: https://doi.org/10.1109/TAC.1974.1100705.
31. Zavorotnyuk DS. MS Spectrum observer repository. Available from: https://github.com/zdens/MS-Spectrum-Observer/releases/tag/1.0 (data obrashhenija: 29 fevralja 2024 g.).
32. Zavorotnyuk DS. MS spectrum observer Demo. Available from: https://zdens.shinyapps.io/ms-spectrum-observer (data obrashhenija: 29 fevralja 2024 g.).

Литература

1. Young RM, Jamshidi A, Davis G, Sherman JH. Current trends in the surgical management and treatment of adult glioblastoma. Ann Transl Med 2015: 1–15. https://doi.org/10.3978/j.issn.2305-5839.2015.05.10.
2. Chanbour H, Chotai S. Review of intraoperative adjuncts for maximal safe resection of gliomas and its impact on outcomes. Cancers. 2022; 14: 5705. Available from: https://doi.org/10.3390/cancers14225705.
3. Pekov SI, Bormotov DS, Nikitin PV, Sorokin AA, Shurkhay VA, Eliferov VA, et al. Rapid estimation of tumor cell percentage in brain tissue biopsy samples using inline cartridge extraction mass spectrometry. Anal Bioanal Chem. 2021; 413: 2913–22. Available from: https://doi.org/10.1007/s00216-021-03220-y.
4. Eberlin LS, Norton I, Orringer D, Dunn IF, Liu X, Ide JL, et al. Ambient mass spectrometry for the intraoperative molecular diagnosis of human brain tumors. Proc Natl Acad Sci. 2013; 110: 1611–6. Available from: https://doi.org/10.1073/pnas.1215687110.
5. Hänel L, Kwiatkowski M, Heikaus L, Schlüter H. Mass spectrometry-based intraoperative tumor diagnostics. Future Sci OA. 2019; 5: FSO373. Available from: https://doi.org/10.4155/fsoa-2018-0087.
6. Li L-H, Hsieh H-Y, Hsu C-C. Clinical application of ambient ionization mass spectrometry. Mass Spectrom. 2017; 6: S0060–S0060. Available from: https://doi.org/10.5702/massspectrometry.S0060.
7. Huang M-Z, Yuan C-H, Cheng S-C, Cho Y-T, Shiea J. Ambient ionization mass spectrometry. Annu Rev Anal Chem. 2010; 3: 43–65. Available from: https://doi.org/10.1146/annurev.anchem.111808.073702.
8. Shi L, Habib A, Bi L, Hong H, Begum R, Wen L. Ambient Ionization Mass Spectrometry: Application and Prospective. Crit Rev Anal Chem. 2022: 1–50. Available from: https://doi.org/10.1080/10408347.2022.2124840.
9. Boiko DA, Kozlov KS, Burykina JV, Ilyushenkova VV, Ananikov VP. Fully automated unconstrained analysis of high-pesolution mass spectrometry data with nachine learning. J Am Chem Soc. 2022; 144: 14590–606. Available from: https://doi.org/10.1021/jacs.2c03631.
10. Liebal UW, Phan ANT, Sudhakar M, Raman K, Blank LM. Machine learning applications for mass spectrometry-based metabolomics. Metabolites. 2020; 10: 1–23. Available from: https://doi.org/10.3390/metabo10060243.
11. Piras C, Hale OJ, Reynolds CK, Jones AK (Barney), Taylor N, Morris M, et al. LAP-MALDI MS coupled with machine learning: an ambient mass spectrometry approach for high-throughput diagnostics. Chem Sci. 2022; 13: 1746–58. Available from: https://doi.org/10.1039/D1SC05171G.
12. Seddiki K, Saudemont P, Precioso F, Ogrinc N, Wisztorski M, Salzet M, et al. Cumulative learning enables convolutional neural network representations for small mass spectrometry data classification. Nat Commun. 2020; 11. Available from: https://doi.org/10.1038/s41467-020-19354-z.
13. Huang YC, Chung HH, Dutkiewicz EP, Chen CL, Hsieh HY, Chen BR, et al. Predicting breast cancer by paper spray ion mobility spectrometry mass spectrometry and machine learning. Anal Chem. 2020; 92: 1653–7. Available from: https://doi.org/10.1021/acs.analchem.9b03966.
14. Iwano T, Yoshimura K, Inoue S, Odate T, Ogata K, Funatsu S, et al. Breast cancer diagnosis based on lipid profiling by probe electrospray ionization mass spectrometry. Br J Surg. 2020; 107: 632–5. Available from: https://doi.org/10.1002/bjs.11613.
15. Zhou M, Guan W, Walker LDE, Mezencev R, Benigno BB, Gray A, et al. Rapid mass spectrometric metabolic profiling of blood sera detects ovarian cancer with high accuracy. Cancer Epidemiol Biomarkers Prev. 2010; 19: 2262–71. Available from: https://doi.org/10.1158/1055-9965.EPI-10-0126.
16. Torp SH, Solheim O, Skjulsvik AJ. The WHO 2021 Classification of central nervous system tumours: a practical update on what neurosurgeons need to know — a minireview. Acta Neurochir (Wien). 2022; 164: 2453–64. Available from: https://doi.org/10.1007/s00701-022-05301-y.
17. Bormotov DS, Eliferov VA, Peregudova OV, Zavorotnyuk DS, Bocharov KV, Pekov SI, et al. Incorporation of a disposable ESI emitter into inline cartridge extraction mass spectrometry improves throughput and spectra stability. J Am Soc Mass Spectrom. 2023; 34:

119–22. Available from: https://doi.org/10.1021/jasms.2c00207.
18. Gibb S, Strimmer K. Maldiquant: A versatile R package for the analysis of mass spectrometry data. Bioinformatics. 2012; 28. Available from: https://doi.org/10.1093/bioinformatics/bts447.
19. Kuhn M. Building predictive models in R using the caret package. J Stat Softw. 2008; 28: 1–26. Available from: https://doi.org/10.18637/jss.v028.i05.
20. Friedman JH, Hastie T, Tibshirani R. Regularization paths for generalized linear models via coordinate descent. J Stat Softw. 2010; 33: 1–22. Available from: https://doi.org/10.18637/jss.v033.i01.
21. Wickham H. ggplot2: Elegant graphics for data analysis. Springer-Verlag, New York; 2016.
22. Rew R, Davis G, Emmerson S, Cormack C, Caron J, Pincus R, et al. Unidata NetCDF 1989. Available from: https://doi.org/10.5065/D6H70CW6.
23. Zavorotnyuk DS, Pekov SI, Sorokin AA, Bormotov DS, Levin N, Zhvansky E, et al. Lipid profiles of human brain tumors obtained by high-resolution negative mode ambient mass spectrometry. Data. 2021; 6: 1–7. Available from: https://doi.org/10.3390/data6120132.
24. Eberlin LS, Norton I, Dill AL, Golby AJ, Ligon KL, Santagata S, et al. Classifying human brain tumors by lipid imaging with mass spectrometry. Cancer Research. 2012; 72 (3): 645–54. Available from: https://doi.org/10.1158/0008-5472.can-11-2465.
25. Friedman JH. Smart user's guide. Stanford Univ CA, Laboratory for Computational Statistics; 1984.
26. Morris JS, Coombes KR, Koomen J, Baggerly KA, Kobayashi R. Feature extraction and quantification for mass spectrometry in biomedical applications using the mean spectrum. Bioinformatics. 2005; 21: 1764–75. Available from: https://doi.org/10.1093/bioinformatics/bti254.
27. Burnham KP, Anderson DR, editors. Model Selection and Multimodel Inference. New York, NY: Springer New York, 2004. Available from: https://doi.org/10.1007/b97636.
28. Gustafsson F, Hjalmarsson H. Twenty-one ML estimators for model selection. Automatica. 1995; 31: 1377–92. Available from: https://doi.org/10.1016/0005-1098(95)00058-5.
29. Шитиков В. К., Мастицкий С. Э. Классификация, регрессия и другие алгоритмы Data Mining с использованием R. 2017. Доступна по ссылке: https://github.com/ranalytics/data-mining.
30. Akaike H. A new look at the statistical model identification. IEEE Trans Autom Control. 1974; 19: 716–23. Available from: https://doi.org/10.1109/TAC.1974.1100705.
31. Zavorotnyuk DS. MS Spectrum observer repository. Available from: https://github.com/zdens/MS-Spectrum-Observer/releases/tag/1.0 (дата обращения: 29 февраля 2024 г.).
32. Zavorotnyuk DS. MS spectrum observer Demo. Available from: https://zdens.shinyapps.io/ms-spectrum-observer (дата обращения: 29 февраля 2024 г.).

SPATIAL ORIENTATION PARAMETERS OF FACE IMAGE RECOGNITION AS PREDICTORS OF LIVER FAILURE SYMPTOMS IN ADOLESCENTS

Nikishina VB, Petrash EA ✉, Engel EYa, Simonenko IA, Shagina ED

Pirogov Russian National Research Medical University, Moscow, Russia

Functional assessment of higher mental functions in case of intoxication or during treatment will make it possible to identify predictors of the symptoms of hepatic encephalopathy associated with portal hypertension. The study was aimed to determine the diagnostic predictors of the emergence of the earliest symptoms of hepatic encephalopathy in adolescents with portal hypertension. The study involved 60 adolescents aged 13–17 years: 28 males, 32 females. The experimental group included 30 adolescents with the diagnosis K76.6 Portal hypertension, unspecified form. The control group included 30 adolescents with normal somatic status, who had no mental disorders, traumatic brain injuries or severe infectious diseases of the brain (based on the records of the annual check-up). The studied groups were matched by sex, age, and social status. The proprietary method, Tobii EyeX hardware and software system (GazeControl software), and Cambridge Face Memory Test for Children (CFMT-C) were used. It has been found that recognition of single face images, multiple face images, and multiple face images camouflaged with noise by adolescents with portal hypertension is associated with the greater efforts (manifested in the increased number and duration of gaze fixations), than recognition of the above by adolescents with normal somatic status. The accuracy of recognition of single face images, multiple face images, and multiple face images camouflaged with noise shown by adolescents with portal hypertension experiencing the toxic effects associated with manifestations of hepatic encephalopathy is significantly reduced compared to that shown by adolescents with normal somatic status. The results obtained can be considered as the diagnostic predictors allowing one to trace the changes in the hepatic encephalopathy severity at various stages of treatment (including after surgical intervention).

Keywords: face image recognition, portal hypertension, hepatic encephalopathy, oculomotor reactions, gaze fixation

Author contribution: the authors contributed to the study and manuscript writing equally.

Compliance with ethical standards: the study was approved by the Ethics Committee of the Pirogov Russian National Research Medical University (protocol № 229 dated 15 May 2023) and conducted in accordance with the requirements of the Fundamentals of the Legislation on the Protection of Citizens' Health; all participants submitted the informed consent to examination.

✉ **Correspondence should be addressed:** Ekaterina A. Petrash
Ostrovityanova, 1, Moscow, 117997, Russia; petrash@mail.ru

Received: 11.03.2024 **Accepted:** 17.04.2024 **Published online:** 30.04.2024

DOI: 10.24075/brsmu.2024.015

ПРОСТРАНСТВЕННО-ОРИЕНТАЦИОННЫЕ ПАРАМЕТРЫ УЗНАВАНИЯ ИЗОБРАЖЕНИЙ ЛИЦ КАК ПРЕДИКТОРЫ СИМПТОМОВ ПЕЧЕНОЧНОЙ НЕДОСТАТОЧНОСТИ У ПОДРОСТКОВ

В. Б. Никишина, Е. А. Петраш ✉, Е. Я. Энгель, И. А. Симоненко, Е. Д. Шагина

Российский национальный исследовательский медицинский университет имени Н. И. Пирогова, Москва, Россия

Функциональная оценка изменений высших психических функций при интоксикационном воздействии, а также в процессе лечения позволит выявить предикторы симптомов печеночной энцефалопатии при портальной гипертензии. Цель работы — определить диагностические предикторы выявления наиболее ранних симптомов печеночной энцефалопатии у подростков с портальной гипертензией. В исследовании участвовали 60 подростков 13–17 лет, 28 человек — мужского пола, 32 человека — женского пола. В экспериментальную группу вошли 30 подростков с диагнозом K76.6 «Портальная гипертензия» без уточнения формы. В контрольную группу вошли 30 подростков с нормативным соматическим статусом без психических, церебрально-травматических и тяжелых инфекционных заболеваний головного мозга (по результатам заключений ежегодной диспансеризации). Исследовательские группы уравнивали по полу, возрасту и социальному статусу. Использовали авторскую методику и программно-аппаратный комплекс Tobii EyeX (ПО «GazeControl»), а также Кембриджский тест запоминания лиц для детей (CFMT-C). Установлено, что узнавание единичных, множественных, множественных зашумленных изображений лиц подростками с портальной гипертензией сопровождается большими усилиями (проявляющимися в увеличении как числа фиксаций взгляда, так и их продолжительности), чем подростками с нормативным соматическим статусом. Точность узнавания единичных, множественных и множественных зашумленных изображений лиц при токсическом влиянии при проявлении печеночной энцефалопатии у подростков с портальной гипертензией значимо снижается по сравнению с подростками с нормативным соматическим статусом. Полученные результаты можно рассматривать в качестве диагностических предикторов, позволяющих отслеживать изменение выраженности симптомов печеночной энцефалопатии на разных этапах лечения (в том числе после оперативного вмешательства).

Ключевые слова: узнавание изображений лиц, портальная гипертензия, печеночная энцефалопатия, глазодвигательные реакции, фиксации взгляда

Вклад авторов: все авторы внесли равнозначный вклад в работу и написание статьи.

Соблюдение этических стандартов: исследование одобрено этическим комитетом РНИМУ им. Н. И. Пирогова (протокол № 229 от 15 мая 2023 г.), проведено в соответствии с требованиями Основ законодательства «Об охране здоровья граждан»; все участники подписали добровольное информированное согласие на обследование.

✉ **Для корреспонденции:** Екатерина Анатольевна Петраш
ул. Островитянова, д. 1, г. Москва, 117997, Россия; petrash@mail.ru

Статья получена: 11.03.2024 **Статья принята к печати:** 17.04.2024 **Опубликована онлайн:** 30.04.2024

DOI: 10.24075/vrgmu.2024.015

The search for predictors of the symptoms of hepatic encephalopathy associated with portal hypertension requires functional assessment of the changes of higher mental functions under conditions of intoxication and in various phases of treatment (including after surgical treatment).

Visual perception represents a combination of the processes underlying construction of a visual image of the surrounding environment. It consists of various structural components: randomness, focus, hand-eye coordination, visual evaluation skills, analytical and synthetic activity of the visual analyzer,

perception volume and constance. Formation of the attention, speech, intelligence functions depends on the visual perception development. Furthermore, visual gnosis can be divided into the following subtypes: visual object, simultaneous, color, and facial gnosis. In turn, facial gnosis reflects the process of face identification.

The changes occurring in this system under the influence of morphological and other factors are a significant indicator and, at the same time, the challenge of the functional rehabilitation training. A number of somatic disorders that seem to be nonspecific for brain disorders are associated with the prominent neurotoxic effects affecting the function of brain structures.

When solving the problem of the gnostic feature specification in adolescents with hepatic encephalopathy, we assessed the prevalence of liver diseases in Russia and found out that 950 individuals per 100,000 population were susceptible to the diseases of this class in 2016 [1], and 60–70% patients with chronic liver diseases developed hepatic encephalopathy of varying severity [2]. It should be also noted that, according to the data obtained in 2007–2016 by comparing children under the age of 14 years with the general population in Russia, the pediatric incidence of some liver diseases exceeded the adult incidence 1.6-fold [3]. Furthermore, the development of liver failure is associated with the generalized intoxication affecting the nervous system [4] that involves the posterior association area [5] responsible for realization of the face recognition function, one of the periods of intense development and differentiation of which is the age between 15–16 years [6].

When assessing the research interest within the framework of the study of face recognition and the spatial orientation factors affecting the process, we performed bibliometric analysis using the eLibrary scientometric database. The depth of analysis was 10 years (2013–2023). The findings suggest insufficient study of the subject: the number of publications reported for the specified period varies between 1–3 scientific papers per year. Thus, it becomes clear that there is a need to study the factor of the spatial orientation characteristics of face images during face image recognition.

Modern domestic concepts of the higher mental function development patterns, specifics of age development and ontogenesis of the psyche [7, 8], perceptual processing patterns, visual perception dynamics and visual phenomena associated with oculomotor activity [9, 10], as well as conceptual provisions and empirical studies of the visual spatial gnosis impairment associated with hepatic encephalopathy [11, 12, 13–16] provided the theoretical and methodological basis for the study.

Visual gnosis represents the process involving reception of the featured visual stimuli that pass through the perceptual filters organized in the existing structures and templates and are later interpreted based on the earlier experience. Human face image is a complex social object. The oculomotor activity associated with face image perception demonstrates a number of specific patterns related to the distribution of gaze fixations depending on the goals of the face photo perception and facial expression. The routes of the gaze associated with face image perception are cyclic and regular [9, 10, 17, 18].

Portal hypertension (K76.6 according to ICD-10) is a syndrome of blood pressure increase in the portal venous system caused by impaired blood flow in the portal vessels, hepatic veins and the inferior vena cava; along with other manifestations (splenomegaly, varicose veins in the esophagus and stomach, ascites), it is associated with the hepatic encephalopathy syndrome. Impaired liver function also results in the toxic effects on the central nervous system (CNS, brain) due to the generalized ammonia and mercaptan intoxication. The effects of intoxication result in the glial edema, which, in turn, affect the neurodynamics (impaired nerve impulse transmission and depression of the CNS function in general) (Fig. 1).

Therefore, the functional impairment resulting from intoxication leads to the difficulty in realization of higher mental functions. Hepatic encephalopathy as a symptom of liver failure (acute or chronic) that belongs to neuropsychiatric syndromes usually represents a potentially reversible brain function impairment manifested in psychomotor, intellectual, emotional and behavioral disorders. Impairment of the visual spatial functions, specifically face image recognition (facial gnosis), is among the earliest manifestations observed during the period, when the other symptoms are subtle. Identification of the above requires using specific psychometric methods.

The study was aimed to assess the spatial orientation parameters of face image recognition in adolescents with portal hypertension.

METHODS

The total size of the research sample was 60 adolescents aged 13–17 years (according to the WHO ICD), the average age was 14.7 ± 1.54 years; among them 28 were males, 32 were females. The experimental group (EG) included 30 adolescents (14 males, 16 females) with the diagnosis of K76.6 Portal hypertension (ICD-10) established by gastroenterologist, among them 16.7% had extrahepatic forms of hepatic encephalopathy, 83.3% had intrahepatic forms of hepatic encephalopathy. In the vast majority of cases (90% of patients), liver failure resulted from the liver disease associated with viral infection. The other subjects (three individuals) had congenital liver failure. The control group (CG) included 30 adolescents (14 males, 16 females) with normal somatic status, who had no mental disorders, traumatic brain injuries or severe infectious diseases of the brain (based on the records of the annual check-up available in May 2023). The studied groups were matched by sex, age, and social status.

Two research method types were used: empirical methods and methods of quantitative and qualitative data processing.

Empirical methods included the following: clinical structured conversation method; archival method involving the analysis of medical history data; method of functional neuropsychological tests represented by the Cambridge Face Memory Test [13]; test for lateralization of higher mental functions.

The visual gnosis characteristics were assessed using the Cambridge Face Memory Test for Children (CFMT-C) [19]. This test represents an adaptation of the initial Cambridge Face Memory Test version designed for adults. The face stimuli were chosen from those used in the CFMT version for adults. The faces represented grayscale images of the children, who posed with the neutral facial expression. Each face was photographed from the same three angles in the same lighting conditions and cropped to remove the hairline and all facial defects. The presentation procedure consisted of five stages.

Stage 1

The adolescents were offered to sequentially memorize six faces in three positions with the limited presentation duration (3 s); then each of three images was displayed together with two faces (distractions), and the adolescents had to choose the face they had just seen. Each correct answer of the subject was assigned one point (the maximum score was 18).

Stage 2

At this stage the adolescents first looked at one screenshot showing six front views of the target faces for 20 s, then they

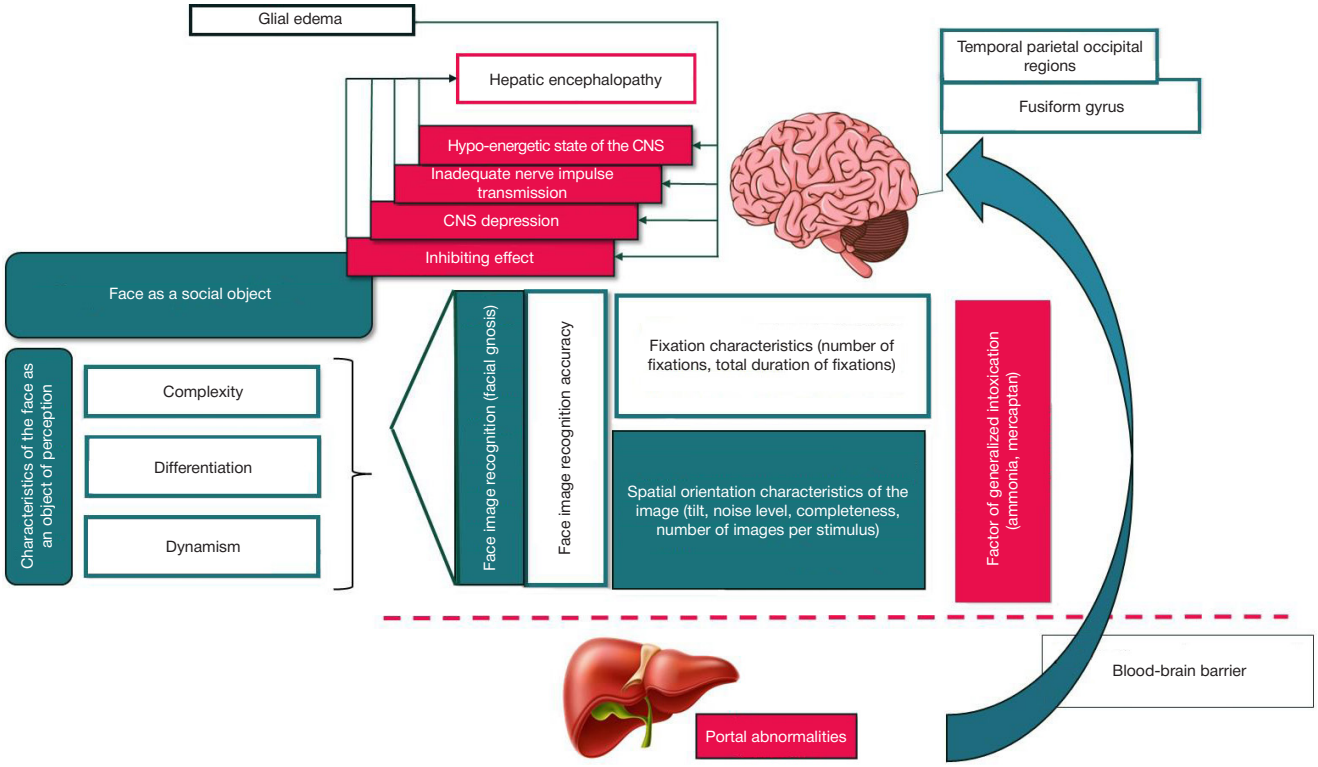

Fig. 1. Scheme of the conceptual model for assessment of the spatial orientation parameters of face image recognition in adolescents with portal hypertension

completed 30 tasks, each of which involved looking at one target face and two distraction faces; the adolescents decided which of the three faces was one of the six target faces they had been offered to memorize. Each correct answer of the subject was assigned one point (the maximum score was 30).

Stage 3

At this stage the adolescents also first looked at one screenshot showing six front views of the target faces for 20 s and then completed 24 tasks, each of which involved looking at one target face and two distraction faces (it should be noted that the images of both target and distraction were camouflaged using the preset Gaussian noise value, which made the process of decision making more difficult than at the 2nd stage). Each correct answer of the subject was assigned one point (the maximum score was 34).

Stage 4

The adolescents had to identify the appropriate entire image, displayed together with two distraction faces during each presentation, by a fragment; the area of the fragment was increased as the adolescents went through the test (from one fragment out of 12 to 12 fragments out of 12).

Stage 5

At the final stage, adolescents were offered to sequentially memorize 10 images of the faces photographed from different angles, each of the faces was later displayed together with two distraction faces, and the adolescents had to choose the face they had just seen. Each correct answer of the subject was assigned one point (the maximum score was 10).

Eventually, assessment was performed based on the following parameters: recognition of single face images; recognition of six face images; recognition of six face images camouflaged with noise; recognition of fragmented face images; recognition of single inverted face images (Fig. 2).

The GP3 HD eye tracker (Tobii Eye; Sweden) was used to assess the characteristics of the subjects' oculomotor responses when they passed the face image recognition test. This model of the device based on the machine vision sensor and image processor is used for eye tracking. The model has the following characteristics: 0.5–1.0 degree of visual angle accuracy; 150 Hz operation frequency; 5–9-point calibration; the range of free head movement relative to the calibrated position within 35 cm (horizontal), 22 cm (vertical), and at least 15 cm on each side. The following parameters were analyzed: total number of fixations on the stimulus image; number of fixations on the upper half of the stimulus image; number of fixations on the lower half of the stimulus image; number of fixations on the left half of the stimulus image; number of fixations on the right half of the stimulus image; number of fixations on the zone between eyes and nose of the stimulus image; number of fixations on the zone between mouth and nose of the stimulus image; number of fixations on the area within the face oval of the stimulus image; number of fixations outside the face oval of the stimulus image; total duration of fixations on the stimulus image.

The lateralization profile of functions was assessed using the following tests for motor and sensory preferences [3; 7]: hand lock test — the finger of the dominant hand is on top; Napoleon pose — the finger of the dominant hand is on top; "handset" test — determining the hand that will reach for the handset and the ear to which the handset will be put; "look-through-the-telescope" test — determining the hand that will reach for the telescope and the eye to which the telescope will be put.

The descriptive, comparative and multivariate statistical methods were used for quantitative and qualitative data processing. Mathematical analysis and data interpretation were performed using the descriptive statistics. The nonparametric Mann–Whitney U test ($p < 0.05$) for independent samples was used for comparative analysis of the ability to recognize static face images based on the fixation characteristics of oculomotor responses and the characteristics of face image recognition depending on the spatial orientation characteristics (image tilt, completeness) in the group of patients with portal hypertension and the group of individuals with normal somatic status (since the distributions of studied traits were non-normal). To determine

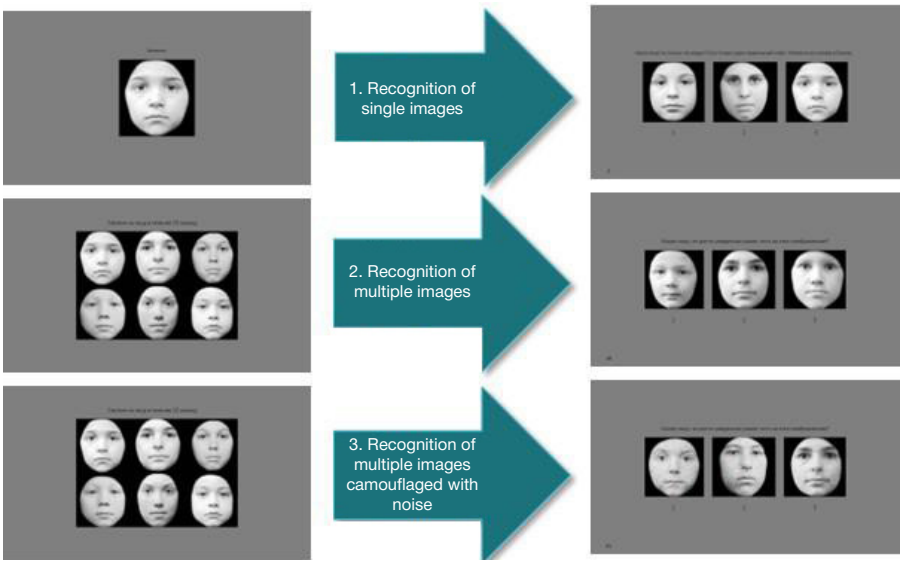

Fig. 2. Examples of the stimulus images used at the stages of the face recognition ability assessment

the factor structure of the static face image recognition based on the fixation characteristics of oculomotor responses and the face image recognition accuracy depending on the spatial orientation characteristics, we performed factor analysis with varimax rotation in order to determine the factor structure of the parameters of oculomotor responses associated with face image recognition considering their spatial orientation characteristics. Statistical processing was performed using the Statistica 13.0 software package (StatSoft; USA).

The study design is provided in Fig. 3.

RESULTS

Assessment of the facial gnosis characteristics using CFMT-C in the group of adolescents with portal hypertension and the group of adolescents with normal somatic status showed that the recognition accuracy observed when presenting single images, multiple images, and multiple images camouflaged with noise demonstrated a significant downward trend in adolescents with portal hypertension relative to appropriate scores of adolescents with normal somatic status (Table).

We revealed significant differences in the facial gnosis scores obtained when performing the test for recognition of single face images between the group of adolescent patients with portal hypertension and the group of adolescents with normal somatic status (*p = 0.001),

We also revealed differences in the facial gnosis scores obtained when performing the test for recognition of multiple face images (*p = 0.012) and the test for recognition of multiple face images camouflaged with noise (*p = 0.003) between the group of adolescent patients with portal hypertension and the group of adolescents with normal somatic status.

The facial gnosis scores obtained upon presentation of a single image (recognition accuracy), multiple face images (recognition accuracy) and multiple face images camouflaged with noise (recognition accuracy) show a significant downward trend in patients with portal hypertension relative to appropriate scores of adolescents with normal somatic status.

The next stage was assessment of the gaze fixation characteristics (total number of fixations; total duration of fixations; number of fixations on the upper and lower halves of face image; number of fixations on the right and left halves of face image; number of fixations on the zones between eyes and nose, mouth and nose; number of fixations on the areas within and outside the face oval of the image) on the presented stimulus images in the group of adolescents with

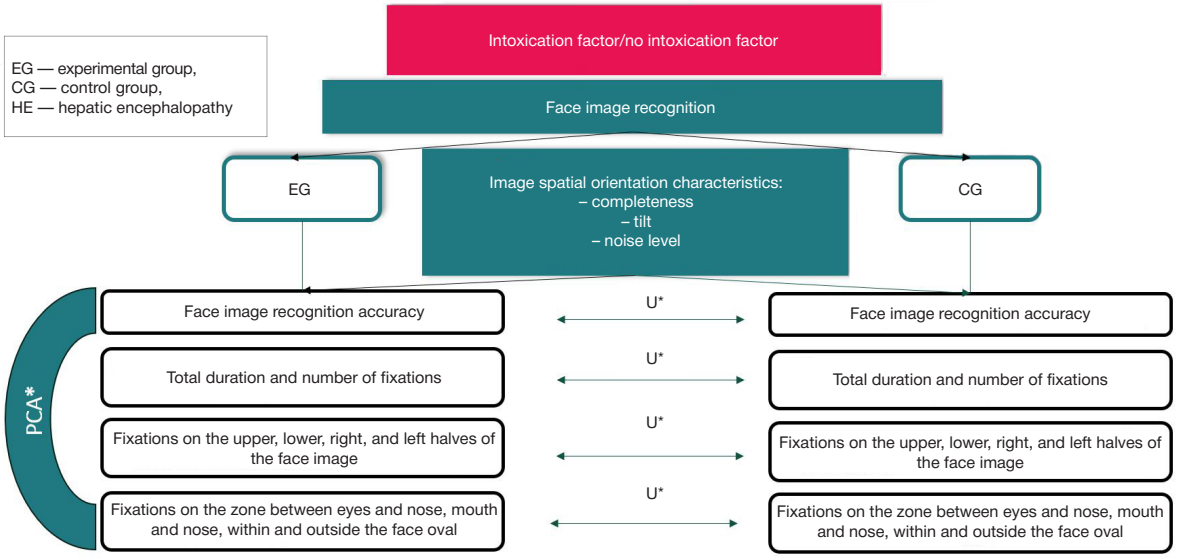

Fig. 3. Design of the study of the spatial orientational parameters of face image recognition in adolescents with portal hypertension

Table. Average face recognition accuracy values in adolescents with portal hypertension and normal somatic status

Tests	Mode (Mo)		Median (Me)		Mean ± standard deviation (M ± σ)	
	EG	CG	EG	CG	EG	CG
1	0.83 0.89 0.94	0.94	0.89	0.94	0.87 ± 0.09	0.93 ± 0.09
2	0.53 0.57 0.73	0.67	0.73	0.83	0.71 ± 0.07	0.79 ± 0.07
3	0.79	0.92	0.75	0.83	0.72 ± 0.06	0.76 ± 0.07
4	0.42	0.33	0.33	0.33	0.28 ± 0.02	0.26 ± 0.02
5	0.8	0.80 0.90 1.0	0.8	0.8	0.75 ± 0.08	0.78 ± 0.07

portal hypertension and the group of individuals with normal somatic status of the same age.

We revealed significant differences in the total number of fixations on the stimulus images obtained when performing tests for recognition of single face images (*p = 0.001), multiple face images (*p = 0.015), multiple face images camouflaged with noise (*p = 0.009) between the group of patients with portal hypertension and the group of adolescents with normal somatic status. We also revealed significant differences in the total duration of fixations obtained when performing tests for recognition of single face images (*p = 0.035), multiple face images camouflaged with noise (*p = 0.005), and single inverted face images (*p = 0.049) between the group of patients with portal hypertension and the group of adolescents with normal somatic status (Fig. 4).

The total number of fixations on the stimulus images obtained when presenting single face images, multiple face images, multiple face images camouflaged with noise shows a significant upward trend in the adolescent patients with portal hypertension relative to appropriate scores of adolescents with normal somatic status. The total duration of fixations on the stimulus images obtained when presenting single face images and multiple face images camouflaged with noise shows a significant upward trend in the adolescent patients with hepatic encephalopathy relative to appropriate scores of adolescents with normal somatic status. Upon presentation of single inverted images, these, on the contrary, show a significant downward trend in adolescents with hepatic encephalopathy along with the increase in adolescents with normal somatic status.

The next stage was assessment of the gaze fixation characteristics considering location in the presented stimulus images according to the criterion of the characteristics' distribution along the vertical axis (right/left half of the image) and distribution along the horizontal axis (upper/lower half of the image).

The study revealed significant differences in the number of fixations on the upper half of the stimulus image obtained when performing tests for recognition of single face images (*p = 0.034), multiple face images (*p = 0.001), multiple face images camouflaged with noise (*p = 0.011) between the group of adolescents with hepatic encephalopathy and the group of adolescents with normal somatic status. We also revealed significant differences in the number of fixations on the lower half of the stimulus image obtained when performing the test for recognition of multiple face images camouflaged with noise (*p = 0.006) between the group of patients with hepatic encephalopathy and the group of adolescents with normal somatic status. There were significant differences in the number of fixations on the right half of the stimulus image obtained when performing the test for recognition of single inverted face images (*p = 0.004) between the group of patients with hepatic encephalopathy and the group of adolescents with normal somatic status (Fig. 5).

The number of fixations on the upper half of the stimulus image obtained when presenting single face images, multiple face images, multiple face images camouflaged with noise shows a significant upward trend in the adolescent patients with hepatic encephalopathy relative to appropriate scores

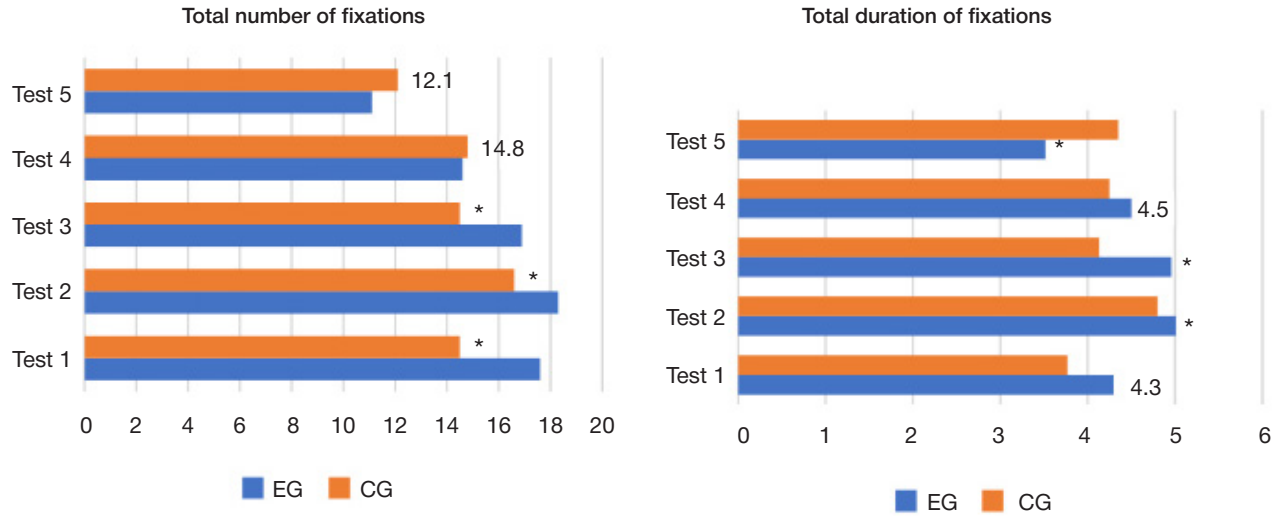

Fig. 4. Average total number and duration of gaze fixations associated with face image recognition

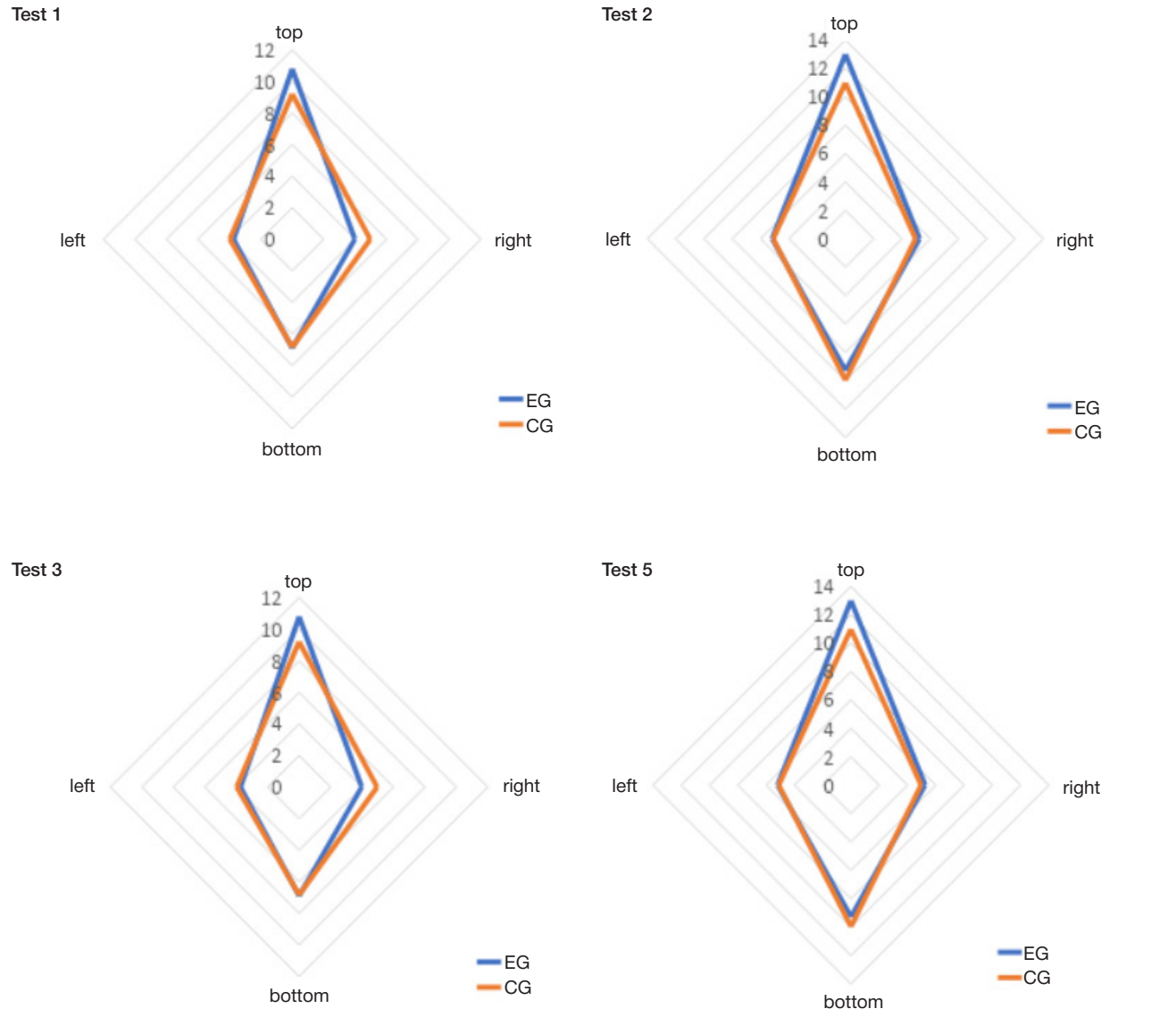

Fig. 5. Average gaze fixation distribution along the vertical (right/left half of the image) and horizontal (upper/lower half of the image) axes in the groups of adolescents

of adolescents with normal somatic status. The number of fixations on the lower half of the image obtained when recognizing multiple face images camouflaged with noise and the number of fixations on the upper half of the image obtained when recognizing single face images, multiple face images, multiple face images camouflaged with noise shows a significant upward trend in the adolescent patients with portal hypertension relative to appropriate scores of adolescents with normal somatic status. The number of fixations on the right half of the image obtained when recognizing single inverted face images shows a significant downward trend in the adolescent patients with hepatic encephalopathy relative to appropriate scores of adolescents with normal somatic status (Fig. 6).

The analysis of the number of fixations on the zones between eyes and nose, mouth and nose of the stimulus image revealed significant differences in the number of fixations on the zone between mouth and nose obtained when recognizing single inverted face images (*$p = 0.006$) between the group of patients with hepatic encephalopathy and the group of adolescents with normal somatic status. Thus, the number of fixations on the zone between mouth and nose obtained when presenting single inverted face images shows a significant downward trend in adolescent patients with hepatic encephalopathy relative to appropriate scores of adolescents with normal somatic status.

When performing factor analysis of the structure of the parameters of oculomotor responses observed during recognition of face images considering their spatial orientation characteristics in adolescents with portal hypertension, the fully explained variance showed that there were 12 factors explaining 87.3% of variance. However, after the analysis of the graph of normalized simple stress we decided to include 1–5.7 factors explaining 73.6% of variance in the analysis as the most significant (Fig. 7).

The conceptual factor parameters are of particular diagnostic value for analysis of neurointoxication effects: the recognition accuracy is determined by the distribution of fixations within the face oval. The spatial orientation factor suggests that recognition of inverted images is ensured by evaluation of comparable spatial relationships outside the face oval. The decrease in the total duration of fixations is correlated to the recognition accuracy increase, which is indicated by the temporal factor content.

DISCUSSION

The study has shown that the recognition accuracy observed when presenting single face images, multiple face images, multiple face images camouflaged with noise demonstrates

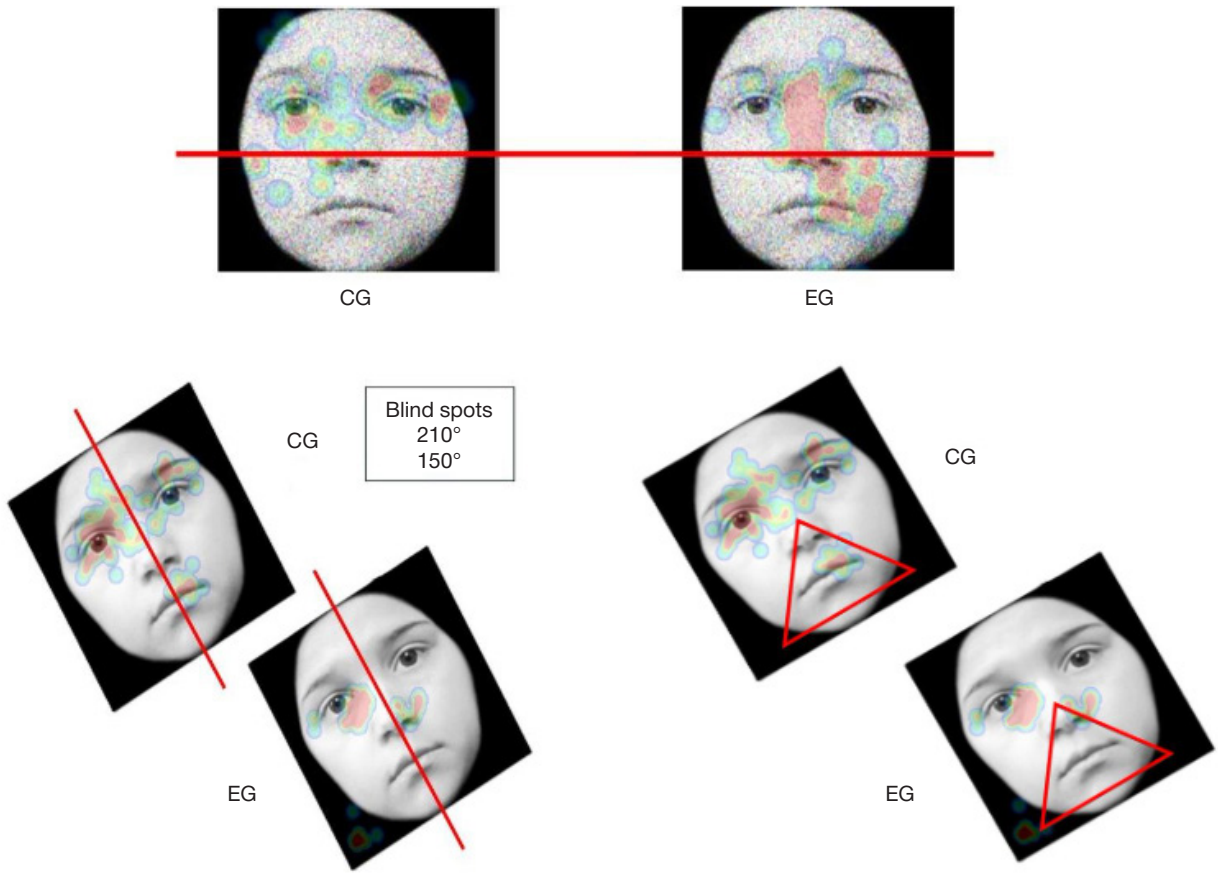

Fig. 6. Examples of the heatmaps of gaze fixation distribution along the vertical (right/left half of the image) and horizontal (upper/lower half of the image) axes in the groups of adolescents

a significant downward trend in patients with symptoms of hepatic encephalopathy relative to appropriate scores of adolescents with normal somatic status.

Taking into account the results of the empirical study of the total number of fixations on the stimulus images, we can say that the parameter demonstrates an upward trend in adolescents with hepatic encephalopathy relative to appropriate scores of adolescents with normal somatic status observed upon presentation of single face images, multiple face images, multiple face images camouflaged with noise.

Taking into account the results of the analysis of the total duration of fixations, we can report an upward trend in adolescent patients with hepatic encephalopathy when comparing with the scores of adolescents with normal somatic status observed upon presentation of single face images and multiple face images camouflaged with noise. The opposite pattern is observed when presenting single inverted images.

The empirical study and comparative analysis of the number of fixations on the upper halves of the stimulus images allow us to conclude that the parameter demonstrates an upward trend upon presentation of single face images, multiple face images, multiple face images camouflaged with noise in adolescent patients with hepatic encephalopathy relative to appropriate scores of adolescents with normal somatic status.

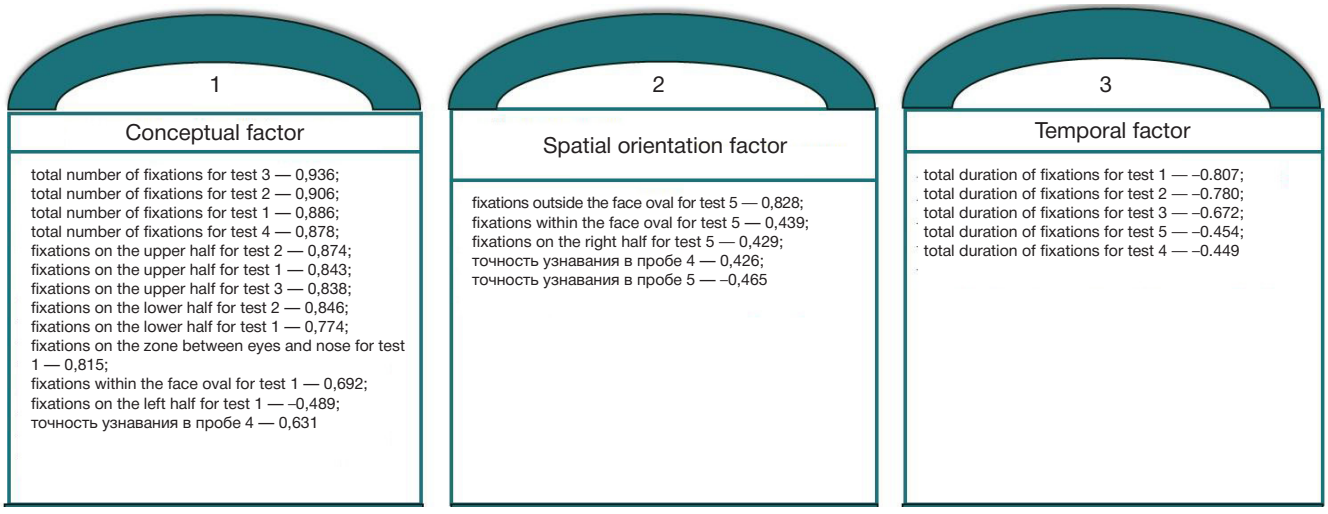

Fig. 7. Factor structure of the parameters of oculomotor responses observed during recognition of face images considering their spatial orientation characteristics in adolescents with portal hypertension

Comparative analysis of the number of fixations on the lower halves of the stimulus images suggests that that the parameter demonstrates an upward trend in adolescents with hepatic encephalopathy relative to appropriate scores of adolescents with normal somatic status obtained upon presentation of multiple face images camouflaged with noise.

Based on the empirical study of the number of fixations on the upper halves of the stimulus images, we managed to reveal a declining trend when performing the test for recognition of single inverted face images in adolescent patients with hepatic encephalopathy relative to appropriate scores of adolescents with normal somatic status.

The empirical study of the number of fixations on the zone between mouth and nose allows us to say that the parameter demonstrates an upward trend in adolescent patients with hepatic encephalopathy relative to appropriate scores of adolescents with normal somatic status obtained when performing the test for recognition of single inverted face images.

Thus, the findings are compliant with the oculomotor activity cyclic and regular nature reported earlier within the framework of studying the parameters of the oculomotor responses associated with face image perception [9, 10]. The processes of face image identification and recognition are characterized by the fact that fixations are distributed mainly within the face oval, in the zone between eyes and nose.

After conducting factor analysis in the group of patients with hepatic encephalopathy, six factors were distinguished. The first factor included the total number of fixations on the stimulus images reported for the tests 1–4, number of fixations on the upper half of the stimulus image reported for the tests 1–3, number of fixations on the lower half of the stimulus image reported for the tests 1–2, number of fixations on the zone between eyes and nose, within and outside the face oval, on the left half of the stimulus image reported for the test 1, as well as the recognition accuracy reported for the test 4. This factor was given the name “factor of fixation characteristics”. The second factor included fixations outside and within the face oval, on the right half of the stimulus image reported for the test 5, and the recognition accuracy reported for the tests 5 and 4; this factor was given the name “image tilt and completeness factor”. The third factor included the total number of fixations reported for the tests 1–5 and fixations on the stimulus images outside the face oval reported for the test 1; this factor was given the name “factor of the total number of fixations”. The fourth factor included fixations on the zone between mouth and nose, within the face oval, on the left half of the stimulus image reported for the test 1, and the recognition accuracy reported for the test 3; this factor was given the name “factor of fixation characteristics associated with recognition of single face images”. The fifth factor included fixations on the left, lower, and right halves, on the zone between mouth and nose, within the face oval, as well as the total number of fixations on the stimulus image reported for the test 5; this factor was given the name “factor of fixation characteristics associated with recognition of inverted images”. The sixth factor included fixations on the upper half and the zone between eyes and nose of the stimulus image reported for the test 5, as well as the recognition accuracy reported for the test 5; this factor was given the name “face image tilt factor”.

CONCLUSIONS

The following conclusions were drawn based on the findings: recognition of single face images, multiple face images, multiple face images camouflaged with noise in adolescents with portal hypertension is associated with the greater efforts (reflected in the increased number and duration of gaze fixations) than that in adolescents with normal somatic status. The accuracy of recognizing single face images, multiple face images, multiple face images camouflaged with noise when experiencing the influence of toxic effects associated with manifestation of hepatic encephalopathy in adolescents with portal hypertension is significantly decreased relative to adolescents with normal somatic status. Based on the factor analysis we distinguished three factors with the greatest uniqueness (conceptual factor, spatial orientation factor, and temporal factor) allowing us to draw the main conclusion that the face image recognition accuracy is determined by the distribution of fixations within the face oval when there is a need to evaluate spatial relationships outside the face oval in case of alteration of its spatial orientation characteristics (tilt). The recognition accuracy is correlated to the total number of fixations. Practical significance of the study is related to identification of the diagnostic predictors that contribute to detection of the hepatic encephalopathy symptoms in adolescents with portal hypertension at its earliest stages on the one hand, and allow one to trace the changes in the severity of the hepatic encephalopathy symptoms during various phases of treatment (including after surgery) on the other hand.

References

1. Pimpin L, Cortez-Pinto H, Negro F, Corbould E, Lazarus J, Webber L, Sheron N. Easl hepahealth Steering Committee. Burden of liver disease in Europe: Epidemiology and analysis of risk factors to identify prevention policies. J Hepatol. 2018; 69 (3): 718–35.
2. Blachier M, Leleu H, Peck-Rado-savljevic M, et al. The burden of liver disease in Europe: a review of available epidemiological data. J Hepatol. 2013; 58 (3): 593–608.
3. Pokrovskij VI, Totolyan AA, redaktory. Virusnye gepatity v Rossijskoj Federacii. Analiticheskij obzor. 11 vypusk. SPb.: FBUN NIIJeM imeni Pastera, 2018; 112 s. Russian.
4. Reis E, Coolen T, Loll V. MRI Findings in acute hyperammonemic encephalopathy: three cases of different etiologies. Journal of the Belgian Society of Radiology. 2020; 104 (1): 2–5.
5. Vizel TG. Osnovy nejropsihologii. Teorija i praktika. 2-e izd. M.: AST, 2021; 544 s. Russian.
6. Mikadze YuV. Nejropsihologija detskogo vozrasta: teorija i metody nejropsihologii detskogo vozrasta. Moskva [i dr.]: Piter, 2008; 284 s. Russian.
7. Lurija AR. Osnovy nejropsihologii. M.: Akademija, 2008; 380 s. Russian.
8. Jelkonin DB. Detskaja psihologija. M.: Akademija, 2011; 383 s. Russian.
9. Barabanshhikov VA, Ananeva KI, Haritonov VN. Organizacija dvizhenij glaz pri vosprijatii izobrazhenij lica. Jeksperimental'naja psihologija. 2009; 2: 31–60. Russian.
10. Barabanshhikov VA, Zhegallo AV. Okulomotornaja aktivnost' pri vosprijatii dinamicheskih i staticheskih vyrazhenij lica. Jeksperimental'naja psihologija. 2018; 11 (1): 5–34. Russian.
11. Damulin IV. Minimal'naja pechenochnaja jencefalopatija: sovremennye klinicheskie i patogeneticheskie aspekty. Terapevticheskij arhiv. 2018; 90 (2): 89–93. Russian.
12. Romanova SV. Nevrologicheskie sindromy v rannej diagnostike pechenochnoj jencefalopatii pri steatogepatoze (discertacija). Saratov, 2010; 22 s. Russian.

13. Greenberg DA, Aminoff MJ, Simon RP. Clinical Neurology. Fifth edition. Chapter 1: Disorders of Consciousness. New York etc.: Lange Medical Books/McGraw–Hill, 2022; p. 1–70.
14. Häussinger D, Butz M, Schnitzler A, Görg B. Pathomechanisms in hepatic encephalopathy. Biological Chemistry. 2021; 402 (9): 1087–102.
15. Montagnese S. Disruption of smooth pursuit eye movements in cirrhosis: Relationship to hepatic encephalopathy and its treatment. Hepatology. 2005; 42 (4): 81.
16. Montemira-Orozco D, et al. Changes in early visual perception in patients with minimal hepatic encephalopathy. Ann Hepatol. 2022; 27: 3.
17. Prokopenko SV, Mozhejko EYu, Rodikov MV, Shvecova IN. Issledovanie osobennostej zritel'no-prostranstvennogo gnozisa u zdorovyh lic v raznye vozrastnye periody zhizni s ispol'zovaniem avtorskogo metoda trehmernogo uznavanija predmeta. Mezhdunarodnyj zhurnal prikladnyh i fundamental'nyh issledovanij. 2015; 8–5: 916–20. Russian.
18. Jarbus AL. Rol' dvizhenij glaz v processe zrenija. Leningrad: Nauka, 1965; 173 s. Russian.
19. Croydon A, Pimperton H, Ewing L, Duchaine BC, Pellicano E. The Cambridge Face Memory Test for Children (CFMT-C): a new tool for measuring face recognition skills in childhood. Neuropsychologia. 2014; 62: 7.

Литература

1. Pimpin L, Cortez-Pinto H, Negro F, Corbould E, Lazarus J, Webber L, Sheron N. Easl hepahealth Steering Committee. Burden of liver disease in Europe: Epidemiology and analysis of risk factors to identify prevention policies. J Hepatol. 2018; 69 (3): 718–35.
2. Blachier M, Leleu H, Peck-Rado-savljevic M, et al. The burden of liver disease in Europe: a review of available epidemiological data. J Hepatol. 2013; 58 (3): 593–608.
3. Покровский В. И., Тотолян А. А., редакторы. Вирусные гепатиты в Российской Федерации. Аналитический обзор. 11 выпуск. СПб.: ФБУН НИИЭМ имени Пастера, 2018; 112 с.
4. Reis E, Coolen T, Loll V. MRI Findings in acute hyperammonemic encephalopathy: three cases of different etiologies. Journal of the Belgian Society of Radiology. 2020; 104 (1): 2–5.
5. Визель Т. Г. Основы нейропсихологии. Теория и практика. 2-е изд. М.: АСТ, 2021; 544 с.
6. Микадзе Ю. В. Нейропсихология детского возраста: теория и методы нейропсихологии детского возраста. Москва [и др.]: Питер, 2008; 284 с.
7. Лурия А. Р. Основы нейропсихологии. М.: Академия, 2008; 380 с.
8. Эльконин Д. Б. Детская психология. М.: Академия, 2011; 383 с.
9. Барабанщиков В. А., Ананьева К. И., Харитонов В. Н. Организация движений глаз при восприятии изображений лица. Экспериментальная психология. 2009; 2: 31–60.
10. Барабанщиков В. А., Жегалло А. В. Окуломоторная активность при восприятии динамических и статических выражений лица. Экспериментальная психология. 2018; 11 (1): 5–34.
11. Дамулин И. В. Минимальная печеночная энцефалопатия: современные клинические и патогенетические аспекты. Терапевтический архив. 2018; 90 (2): 89–93.
12. Романова С. В. Неврологические синдромы в ранней диагностике печеночной энцефалопатии при стеатогепатозе (диссертация). Саратов, 2010; 22 с.
13. Greenberg DA, Aminoff MJ, Simon RP. Clinical Neurology. Fifth edition. Chapter 1: Disorders of Consciousness. New York etc.: Lange Medical Books/McGraw–Hill, 2022; p. 1–70.
14. Häussinger D, Butz M, Schnitzler A, Görg B. Pathomechanisms in hepatic encephalopathy. Biological Chemistry. 2021; 402 (9): 1087–102.
15. Montagnese S. Disruption of smooth pursuit eye movements in cirrhosis: Relationship to hepatic encephalopathy and its treatment. Hepatology. 2005; 42 (4): 81.
16. Montemira-Orozco D, et al. Changes in early visual perception in patients with minimal hepatic encephalopathy. Ann Hepatol. 2022; 27: 3.
17. Прокопенко С. В., Можейко Е. Ю., Родиков М. В., Швецова И. Н. Исследование особенностей зрительно-пространственного гнозиса у здоровых лиц в разные возрастные периоды жизни с использованием авторского метода трехмерного узнавания предмета. Международный журнал прикладных и фундаментальных исследований. 2015; 8–5: 916–20.
18. Ярбус А. Л. Роль движений глаз в процессе зрения. Ленинград: Наука, 1965; 173 с.
19. Croydon A, Pimperton H, Ewing L, Duchaine BC, Pellicano E. The Cambridge Face Memory Test for Children (CFMT-C): a new tool for measuring face recognition skills in childhood. Neuropsychologia. 2014; 62: 7.

INTERDISCIPLINARY APPROACH TO ORTHODONTIC TREATMENT INVOLVING AN OSTEOPATH AND A DENTIST (PROTOCOL)

Aptekar IA[1]✉, Abramova EV[1,2], Postnikov MA[5], Kopetsky IS[3], Eremin DA[3], Postnikova EM[4], Poluianova EB[5], Aptekar VI[2], Muravyov IO[2]

[1] Tyumen Institute of Manual Medicine, Tyumen, Russia
[2] Tyumen State Medical University, Tyumen, Russia
[3] Pirogov Russian National Research Medical University, Moscow, Russia
[4] I.M. Sechenov First Moscow State Medical University (Sechenov University), Moscow, Russia
[5] Samara State Medical University, Samara, Russia

Contemporary approaches to orthodontic treatment are complex: in complicated cases, they combine removable/fixed orthodontic appliances and surgical treatment, i.e., extraction of permanent teeth. In order to prevent negative outcomes and complications that can follow correction of dentofacial abnormalities and deformities, children and adults alike need to be thoroughly examined and prepared to the orthodontic stage of treatment. Many studies point to the relationship between orthodontic treatment and development of somatic dysfunctions. The purpose of this work was to develop an osteopathic disorders correction algorithm that can be introduced to an interdisciplinary protocol uniting efforts by an osteopath and an orthodontist with the aim to improve the quality of specialized orthodontic medical care.

Keywords: orthodontic treatment, osteopathic correction, somatic dysfunction, interdisciplinary interaction

Acknowledgements: authors thank Department of Restorative Dentistry of the Samara State Medical University for assistance in preparation of the materials and design of the manuscript.

Author contribution: Aptekar IA — study design and planning, literature analysis, data interpretation, manuscript authoring; Abramova EV — literature analysis, osteopathic data collection, data analysis and interpretation, manuscript authoring; Postnikov MA — editing; Kopetskiy IS, Postnikova EM, Poluianova EB — manuscript authoring; Eremin DA — analysis of the results; Aptekar VI, Muravyov IO — clinical trials, literature analysis, data interpretation, manuscript authoring.

Compliance with ethical standards: the study was approved by the Ethics Committee of the Research Centre for Medical Genetics (protocol № 4/2 dated 19 April 2021). The patients submitted the informed consent to participation in scientific research.

✉ **Correspondence should be addressed:** Igor A. Aptekar
Popova, 7a, Tyumen, 625048, Russia; aptekar72@mail.ru

Received: 15.01.2024 **Accepted:** 28.02.2024 **Published online:** 14.04.2024

DOI: 10.24075/brsmu.2024.011

ПРОТОКОЛ МЕЖДИСЦИПЛИНАРНОГО ВЗАИМОДЕЙСТВИЯ ОСТЕОПАТА И СТОМАТОЛОГА В ПРОЦЕССЕ ОРТОДОНТИЧЕСКОГО ЛЕЧЕНИЯ

И. А. Аптекарь[1]✉, Е. В. Абрамова[1,2], М. А. Постников[5], И. С. Копецкий[3], Д. А. Еремин[3], Е. М. Постникова[4], Э. Б. Полуянова[5], В. И. Аптекарь[2], И. О. Муравьев[2]

[1] Тюменский институт мануальной медицины, Тюмень, Россия
[2] Тюменский государственный медицинский университет, Тюмень, Россия
[3] Российской национальный исследовательский медицинский университет имени Н. И. Пирогова, Москва, Россия
[4] Первый московский государственный медицинский университет имени И. М. Сеченова (Сеченовский Университет), Москва, Россия
[5] Самарский государственный медицинский университет, Самара, Россия

Современное ортодонтическое лечение носит комплексный характер и включает не только использование съемных и несъемных ортодонтических конструкций, но и оперативное лечение (экстракцию постоянных зубов) в сложных случаях. Необходимы тщательное обследование и подготовка пациентов перед ортодонтическим этапом лечения для профилактики отрицательных результатов и осложнениий коррекции зубочелюстных аномалий и деформаций, как у детей, так и у взрослых. Результаты многих исследований указывают на взаимосвязь между ортодонтическим лечением и формированием соматических дисфункций. Целью работы было разработать алгоритм коррекции остеопатических нарушений, который может быть внедрен в практику междисциплинарного взаимодействия врача-остеопата и стоматолога-ортодонта для повышения качества специализированной ортодонтической медицинской помощи.

Ключевые слова: ортодонтическое лечение, остеопатическая коррекция, соматическая дисфункция, междисциплинарное взаимодействие

Благодарности: авторы благодарят сотрудников кафедры терапевтичекой стоматологии ФГБОУ ВО СамГМУ Минздрава России за помощь в подготовке материалов и дизайна рукописи.

Вклад авторов: И. А. Аптекарь — дизайн и планирование исследования, анализ литературы, интерпретация данных, подготовка рукописи; Е. В. Абрамова — анализ литературы, сбор данных в сфере остеопатии, анализ и интерпретация данных, подготовка рукописи; М. А. Постников — редактирование; И. С. Копецкий, Е. М. Постникова, Э. Б. Полуянова — подготовка рукописи; Д. А. Еремин — анализ результатов; В. И. Аптекарь, И. О. Муравьев — проведение клинических исследований, анализ литературы, интерпретация данных, подготовка рукописи.

Соблюдение этических стандартов: исследование одобрено этическим комитетом ФГБНУ «МГНЦ» (протокол № 4/2 от 19 апреля 2021 г.). Получено добровольное информированное согласие на участие пациентов в научном исследовании.

✉ **Для корреспонденции:** Игорь Александрович Аптекарь
ул. Попова, д. 7а, г. Тюмень, 625048, Россия; aptekar72@mail.ru

Статья получена: 15.01.2024 **Статья принята к печати:** 28.02.2024 **Опубликована онлайн:** 14.04.2024

DOI: 10.24075/vrgmu.2024.011

According to the literature, dentofacial abnormalities registered in the population of the Russian Federation are highly variable. Most researchers believe that prevalence of such abnormalities grows with age and ranges from 30 to 80% [1–3]. In complicated cases, contemporary orthodontic treatment protocols combine removable/fixed orthodontic appliances and surgery.

As previous studies indicate, extraction of individual teeth can help establish multiple stable contacts between dental arches and normalize functionality of the dentofacial system. The teeth pulled most often in the context of orthodontic treatment, including protocols that employ braces, are third molars, followed by first molars [4–6]. A complex therapy of dentofacial abnormalities may justifiably imply cooperation of dentists specializing in related fields [7], with the goals of such therapy being normalization of occlusion, restoration of the dentofacial system's functions, and aesthetic reconstruction.

From the point of view of osteopathic diagnosis, a dominant somatic dysfunction in the human body can stem from specific somatic dysfunctions, namely, their intraocclusive variations, which are directly related to the anatomical features conditioning occlusion. The dominant somatic dysfunctions developing in such a case are disorders of venous return from the head, vestibulopathies, disorders of the temporomandibular joint. This, in turn, affects the patient's quality of life [3, 6–9]. Therefore, it is important for an orthodontist to professionally cooperate not only with fellow dentists, but also with medical doctors specializing in other fields, including osteopaths [8–12].

Previous studies have shown that osteopathic correction added to dental and orthodontic treatment significantly reduces the frequency and severity of somatic dysfunctions of head and neck, thus significantly improving the quality of life of patients [13–17]. There is no single protocol of interdisciplinary interaction involving an osteopath and an orthodontist described in the literature. Moreover, no paper presents an intraocclusive somatic dysfunctions remedying algorithm, which may include, firstly, curing compression as the cause of disorders of the peripheral nervous system and vascular hydrodynamic disorders, and secondly, remediation of hypercapnia, a marker of impaired venous circulation and hypoxia, which signals arterial circulation disruptions [18].

This study aimed to develop an interdisciplinary cooperation algorithm involving a dentist and an osteopath in the context of preparing a patient for specialized dental treatment and subsequent comprehensive rehabilitation seeking to mitigate the risk of complications manifesting as tension headaches.

METHODS

The study analyzed the data from outpatient records of 340 patients who applied to the clinic in 2014 through 2023, with an established tension headaches diagnosis (ICD G44.2) being the inclusion requirement. Among the clinical symptoms, patients mentioned moderate pain, generalized, more often of a squeezing, compressive nature, episodic or chronic. As a rule, headache originated in the occipital or frontal part of the head, and spread further to all parts thereof. The participants were divided into two groups, 170 patients in each.

Treatment group inclusion criteria: application to the osteopathic clinic during ongoing orthodontic treatment that began 1–3 months before that application; complaints of cephalgia, cervicalgia.

Control group inclusion criteria: complaints of cephalgia, cervicalgia; no history of orthodontic treatment. All participants underwent osteopathic examination (standardized protocol) and osteopathic correction of the identified somatic dysfunctions.

Exclusion criteria: diagnosis of «tension headaches associated with somatic pathology».

Tension headache is not associated with such etiological factors as physical activity and active stimuli like light, smell or sound. Unlike migraines, such headaches are not typically concomitant with nausea and vomiting. Tension headaches stem from the following: sleep and rest disorders, emotional stress, somatic dysfunctions of the temporomandibular joint (TMJ), degenerative disk disease (in cervical spine, in particular), and eye strain, especially that caused by electronic devices with excessively bright screens. The headaches can last from 30 minutes to 2–3 days. Clinically, there are episodic and chronic tension headaches distinguished. Fire percent of this group's patients had a third molar extracted 1–3 months before the onset of cephalgia.

Processing the results, we applied parametric and nonparametric methods. The data were systematized and visualized using Microsoft Office Excel 2013. SPSS Statistics (version 2) enabled statistical processing. The differences were considered significant at $p = 0.05$.

RESULTS

Following a standardized protocol, we diagnosed the dominant somatic dysfunction and identified the primary biomechanical, neurodynamic, and hydrodynamic components underpinning it [19, 20].

Figure 1 presents the comparison of the osteopathic status indicators registered in treatment and control groups before osteopathic intervention. All patients with a history of orthodontic treatment had the said status dominated by local somatic dysfunctions in the head area (sphenobasilar synchondrosis, locally — interstitial somatic dysfunctions in the palatomaxillary suture, zygomaxillary suture, intermaxillary suture, frontomaxillary suture, temporomandibular joint, intraosseous somatic dysfunctions of the upper and lower jaws). In addition, at the regional level, we registered neck somatic dysfunctions (local dysfunction of C0–C1 and the below cervical spine segments) and pelvic somatic dysfunctions (local dysfunction of L5–S1).

Manual osteopathic correction techniques were chosen individually for each patient. In the context of osteopathic treatment, the physician proceeded top down, i.e., remedied global somatic dysfunctions first, then moved to the regional and subsequently local levels. "Somatic dysfunction" clinical guidelines were observed when correcting the dominant somatic dysfunction [19].

For most patients, the sequence of application of osteopathic techniques was as follows: pubic joint decompression, sacrococcygeal joint mobility restoration, L5–S1 mobility restoration, thoracic diaphragm balancing, upper aperture balancing, C0–C1 mobility restoration, sphenobasilar synchondrosis decompression, correction of the revealed interstitial somatic dysfunctions.

All patients underwent a control osteopathic examination (standardized protocol) after osteopathic correction of the identified somatic dysfunctions. Figure 2 presents the comparison of the osteopathic status indicators registered in treatment and control groups before and after osteopathic intervention.

Repeated examination confirmed a statistically significant decrease of the frequency of somatic dysfunctions, including those found in the dentofacial system and neck region, as well as their clinical manifestations.

DISCUSSION

This work investigates the effect of extraction of first or third molar as a significant etiological factor in the development of

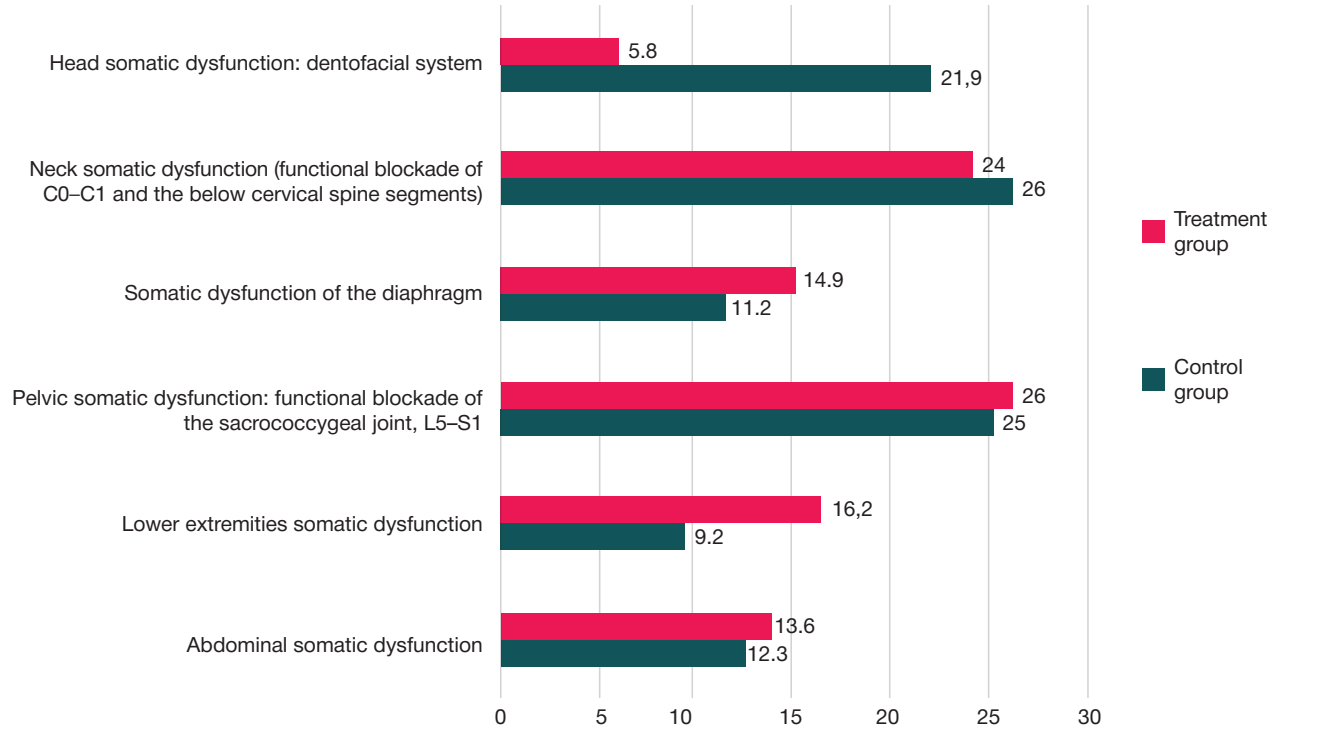

Fig. 1. Comparison of osteopathic status indicators, treatment group and groups, before osteopathic correction (%). * — $p \leq 0.05$

tension headache. The most prominent component of this factor are the traction and compression forces accompanying dental treatment.

We studied biomechanical, neurodynamic, hydrodynamic functional, and in some cases pathogenetic adaptation chains leading to the development of regional somatic dysfunctions, with such in the head and neck region being most common.

History of extraction of first or third molar and predominance of head somatic dysfunctions in the treatment group, including those affecting dentofacial system, allowed exposing the sequence of adaptive reactions of the body that translate into tension headaches initiated by etiological factors of intraocclusive nature.

Tooth extraction is associated with a combined effect of traction and compression forces on the upper or lower jaw. Consequently, there arise compression forces inside the bone, which initiate allostatic adaptive reactions at the local level. As a result, there develop somatic dysfunctions with a dominant biomechanical component, from the occipital bone and C1–C2 cervical vertebrae in the first place.

Pulling an upper jaw molar, dentist applies force to the entire head and neck region, which means that initially, before a more localized reaction, there appears sphenobasilar synchondrosis, mainly in the form of compression and torsion of varying severity. This condition may compromise the existing pattern of interaction between the sphenoid and occipital bones, and subsequently trigger adaptive reactions that contribute to the development of cephalgia. In the context of a tooth extraction, palatal bones accept biomechanical stress and, through the chain of interosseous suture interactions, transfer it to the sphenoid bone, and adaptation through connections with the zygomatic bone stresses the temporal bone. After extraction of a mandibular molar, diagnostics revealed somatic dysfunctions of the temporal bone in the first place.

In the context of adaptation to the mechanical etiological factors, anatomical biomechanical connections cause

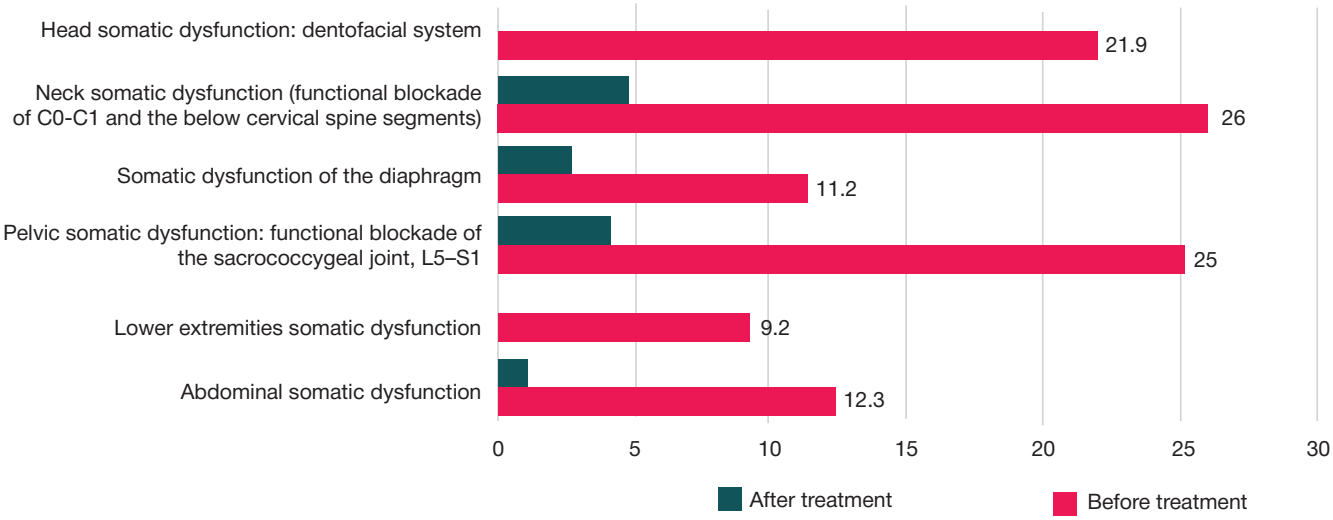

Fig. 2. Comparison of osteopathic status indicators, treatment group and groups, after osteopathic correction (%). * — $p \leq 0.05$

compression in the sutures between skull bones and brain membranes. By severity, the most common compressions are those in the zygomaticomaxillary, palatomaxillary, intermaxillary and frontomaxillary sutures; they cause functional intersuture somatic dysfunction.

The latter compromises mobility of the brain membranes. Somatic dysfunctions of the brain membranes affect venous circulation of the head region and cerebrospinal fluid dynamics. In turn, this can lead to a reflex response from the central nervous system and the autonomic nervous system, growth of the arterial and intracranial pressure. Increased intracranial pressure irritates receptors of the brain membranes' nerve endings and thus causes pain in the region of the head.

Based on the data yielded by this study, it can be assumed that the etiotropic trigger of development of the adaptation associated with tension headaches after molar extraction is the somatic dysfunction as part of the sphenobasilar synchondrosis, which is an adaptive reaction aimed at maintaining constancy of the internal environment.

As an adaptive reaction, somatic dysfunction is based on the pattern of skull bone positions formed at birth. As a result, there develop somatic dysfunctions that have neurodynamic and hydrodynamic components as the prevailing ones.

Other factors that condition development of somatic dysfunctions are extraction technique and position of the dentist relative to the patient during the procedure. Duration of extraction depends on complexity of the case; at a minimum, it lasts 40-60 minutes.

Mouth opened for a long time, rotations of the head and lateroflexion in the opposite direction may cause additional somatic dysfunctions in C0–C1, C1–C2, pleural dome ligaments, first rib, hyoid bone, musculoskeletal system of the stomatognathic system.

It should be noted that such position of the patient is peculiar not only to molar extraction but also to many other procedures in the context of orthodontic treatment.

Osteopathic diagnostics allows a conclusion that the primary somatic dysfunction is an intraosseous somatic dysfunction of the upper or lower jaw in the projection of the extracted molar. This is the area of primary damage. In such cases, the osteopath rehabilitates the patient by correcting somatic dysfunctions resulting from extraction of the first or third molar.

For this study, we used the osteopathic assistance protocol designed to remedy somatic dysfunctions (given below). It should be noted that the algorithm was developed following studies that investigated changes of functional activity of fibroblasts against the background of compression, hypercapnia, and hypoxia (simulated). It has been shown that compression, a local spike of pressure in the tissues, disrupts adaptive capabilities of connective tissue the most. Hypercapnia, reaction to high CO_2 content, was the second most potent etiological factor promoting development of the somatic dysfunction's hydrodynamic component at the local level. Hypoxia was shown to have the least effect thereon [18].

Thus, the revealed ranking of etiological factors affecting development of the somatic dysfunction at the local level can be expressed by the following algorithm. Remediation of compression at the local and regional level. Osteopathic techniques (standardized method) enabled decompression. In case of a diagnosed sphenobasilar synchondrosis compression, the decompression sequence began with the sacrum, L5–S1, thoracic diaphragm, and then C0–C1; afterwards, we retested and rebalanced integrity of the body's biomechanical mobility.

Initial correction of the thoracic diaphragm and pelvic diaphragm and adjustment of the venous sinuses after correction of sphenobasilar synchondrosis allow, in turn, to improve and restore venous circulation function and minimize the effects of hypercapnia at the local and regional levels.

However, it should be noted that, in connection with a molar extraction, there are two more reasons for cooperation between an osteopath and an orthodontist:

the patient may apply for osteopathic assistance after emergency extraction of any tooth, with rehabilitation and correction of the resulting somatic dysfunctions often preceding complaints;

the patient may apply for osteopathic assistance before a scheduled extraction of any tooth, with dental and osteopathic prevention measures taken to mitigate complications that may arise following the said extraction.

In such a case, osteopath's task is to diagnose somatic dysfunctions that may aggravate after tooth extraction.

Many orthodontists know that inviting an osteopath to participate in the post-extraction rehabilitation makes the entire process more effective and minimizes risks and complications. Therefore, the patient is referred for consultation to an osteopath before scheduled tooth extraction, and if extraction is emergency — after it, for rehabilitation.

Depending on the algorithm used, treatment can consists of several stages; its plan, as well as that of diagnostics, is similar for cases of emergency molar extraction and patient referrals driven by complaints.

Scheduled treatment implies dental and osteopathic preparation of the patient for tooth extraction:

Stage 1: consultation with a dentist before scheduled tooth extraction, US examination of head and neck vessels with the aim to diagnose disorders of venous and arterial circulation in the head region, and learn the effect of these factors on the adaptive abilities of fibroblasts, including synthesis of collagen, elastin and glycosaminoglycans;

Stage 2: primary visit to the osteopath, including diagnosing of primary or leading somatic dysfunction, osteopathic correction of the dominant somatic dysfunction and elimination of its cause, improvement of the body's adaptive capabilities with the aim to ensure homeostatic constancy of the internal environment;

Stage 3: if necessary, two or three more visits to the osteopath within two weeks. In case there is limited time available before dental treatment, the therapeutic part of osteopathic care should be performed 72 hours before it. This period of time was established based on the results of investigation of adaptive capabilities of fibroblasts (main connective tissue cells) after elimination of the etiological factors triggering somatic dysfunction, and tissue's return to the normosthenic conditions at the local and regional levels;

Stage 4: repeated dentist appointment before tooth extraction, followed by the specialized dental intervention;

Stage 5: implementation of rehabilitation measures, which may include the provision of osteopathic assistance and physiotherapy.

The algorithm of osteopathic care for patients during orthodontic treatment developed by us in the context of this study has been introduced to the practice of the Tyumen Institute of Manual Medicine.

CONCLUSIONS

The algorithm implies sequential elimination of compression factors (using osteopathic techniques) as markers of

neurodynamic and hydrodynamic disorders, subsequent remediation of hypercapnia that stems from the impairments of venous circulation and lymphodynamics, restoration of arterial circulation, and remediation of hypoxia and tissue nutrition disorders. Practiced, this protocol, involving interdisciplinary cooperation between an osteopath and an orthodontist, with joint patient management and cross-counseling, allows early diagnosis and timely correction of the identified somatic dysfunctions of dentofacial system, and, moreover, prevention of their development during orthodontic treatment. Osteopathic adjustments are a non-invasive component of the comprehensive dentofacial system abnormalities treatment programs, which allows their active application with the aim to optimize the treatment algorithm, improve the quality of medical care and effectiveness of specialized orthodontic therapy.

References

1. Persin LS. Ortodontija. Nacional'noe rukovodstvo. Lechenie zubocheljustnyh anomalij. M.: GJeOTAR-Media; 2020; 2: 376. Russian.
2. Popova NV, Arsenina OI, Gavrilova MV, Gluhova NV. Ob"ektivnaja i sub"ektivnaja ocenka kachestva i jeffektivnosti ortodonticheskogo lechenija. Stomatologija. 2021; 100 (5): 82–87. Russian.
3. Zubareva A. Garaeva KL, Isaeva AI. Rasprostranennost' zubocheljustnyh anomalij u detej i podrostkov (obzor literatury). European Research. 2015; 10 (11): 128–32. Russian.
4. Mihalin AN, Nikandrov RA. Sovremennye sredstva lechenija zubocheljustnyh anomalij. Juvenis scientia. 2017; 12: 19–21. Russian.
5. Megrabjan OA, Konkova AM. Osobennosti lechenija pacientov s distal'noj okkljuziej zubnyh rjadov v razlichnye vozrastnye periody (obzor literatury). Acta medica Eurasica. 2018; 4: 19–29. Russian.
6. Ibragimova IF, Timerbulatova GA, Mannanova FF, Galiullina MV, Junusov RR. Klinicheskie nabljudenija nekotoryh otricatel'nyh rezul'tatov i oslozhnenij posle proteticheskoj korrekcii zubocheljustnyh anomalij i deformacij. Problemy stomatologii. 2018; 14 (4): 117–20. DOI: 10.18481/2077-7566-2018-14-4-117-120. Russian.
7. Abramova MYa, Medvedickova AI, Lukina GI. Personificirovannyj podhod pri lechenii pacientov s anomalijami zubocheljustnoj sistemy s privlecheniem vrachej-stomatologov smezhnyh special'nostej. Rossijskaja stomatologija. 2022; 15 (1): 20–24. Dostupno po ssylke: https://doi.org/10.17116/rosstomat20221501120. Russian.
8. Aptekar IA, Abramova EV, Aptekar VI, Judina, Aleshina OA. Ocenka sostojanija ortodonticheskoj pomoshhi naseleniju v aspekte mezhdisciplinarnogo podhoda lechenija pacientov s zubocheljustnymi anomalijami. Mediko-farmacevticheskij zhurnal «Pul's». 2020; 6 (22): 31–34. Dostupno po ssylke: http://dx.doi.org/10.26787/nydha-2686-6838-2020-22-6-31-34. Russian.
9. Medvedickova AI, Abramova MYa, Lukina GI. Problemno-orientirovannyj analiz jeffektivnosti mezhdisciplinarnogo podhoda v kompleksnom lechenii pacientov s zubocheljustnymi anomalijami i deformacijami. Rossijskaja stomatologija. 2021; 14 (4): 46–50. Dostupno po ssylke: https://doi.org/10.17116/rosstomat20211404146. Russian.
10. Milutka YuA, Yushmanov IG, Badmaeva AN. Vozmozhnosti osteopaticheskoj korrekcii v kompleksnoj terapii disfunkcii visochno-nizhnecheljustnogo sustava. Rossijskij osteopaticheskij zhurnal. 2019; (1–2): 43–50. Dostupno po ssylke: https://doi.org/10.32885/2220-0975-2019-1-2-43-50. Russian.
11. Aptekar IA, Abramova EV, Aptekar VI, Yudina AA, Lebedev IA, Borsukov AP, Anatomo-fiziologicheskoe obosnovanie jeffektivnosti osteopaticheskoĭ korrekcii v kompleksnoĭ reabilitacii pacientov posle jekstrakcii pervogo moljara. Ural'skiĭ medicinskiĭ zhurnal. 2020; 09 (192): 133–137. DOI 10.25694/ URMJ.2020.09.27. Russian.
12. Atjakshev AV, Tekuteva NV. Ocenka gemodinamicheskih cerebral'nyh narushenij pri jekstrakcii tret'ih moljarov i jeffektivnost' osteopaticheskoj reabilitacii posle jekstrakcii zubov. Rossijskij osteopaticheskij zhurnal. 2016; (1–2): 60–66. Dostupno po ssylke: https://doi.org/10.32885/2220-0975-2016-1-2-60-66. Russian.
13. Yushmanov IG, Kalimullin MN, Zaripov IT, Zlatkovskaya MV. Vlijanie osteopaticheskoj korrekcii na kachestvo zhizni pacienta pri s"emnom stomatologicheskom protezirovanii. Rossijskij osteopaticheskij zhurnal. 2018; (1–2): 14–18. Dostupno po ssylke: https://doi.org/10.32885/2220-0975-2018-1-2-14-18. Russian.
14. Abramova EV, Aptekar IA, Pozdeev SYu. Osteopaticheskaja pomoshh' posle jekstrakcii tret'ego moljara kak jelement korrekcii golovnyh bolej naprjazhenija. Sbornik nauchnyh materialov IV Mezhdunarodnogo Kongressa «Fizioterapija. Lechebnaja fizkul'tura. Reabilitacija. Sportivnaja medicina». Moskva, 2018; s. 14. Russian.
15. Postnikov MA, Trunin DA, Malkina VD, Pankratova NV, Klochkov FG, Poştaru C. Osteopaticheskaja korrekcija v kompleksnom lechenii pacientov s zubocheljustno-licevymi anomalijami. Rossijskij osteopaticheskij zhurnal. 2018; (1–2): 91–99. Dostupno po ssylke: https://doi.org/10.32885/2220-0975-2018-1-2-91-99. Russian.
16. Basieva YeV, Milutka YuA, Tarasov NA, Silin AV, Mohov DE. Jeffektivnost' ortodonticheskoj i osteopaticheskoj korrekcii u pacientov s zubocheljustnymi anomalijami i myshechno-sustavnymi disfunkcijami visochno-nizhnecheljustnogo sustava pri nalichii soputstvujushhih somaticheskih disfunkcij i bez nih. Rossijskij osteopaticheskij zhurnal. 2021; (4): 63–74. Dostupno po ssylke: https://doi.org/10.32885/2220-0975-2021-4-63-74. Russian.
17. Bajramova LN, Belousova MV. Mezhdisciplinarnoe vzaimodejstvie v organizacii pomoshhi detjam s rechevymi i zubocheljustnymi narushenijami. Rossijskij osteopaticheskij zhurnal. 2017; (1–2): 31–36. Dostupno po ssylke: https://doi.org/10.32885/2220-0975-2017-1-2-31-36. Russian.
18. Aptekar IA, Kostolomova EG, Suhovej YuG. Izmenenie funkcional'noj aktivnosti fibroblastov v processe modelirovanija kompressii, giperkapnii i gipoksii. Rossijskij osteopaticheskij zhurnal. 2019; (1–2): 72–84. Dostupno po ssylke: https://doi.org/10.32885/2220-0975-2019-1-2-72-84. Russian.
19. Klinicheskie rekomendacii «Somaticheskaja disfunkcija» (odobreny Minzdravom Rossii). Moskva, 2023; 121 s. Dostupno po ssylke: https://diseases.medelement.com/disease/%D1%81%D0%BE%D0%BC%D0%B0%D1%82%D0%B8%D1%87%D0%B5%D1%81%D0%BA%D0%B0%D1%8F-%D0%B4%D0%B8%D1%81%D1%84%D1%83%D0%BD%D0%BA%D1%86%D0%B8%D1%8F-%D0%BA%D0%BF-%D1%80%D1%84-2023/17537?ysclid=luqpgv6t9b900850830. Russian.
20. Porjadok okazanija medicinskoj pomoshhi naseleniju po profilju «Osteopatija», utverzhdennyj MZ RF v 2018 g. # 21n. Dostupno po ssylke: https://base.garant.ru/71872688/. Russian.

Литература

1. Персин Л. С. Ортодонтия. Национальное руководство. Лечение зубочелюстных аномалий. М.: ГЭОТАР-Медиа, 2020; 376 с.
2. Попова Н. В., Арсенина О. И., Гаврилова М. В., Глухова Н. В. Объективная и субъективная оценка качества и эффективности ортодонтического лечения. Стоматология. 2021; 100 (5): 82–87.
3. Зубарева А. В., Гараева К. Л., Исаева А. И. Распространенность зубочелюстных аномалий у детей и подростков (обзор литературы). European Research. 2015; 10 (11): 128–32.
4. Михалин А. Н., Никандров Р. А. Современные средства лечения зубочелюстных аномалий. Juvenis scientia. 2017; 12: 19–21.
5. Меграбян О. А., Конькова А. М. Особенности лечения пациентов с дистальной окклюзией зубных рядов в различные возрастные периоды (обзор литературы). Acta

medica Eurasica. 2018; 4: 19–29.
6. Ибрагимова И. Ф., Тимербулатова Г. А., Маннанова Ф. Ф., Галиуллина М. В., Юнусов Р. Р. Клинические наблюдения некоторых отрицательных результатов и осложнений после протетической коррекции зубочелюстных аномалий и деформаций. Проблемы стоматологии. 2018; 14 (4): 117–20. DOI: 10.18481/2077-7566-2018-14-4-117-120.
7. Абрамова М. Я., Медведицкова А. И., Лукина Г. И. Персонифицированный подход при лечении пациентов с аномалиями зубочелюстной системы с привлечением врачей-стоматологов смежных специальностей. Российская стоматология. 2022; 15 (1): 20–24. Доступно по ссылке: https://doi.org/10.17116/rosstomat20221501120.
8. Аптекарь И. А., Абрамова Е. В., Аптекарь В. И., Юдина, Алешина О. А. Оценка состояния ортодонтической помощи населению в аспекте междисциплинарного подхода лечения пациентов с зубочелюстными аномалиями. Медико-фармацевтический журнал «Пульс». 2020; 6 (22): 31–34. Доступно по ссылке: http://dx.doi.org/10.26787/nydha-2686-6838-2020-22-6-31-34
9. Медведицкова А. И., Абрамова М. Я., Лукина Г. И. Проблемно-ориентированный анализ эффективности междисциплинарного подхода в комплексном лечении пациентов с зубочелюстными аномалиями и деформациями. Российская стоматология. 2021; 14 (4): 46–50. Доступно по ссылке: https://doi.org/10.17116/rosstomat20211404146.
10. Милутка Ю. А., Юшманов И. Г., Бадмаева А. Н. Возможности остеопатической коррекции в комплексной терапии дисфункции височно-нижнечелюстного сустава. Российский остеопатический журнал. 2019; (1–2): 43–50. Доступно по ссылке: https://doi.org/10.32885/2220-0975-2019-1-2-43-50.
11. Аптекарь И. А., Абрамова Е. В., Аптекарь В. И., Юдина А. А., Лебедев И. А., Борсуков А. П., Анатомо-физиологическое обоснование эффективности остеопатической коррекции в комплексной реабилитации пациентов после экстракции первого моляра. Уральский медицинский журнал. 2020; 09 (192): 133–137. DOI 10.25694/ URMJ.2020.09.27.
12. Атякшев А. В., Текутьева Н. В. Оценка гемодинамических церебральных нарушений при экстракции третьих моляров и эффективность остеопатической реабилитации после экстракции зубов. Российский остеопатический журнал. 2016; (1–2): 60–66. Доступно по ссылке: https://doi.org/10.32885/2220-0975-2016-1-2-60-66.
13. Юшманов И. Г., Калимуллин М. Н., Зарипов И. Т., Златковская М. В. Влияние остеопатической коррекции на качество жизни пациента при съемном стоматологическом протезировании. Российский остеопатический журнал. 2018; (1–2): 14–18. Доступно по ссылке: https://doi.org/10.32885/2220-0975-2018-1-2-14-18.
14. Абрамова Е. В., Аптекарь И. А., Поздеев С. Ю. Остеопатическая помощь после экстракции третьего моляра как элемент коррекции головных болей напряжения. Сборник научных материалов IV Международного Конгресса «Физиотерапия. Лечебная физкультура. Реабилитация. Спортивная медицина». Москва, 2018; с. 14.
15. Постников М. А., Трунин Д. А., Малкина В. Д., Панкратова Н. В., Клочков Ф. Г., Poştaru C. Остеопатическая коррекция в комплексном лечении пациентов с зубочелюстно-лицевыми аномалиями. Российский остеопатический журнал. 2018; (1–2): 91–99. Доступно по ссылке: https://doi.org/10.32885/2220-0975-2018-1-2-91-99.
16. Басиева Э. В., Милутка Ю. А., Тарасов Н. А., Силин А. В., Мохов Д. Е. Эффективность ортодонтической и остеопатической коррекции у пациентов с зубочелюстными аномалиями и мышечно-суставными дисфункциями височно-нижнечелюстного сустава при наличии сопутствующих соматических дисфункций и без них. Российский остеопатический журнал. 2021; (4): 63–74. Доступно по ссылке: https://doi.org/10.32885/2220-0975-2021-4-63-74.
17. Байрамова Л. Н., Белоусова М. В. Междисциплинарное взаимодействие в организации помощи детям с речевыми и зубочелюстными нарушениями. Российский остеопатический журнал. 2017; (1–2): 31–36. Доступно по ссылке: https://doi.org/10.32885/2220-0975-2017-1-2-31-36.
18. Аптекарь И. А., Костоломова Е. Г., Суховей Ю. Г. Изменение функциональной активности фибробластов в процессе моделирования компрессии, гиперкапнии и гипоксии. Российский остеопатический журнал. 2019; (1–2): 72–84. Доступно по ссылке: https://doi.org/10.32885/2220-0975-2019-1-2-72-84.
19. Клинические рекомендации «Соматическая дисфункция» (одобрены Минздравом России). Москва, 2023; 121 с. Доступно по ссылке: https://diseases.medelement.com/disease/%D1%81%D0%BE%D0%BC%D0%B0%D1%82%D0%B8%D1%87%D0%B5%D1%81%D0%BA%D0%B0%D1%8F-%D0%B4%D0%B8%D1%81%D1%84%D1%83%D0%BD%D0%BA%D1%86%D0%B8%D1%8F-%D0%BA%D0%BF-%D1%80%D1%84-2023/17537?ysclid=luqpgv6t9b900850830.
20. Порядок оказания медицинской помощи населению по профилю «Остеопатия», утвержденный МЗ РФ в 2018 г. № 21н. Доступно по ссылке: https://base.garant.ru/71872688/.

TREATMENT OF GONARTHROSIS USING AUTOLOGOUS PLATELET-RICH PLASMA

Egiazaryan KA, Danilov MA ✉, Abdusalamov RM

Pirogov Russian National Research Medical University, Moscow, Russia

Injections of platelet-rich plasma are considered to be a promising treatment. Medicines acting on the subchondral bone can improve tissue's structure and slow down destruction of the articular cartilage. This study aimed to analyze the results of intraarticular and intraosseous administration of platelet-rich plasma (PRP) in gonarthrosis cases. One hundred and eighty-seven participants (gonarthrosis stages 1 through 3) were divided into three groups. Group 1 (treatment group) received intraarticular PRP injections, group 2 (comparison group) — intraosseous PRP injections. For assessment purposes, we used the SF-36 survey and visual analog scale. Three months after the treatment, initial pain level decreased in both groups 1 and 2. In group 1, the prevalence of synovitis went down after 3 months, in group 2 — after 6 months (21.9 and 31.3%, respectively; $p < 0.05$). Six months after the treatment, soft tissue swelling around the joint was registered less often in groups 1 and 2 (8.2 and 8.3%, respectively). As for the physical component of the quality of life, it improved in group 1 after 3 months (70.40%), in group 2 — after 6 months (69.80%); as for the mental component, the dynamics was acknowledged positive 3 months after the treatment in groups 1 and 2 (64.30 and 65.10%, respectively), and 6 months after the treatment (65.10 and 66.40%, respectively). Thus, administration of PRP in gonarthrosis cases attenuate pain and improves the quality of life. In terms of alleviation of the clinical symptoms and improvement of the physical component of patients' lives, intraosseous PRP injections performed significantly better.

Keywords: quality of life, pain, intraarticular injection, intraosseous injection

Author contribution: Egiazaryan KA, Danilov MA — study design development, analysis of results; Danilov MA, Abdusalamov RM — data collection, literature review, preparation administration, assessment of the results.

Compliance with ethical standards: the study was approved by the Ethics Committee of the N.I. Pirogov Russian National Research Medical University (Minutes #213 of December 13, 2021).

✉ **Correspondence should be addressed:** Maxim A. Danilov
Ostrovityanova, 1, Moscow, 117997, Russia; md.danilov@gmail.com

Received: 30.01.2024 **Accepted:** 02.03.2024 **Published online:** 19.04.2024

DOI: 10.24075/brsmu.2024.012

ЛЕЧЕНИЕ ГОНАРТРОЗА С ПРИМЕНЕНИЕМ АУТОЛОГИЧЕСКОЙ ОБОГАЩЕННОЙ ТРОМБОЦИТАМИ ПЛАЗМЫ

К. А. Егиазарян, М. А. Данилов ✉, Р. М. Абдусаламов

Российский национальный исследовательский медицинский университет имени Н. И. Пирогова, Москва, Россия

Инъекции плазмы с тромбоцитами рассматривают как перспективный метод лечения. Препараты, воздействующие на субхондральную кость, могут способствовать улучшению структуры ткани и замедлению разрушения суставного хряща. Целью работы было изучить результаты лечения пациентов с гонартрозом путем внутрисуставного и внутрикостного введения обогащенной тромбоцитами плазмы (ОТП). В исследование включены 187 пациентов с 1–3-й стадией, разделенные на три группы. В группе 1 (основная) осуществляли внутрисуставное введение ОТП, в группе 2 (сравнения) — внутрикостные инъекции ОТП. Для оценки использовали визуально-аналоговую шкалу и опросник «SF-36». В группе 1 и 2 было зарегистрировано снижение показателя стартовой боли уже через 3 месяца после проведенного лечения. Снижение частоты синовитов отмечено у пациентов группы 1 через 3 месяца; в группе 2 — через 6 месяцев (21,9 и 31,3% соответственно; $p < 0,05$). Частота регистрации отечности мягких тканей области сустава снижалась через 6 месяцев у пациентов группы 1 и группы 2 (8,2 и 8,3% соответственно). У пациентов группы 1 была выявлена положительная динамика через 3 месяца (70,40%), группы 2 — через 6 месяцев (69,80%) по физическому компоненту качества жизни; у пациентов группы 1 и группы 2 через 3 месяца (64,30 и 65,10% соответственно), через 6 месяцев (65,10 и 66,40% соответственно) — по психическому компоненту. Таким образом, использование ОТП при гонартрозе свидетельствует о снижении боли, улучшении параметров жизни. Внутрикостные инъекции ОТП значительно улучшают клинические симптомы и физическое качество жизни пациентов.

Ключевые слова: качество жизни, боль, внутрисуставное введение, внутрикостное введение

Вклад авторов: К. А. Егиазарян, М. А. Данилов — разработка дизайна исследования, анализ результатов; М. А. Данилов, Р. М. Абдусаламов — сбор данных, обзор литературы, проведение процедур введения, оценка результатов.

Соблюдение этических стандартов: исследование одобрено этическим комитетом ФГАОУ ВО РНИМУ им. Н. И. Пирогова (протокол № 213 от 13 декабря 2021 г.).

✉ **Для корреспонденции:** Максим Александрович Данилов
ул. Островитянова, д. 1, г. Москва, 117997, Россия; md.danilov@gmail.com

Статья получена: 30.01.2024 **Статья принята к печати:** 02.03.2024 **Опубликована онлайн:** 19.04.2024

DOI: 10.24075/vrgmu.2024.012

Osteoarthritis (OA) of the knee (gonarthrosis) is a degenerative progressing joint disease involving loss of articular cartilage [1].

About 13% of women and 10% of men aged 60 and above suffer from symptomatic knee OA. After 70, the prevalence of this pathology increases to 40%. Disregarding age as a factor, the frequency of symptomatic gonarthrosis is approximately 240 cases per 100,000 people per year [2].

Gonarthrosis is a progressive disease; as a rule, the specifics of its pathogenesis lead to a disability.

The causes of damage to the cartilage associated with osteoarthritis are not fully understood, but may stem from constitutional and genetic factors, trauma, overload disease, etc. Recently, pathological changes in the subchondral bone — ischemia and local necrosis — have been receiving

increasing attention as the disease's pathogenetic factors [3]. A history of knee injuries is also considered to be an important aspect [4].

Physical activity restrictions, pain and discomfort associated with movements undermine patients' daily routines and social life, which degrades their quality of life (QOL) [5].

In this connection, investigation of methods of treatment of knee OA is considered to be an important task. With varying efficacy, conservative approaches aim to eliminate clinical manifestations (pain) and partially improve the joint's functional state [6]. However, the respective therapeutic strategies have no effect on the OA pathogenesis and do not help to improve the patients' QOL.

Contemporary orthopedics sees promise in the development and introduction of the new OA treatment techniques that would not only address clinical symptoms but also prevent progression of the pathological process. Injections of platelet-rich plasma (PRP) is one of such techniques [7, 8]. The effects of PRP mainly depend on the platelet secretion products. In addition to organelles, platelet cytoplasm contains many granules carrying over 300 different biologically active substances. There are three types of platelet secretory granules: dense granules (or γ-granules), α-granules and lysosomes. The latter are commonly represented by various enzymes (acid hydrolases). Dense granules contain catecholamines, serotonin, ADP, ATP and calcium, which are involved in the activation of the coagulation cascade. Driven by the growth factors, fibroblasts, endothelial cells and epithelial cells migrate to the injury and multiply there. Subsequently, there forms an extracellular matrix, new vessels grow, and connective tissue matures and remodels. Mediators of α-granules HGF, TNFa, TGFß1, VEGF and EGF deliver the anti-inflammatory effect, and attenuation of inflammation also has an analgesic effect [9–12].

The prupose of this study is to analyze the results of intraarticular and intraosseous administration of platelet-rich plasma (PRP) in knee OA cases.

METHODS

From 2018 through 2022, we examined and treated 187 patients with knee OA, stages 1 through 3 (ages 40 through 70), and subsequently monitored the dynamics of the symptoms and signs of the disease. This part of the study was conducted at the premises of the N. I. Pirogov State Clinical Hospital #1, Moscow, and the Republican Clinical Hospital, Makhachkala (Republic of Dagestan).

The knee OA diagnosis was verified under the applicable regulations [13–15].

The inclusion criteria were: age from 40 to 70 years; knee AO confirmed by radiographic examination; disease stage 1 through 3 under Kellgren classification; walking-associated pain intensity ≥40 mm on the visual analog scale (VAS) over the past 2 weeks; no intake of systemic chondroprotectors and/or cartilage regeneration stimulating drugs within 2 months before the study; no intake of nonsteroidal anti-inflammatory drugs (NSAIDs) for 2 weeks before the study; voluntary consent to participate in the study and adequately cooperate in its context.

The exclusion criteria were: age under 40 and over 70; refusal to participate in the study and/or sign the informed consent form; walking-associated pain intensity <40 mm on VAS; stage 4 damage under Kellgren classification; surgical treatment of gonarthrosis during the previous 6 months; pronounced deformity of the knee joint; exacerbation lasting more than a month; pregnancy and/or lactation; serious or unstable somatic diseases (severe diseases of the liver, cardiovascular system, lungs or kidney, oncological, mental diseases), decompensated diabetes mellitus; intake of tissue regeneration drugs, systemic chondroprotectors withing 2 months before the study; intake of NSAIDs within 2 weeks before the study.

Depending on the technique applied, the patients were divided into three groups. Treatment group (group 1) included 73 patients, 21 male and 52 female, mean age 57.4 ± 2.87 years; they received intraarticular injections of PRP. Comparison group (group 2) included 48 patients, 15 male and 33 female, mean age 56.9 ± 2.85 years; the received intraosseous injections of PRP. Control group (group 3) consisted of 66 people, 21 male and 45 female, means age 57.1 ± 2.86 years; their treatment plan included NSAIDs, a course of chondroprotectors, and a course of glucorticoids administared intraarticularly. In group 1, autologous PRP was injected intraarticularly in a single course, three injections once a week, once a year; in group 2, PRP was injected intraosseously, two injections every two weeks, once a year.

In all groups, the most common stage was 2nd: 37 (50.7%) patients in group 1, 22 patients (45.8%) in group 2, and in 27 (40.9%) patients in the control group. We found no statistically significant intergroup differences in the frequency stage-wise OA diagnosis within the sample.

All patients underwent a comprehensive examination, which included registration of complaints, study of the medical and life history, physical examination and analysis of the objective signs of joint pathology, and assessment of the severity of damage.

Radiography, ultrasonography, and magnetic resonance imaging (MRI) were also parts of the comprehensive primary examination.

The intensity of pain was recorded with the help of the visual analog scale (VAS), and QOL indicators registered with a non-specific SF-36 survey (before treatment, three and six months thereafter).

Statsoft's STATISTICA 10 and Microsoft Excel 2016 (USA) were used for statistical data analysis.

In case of normal distribution of indicators, we applied the Student's test to compare groups, and used the Mann–Whitney test when distribution was nonparametric. Normality of distribution was assessed with the help of the Shapiro-Wilk test. The null hypothesis (α) was considered significant at $p = 0.05$ (all intergroup comparisons).

RESULTS

Figure 1 shows the initial pain intensity dynamics after over 30 minutes of rest.

These data indicate that before the treatment, all patients (100%) experienced pain after resting for more than 30 minutes.

Three months after treatment, in groups 1 and 2, initial pain after over 30 minutes of rest decreased to 64.4 and 47.90%, respectively, from 100%.

After six and twelve months, the intensity of pain in the treatment group increased to 72.60 and 79.50%, respectively, that in the comparison group — to 62.50 and 68.80%, respectively.

In the control group, the dynamics of the initial pain was not significant; it amounted to 92.40% after three months, 93.90% after six months, and 97.0% after twelve months.

Figure 2 shows the dynamics of indicators of morning joint stiffness in the entire sample.

Compared to the control group, both group 1 and group 2 exhibited a significant decrease in the number of complaints about morning joint stiffness.

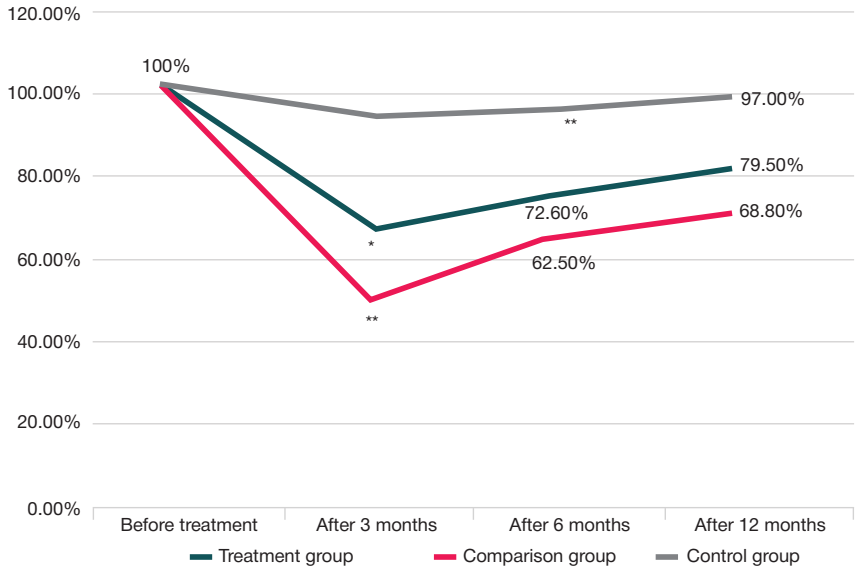

Fig. 1. Initial pain intensity dynamics after over 30 minutes of rest, all groups, percentages. * — significance of differences ($p < 0.05$) between indicators of the control group and those registered for groups 1 and 2; ** — significance of differences ($p < 0.001$) between indicators of the control group and group 2

Table presents the knee OA parameters as registered with ultrasonography.

It should be noted that before treatment, the prevalence of synovitis, soft tissue edema, osteophytes, and subchondral sclerosis was comparable between the groups. In the treatment group, the differences in the prevalence of synovitis became significant (compared to baseline) after three months (27.4%); in the treatment and comparison groups — after six months (21.9 and 31.3%, respectively). As for the prevalence of swelling around the joint, the differences in prevalence thereof became significant after 6 months (treatment and comparison groups, 8.2 and 8.3%, respectively). After 12 months, the differences registered between groups have lost significance, but the lowest values were recorded (ultrasonography) in the treatment group.

Figures 3 and 4 show the results of a comparative analysis of physical and mental components of QOL, as registered with the SF-36 survey; time points — before treatment, 3 and 6 months after treatment.

With treatment in the background, groups 1 and 2 exhibited significant positive dynamics: groups 1 after three months (70.40%), group 2 after six months (69.80%).

Six months after treatment, values of the indicators were above baseline in both group 1 and group 2, with group 2 performing better. In control group, the physical component of QOL, according to the SF-36 survey, did not change throughout the study (51.20% — before treatment; 53.50% — after 3 months; 54.0% — after 6 months).

As registered with the SF-36, against the background of treatment, both group 1 and group 2 have shown positive dynamics of the mental component of QOL after 3 months (64.30 and 65.10%, respectively), and after 6 months (65.10% and 66.40%, respectively). In control group, the situation remained largely unchanged (42.20% before treatment, 44.30% after 3 months, and 44.60% after 6 months).

Figure 5 shows pain intensity as recorded with the help of VAS.

Against the background of treatment, groups 1 and 2 exhibited significant ($p < 0.05$) positive dynamics after 3 and 6 months; after 3 months, the values were better in group 1 (2.80 ± 0.14 and 3.90 ± 0.19, respectively), and after 6 months — in group 2 (3.40 ± 0.17 and 3.0 ± 0.15, respectively). In the control group, therapy failed to relief the pain, and the values remained on the same level throughout the study (before treatment —

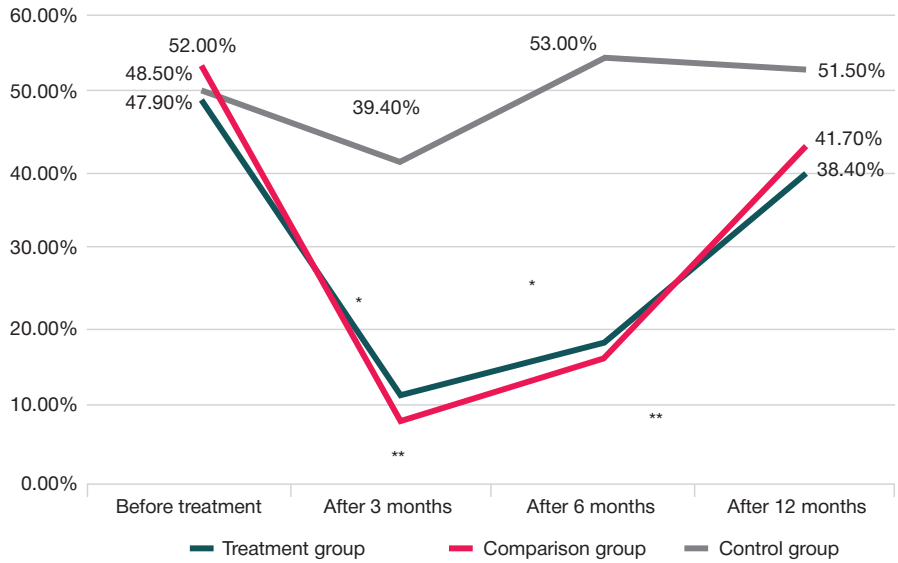

Fig. 2. Morning joint stiffness dynamics, all participants, percentages. * — significance of differences ($p < 0.05$) between indicators of the control group and those registered for groups 1 and 2; ** — significance of differences ($p < 0.001$) between indicators of the control group and groups 1 and 2

Table. Dynamics of ultrasonography indicators of the knee OA against the background of treatment, all patients

Indicators	Treatment group (n = 73)		Comparison group (n = 48)		Control group (n = 66)	
	Abs.	%	Abs.	%	Abs.	%
Before treatment						
Synovitis	55	75.3	37	77.0	49	74.2
Swelling of soft tissues in the joint area	11	15.1	8	16.7	12	18.1
Osteophytes	59	80.8	40	83.3	54	81.8
Subchondral sclerosis	61	83.6	41	85.4	56	84.8
3 months after treatment						
Synovitis	20	27.4*	30	62.5	47	71.2
Swelling of soft tissues in the joint area	8	10.9	6	12.5	5	4.5*
Osteophytes	59	80.8	40	83.3	54	81.8
Subchondral sclerosis	61	83.6	41	85.4	56	84.8
6 months after treatment						
Synovitis	16	21.9*	15	31.3*	45	68.2
Swelling of soft tissues in the joint area	6	8.2*	4	8.3*	5	7.5*
Osteophytes	57	78.1	39	81.3	54	81.8
Subchondral sclerosis	59	80.8	40	83.3	56	84.8
12 months after treatment						
Synovitis	24	32.9	22	45.8	48	72.7
Swelling of soft tissues in the joint area	10	13.7	8	16.7	11	16.7
Osteophytes	57	78.1	39	81.3	54	81.8
Subchondral sclerosis	59	80.8	40	83.3	56	84.8

Note: * — significance of differences ($p < 0.05$) of the indicator values before and after treatment, intragroup.

6.0 ± 0.3; after 3 months — 5.60 ± 0.28; after 6 months — 5.80 ± 0.29; after 12 months — 5.90 ± 0.30).

DISCUSSION

Knee OA is a pathology that grows more prevalent as the life expectancy of the population increases. This diseases poses a significant social, economic and medical problem, the solution of which should employ non-pharmacological, pharmacological, and surgical methods of treatment at different stages. Surgery, in the form of partial or complete knee replacement, is most often resorted to at late stages of knee OA [16–17]. Regenerative approaches, such as those involving PRP and cell therapy, aim to expand the therapeutic arsenal to prevent or delay surgery. While cell therapy is still in its infancy and has to overcome a number of problems, PRP has been used for more than 15 years, and there is a consolidated position about it in the context of treatment of this disease. An increasing number of randomized clinical trials are being conducted to obtain convincing conclusions about the effectiveness and safety of PRP. Despite the fact that intraarticular injection of PRP as knee OA treatment shows promising results, this method, according to a number of authors, affects only the articular cartilage and the synovial membrane, without affecting the subchondral bone. Intraosseous injections to the subchondral bone can make the protocol more comprehensive [18, 19].

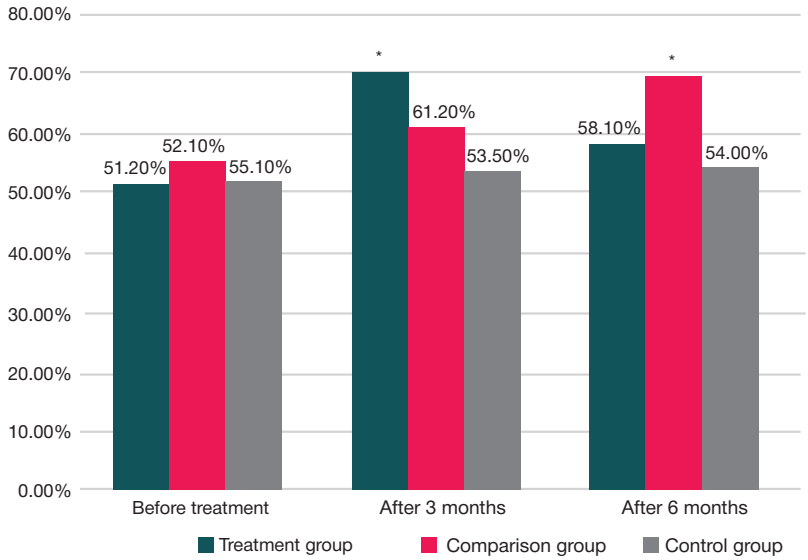

Fig. 3. Dynamics of the physical indicators of QOL, as registered with a SF-36 survey before treatment, 3 and 6 months thereafter. * — significance of differences ($p < 0.05$), indicator's value before and after treatment, intragroup; ** — significance of differences ($p < 0.001$), indicator's values, treatment group and comparison group, 3 and 6 months after treatment

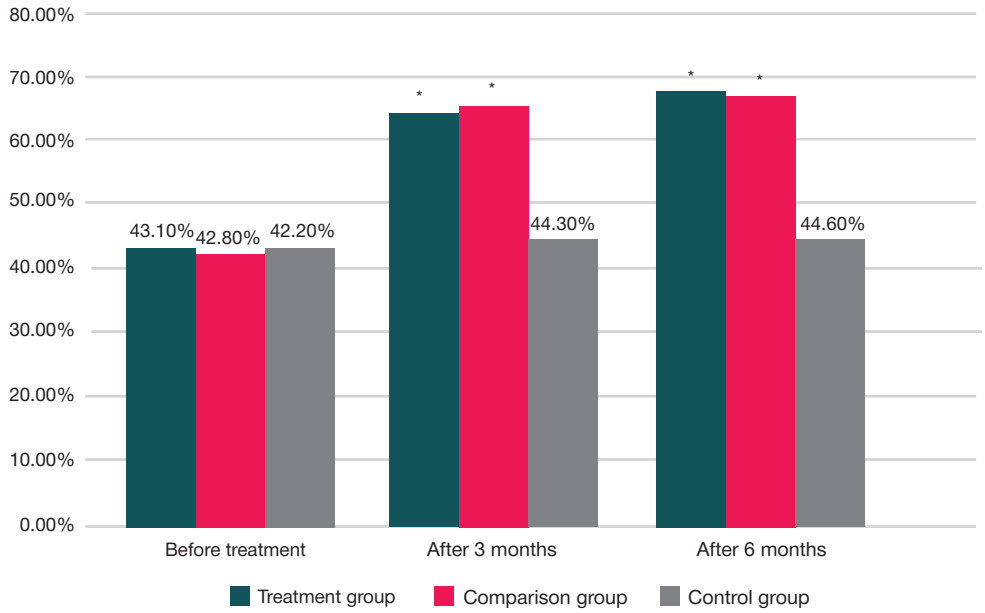

Fig. 4. Dynamics of the mental indicators of QOL, as registered with a SF-36 survey before treatment, 3 and 6 months thereafter. * — significance of differences ($p < 0.05$) of the indicator values before and after treatment.

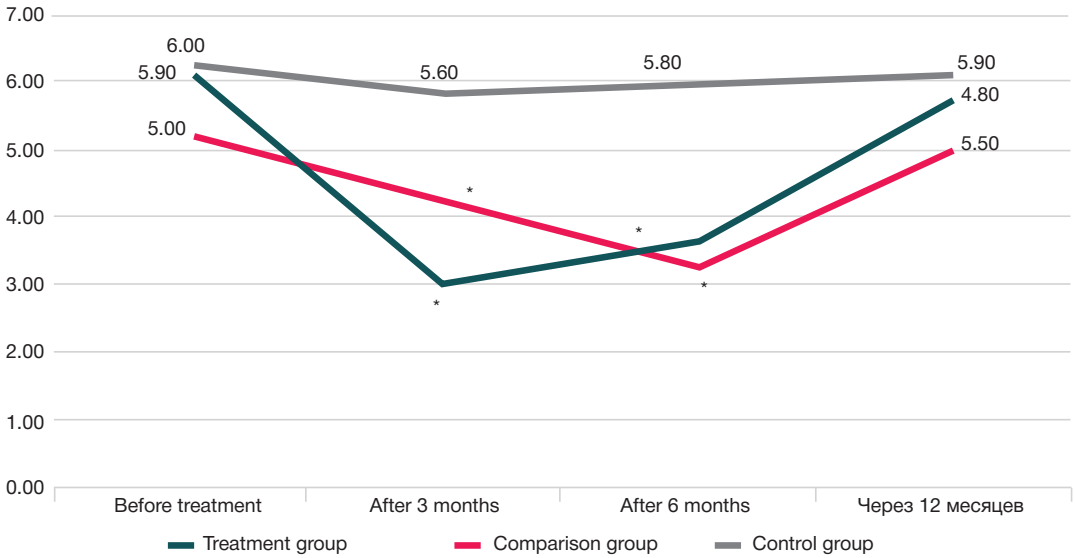

Fig. 5. Pain intensity, VAS registration, all patients (points). * — significance of differences ($p < 0.05$), indicator's value compared to control group; ** — significance of differences ($p < 0.001$), indicator's values, treatment group and comparison group compared

Currently, clinical studies of intraosseous administration of PRP in treatment of knee OA are in the early stages. The rationale for this method largely depends on the growing knowledge about the role of the bone-cartilaginous functional unit in the development of knee OA, as well as on growth of the number of preclinical studies and intraosseous methods of treatment of other bone pathologies [20, 21]. Further research is needed in this area to better understand cellular processes underlying the mechanism of action and to plan further pathways of intraosseous injections.

CONCLUSIONS

Compared to standard therapy, which relies on NSAIDs, chondroprotectors, and intraarticular administration of glucocorticoids, administration of PRP in OA cases yields significantly better results in terms of pain intensity and QOL parameters. Intraosseous injection of PRP allows achieving significantly better results in terms of clinical symptoms and physical component of the patients' QOL.

References

1. Hsu H, Siwiec RM. Knee Osteoarthritis. [Updated 2023 Jun 26]. In: StatPearls [Internet]. Treasure Island (FL): StatPearls Publishing. 2023. Available from: https://www.ncbi.nlm.nih.gov/books/NBK507884/.
2. Magnusson K, Turkiewicz A, Englund M. Nature vs nurture in knee osteoarthritis — the importance of age, sex and body mass index. Osteoarthritis Cartilage. 2019; 27 (4): 586–92.
3. Egiazaryan KA, Lazishvili GD, et al. Knee osteochondritis desiccans: surgery algorithm. Bulletin of RSMU. 2018; 2: 73–78.
4. Egiazaryan KA, Cherkasov SN, Attaeva LZh. Analiz struktury pervichnoj zabolevaemosti po klassu travmy, otravlenija i nekotorye drugie posledstvija vozdejstvija vneshnih prichin vzroslogo naselenija Rossijskoj Federacii. Kafedra travmatologii i

ortopedii. 2017; 1: 25–27. Russian.
5. Li JS, Tsai TY, Clancy MM, Li G, Lewis CL, Felson DT. Weight loss changed gait kinematics in individuals with obesity and knee pain. Gait Posture. 2019; 68: 461–5.
6. Vasileva LV, Lahin DI. Vlijanie metabolicheskogo sindroma na klinicheskuju kartinu osteoartroza. Medicinskij Vestnik Severnogo Kavkaza. 2017; 12 (1): 8–11. Russian.
7. Guseva AI, Tagilceva YuS. Primenenie obogashhennoj trombocitami plazmy v lechenii zabolevanij oporno-dvigatel'nogo apparata. Alleja nauki. 2018; 6 (5): 148–51. Russian.
8. Cui Y, Lin L, Wang Z, Wang K, Xiao L, Lin W, et al. Research trends of platelet-rich plasma therapy on knee osteoarthritis from 2011 to 2021: A review. Medicine (Baltimore). 2023; 102 (2): e32434.
9. Wang L, et al. Comparison of the effects of autologous and allogeneic purified platelet-rich plasma on cartilage damage in a rabbit model of knee osteoarthritis. Front Surg. 2022; 9: 911468.
10. Wang Y, et al. Clinical efficacy of platelet-rich plasma as adjuvant therapy in patients undergoing arthroscopic repair of meniscal injury. J Int Med Res. 2020; 48 (9): 300060520955059.
11. Sheean AJ, Anz AW, Bradley JP. Platelet-rich plasma: fundamentals and clinical applications. Arthroscopy. 2021; 37 (9): 2732–4.
12. dos Santos RG; et al. The regenerative mechanisms of platelet-rich plasma: A review. Cytokine. 2021; 144: 155560.
13. Ob utverzhdenii standarta pervichnoj mediko-sanitarnoj pomoshhi pri gonartroze i shodnyh s nim klinicheskih sostojanijah. Prikaz Ministerstva zdravoohranenija RF ot 24 dekabrja 2012 g. # 1498n. M., 2012. Russian.
14. Nasonov EL, redaktor. Rossijskie klinicheskie rekomendacii. Revmatologija pod red. M.: GJeOTAR-Media, 2017; 464 s. Russian.
15. Bruyère O, et al. A consensus statement on the European Society for Clinical and Economic Aspects of Osteoporosis and Osteoarthritis (ESCEO) algorithm for the management of knee osteoarthritis — from evidence-based medicine to the real-life setting. Seminars in arthritis and rheumatism. WB Saunders. 2016; 45 (4): S3-S11.
16. Moretti L, Maccagnano G, Coviello M, Cassano GD, Franchini A, Laneve A, et al. Platelet rich plasma injections for knee osteoarthritis treatment: A prospective clinical study. J Clin Med. 2022; 11 (9): 2640.
17. Cui Yubo, Lin Liqiong, Wang Zhiwei, Wang Kai, Xiao Lili, Lin Wentao, et al. Research trends of platelet-rich plasma therapy on knee osteoarthritis from 2011 to 2021: A review. Medicine. 2023; 102 (2): e32434.
18. Patel S, Rajnish RK, Baburaj V, Kumar P, Sharma S, Kumar V. Intraosseous infiltration of platelet-rich plasma for knee osteoarthritis: A systematic review of literature and limited meta-analysis. Indian J Orthop. 2022; 56 (11): 1847–57. DOI: 10.1007/s43465-022-00737-x. PMID: 36310547; PMCID: PMC9561501.
19. Sánchez M, Jorquera C, de Dicastillo LL, et al. Real-world evidence to assess the effectiveness of platelet-rich plasma in the treatment of knee degenerative pathology: a prospective observational study. Therapeutic Advances in Musculoskeletal Disease. 2022; 14. DOI: 10.1177/1759720X221100304.
20. Torres-Torrillas M, Damia E, Romero Ad, Pelaez P, Miguel-Pastor L, Chicharro D, et al. Intra-osseous plasma rich in growth factors enhances cartilage and subchondral bone regeneration in rabbits with acute full thickness chondral defects: Histological assessment. Front Vet Sci. 2023; 10: 1131666. DOI: 10.3389/fvets.2023.1131666.
21. Torres-Torrillas M, Damiá E, Peláez P, Miguel-Pastor L, Cuervo B, Cerón JJ, et al. Intra-osseous infiltration of adipose mesenchymal stromal cells and plasma rich in growth factors to treat acute full depth cartilage defects in a rabbit model: serum osteoarthritis biomarkers and macroscopical assessment. Front Vet Sci. 2022; 9: 1057079. DOI: 10.3389/fvets.2022.1057079.

Литература

1. Hsu H, Siwiec RM. Knee Osteoarthritis. [Updated 2023 Jun 26]. In: StatPearls [Internet]. Treasure Island (FL): StatPearls Publishing. 2023. Available from: https://www.ncbi.nlm.nih.gov/books/NBK507884/.
2. Magnusson K, Turkiewicz A, Englund M. Nature vs nurture in knee osteoarthritis — the importance of age, sex and body mass index. Osteoarthritis Cartilage. 2019; 27 (4): 586–92.
3. Егиазарян К. А., Лазишвили Г. Д. и др. Алгоритм хирургического лечения больных с рассекающим остеохондритом коленного сустава. Вестник Российского государственного медицинского университета. 2018; 2: 77–83.
4. Егиазарян К. А., Черкасов С. Н., Аттаева Л. Ж. Анализ структуры первичной заболеваемости по классу травмы, отравления и некоторые другие последствия воздействия внешних причин взрослого населения Российской Федерации. Кафедра травматологии и ортопедии. 2017; 1: 25–27.
5. Li JS, Tsai TY, Clancy MM, Li G, Lewis CL, Felson DT. Weight loss changed gait kinematics in individuals with obesity and knee pain. Gait Posture. 2019; 68: 461–5.
6. Васильева Л. В., Лахин Д. И. Влияние метаболического синдрома на клиническую картину остеоартроза. Медицинский Вестник Северного Кавказа. 2017; 12 (1): 8–11.
7. Гусева А. И., Тагильцева Ю. С. Применение обогащенной тромбоцитами плазмы в лечении заболеваний опорно-двигательного аппарата. Аллея науки. 2018; 6 (5): 148–51.
8. Cui Y, Lin L, Wang Z, Wang K, Xiao L, Lin W, et al. Research trends of platelet-rich plasma therapy on knee osteoarthritis from 2011 to 2021: A review. Medicine (Baltimore). 2023; 102 (2): e32434.
9. Wang L, et al. Comparison of the effects of autologous and allogeneic purified platelet-rich plasma on cartilage damage in a rabbit model of knee osteoarthritis. Front Surg. 2022; 9: 911468.
10. Wang Y, et al. Clinical efficacy of platelet-rich plasma as adjuvant therapy in patients undergoing arthroscopic repair of meniscal injury. J Int Med Res. 2020; 48 (9): 300060520955059.
11. Sheean AJ, Anz AW, Bradley JP. Platelet-rich plasma: fundamentals and clinical applications. Arthroscopy. 2021; 37 (9): 2732–4.
12. dos Santos RG; et al. The regenerative mechanisms of platelet-rich plasma: A review. Cytokine. 2021; 144: 155560.
13. Об утверждении стандарта первичной медико-санитарной помощи при гонартрозе и сходных с ним клинических состояниях. Приказ Министерства здравоохранения РФ от 24 декабря 2012 г. № 1498н. М., 2012.
14. Насонов Е. Л., редактор. Российские клинические рекомендации. Ревматология под ред. М.: ГЭОТАР-Медиа, 2017; 464 с.
15. Bruyère O, et al. A consensus statement on the European Society for Clinical and Economic Aspects of Osteoporosis and Osteoarthritis (ESCEO) algorithm for the management of knee osteoarthritis — from evidence-based medicine to the real-life setting. Seminars in arthritis and rheumatism. WB Saunders. 2016; 45 (4): S3-S11.
16. Moretti L, Maccagnano G, Coviello M, Cassano GD, Franchini A, Laneve A, et al. Platelet rich plasma injections for knee osteoarthritis treatment: A prospective clinical study. J Clin Med. 2022; 11 (9): 2640.
17. Cui Yubo, Lin Liqiong, Wang Zhiwei, Wang Kai, Xiao Lili, Lin Wentao, et al. Research trends of platelet-rich plasma therapy on knee osteoarthritis from 2011 to 2021: A review. Medicine. 2023; 102 (2): e32434.
18. Patel S, Rajnish RK, Baburaj V, Kumar P, Sharma S, Kumar V. Intraosseous infiltration of platelet-rich plasma for knee osteoarthritis: A systematic review of literature and limited meta-analysis. Indian J Orthop. 2022; 56 (11): 1847–57. DOI: 10.1007/s43465-022-00737-x. PMID: 36310547; PMCID: PMC9561501.
19. Sánchez M, Jorquera C, de Dicastillo LL, et al. Real-world evidence to assess the effectiveness of platelet-rich plasma in the treatment of knee degenerative pathology: a prospective observational study. Therapeutic Advances in Musculoskeletal Disease. 2022; 14. DOI: 10.1177/1759720X221100304.
20. Torres-Torrillas M, Damia E, Romero Ad, Pelaez P, Miguel-Pastor L, Chicharro D, et al. Intra-osseous plasma rich in growth factors enhances cartilage and subchondral bone regeneration in rabbits with acute full thickness chondral defects: Histological

assessment. Front Vet Sci. 2023; 10: 1131666. DOI: 10.3389/fvets.2023.1131666.
21. Torres-Torrillas M, Damiá E, Peláez P, Miguel-Pastor L, Cuervo B, Cerón JJ, et al. Intra-osseous infiltration of adipose mesenchymal stromal cells and plasma rich in growth factors to treat acute full depth cartilage defects in a rabbit model: serum osteoarthritis biomarkers and macroscopical assessment. Front Vet Sci. 2022; 9: 1057079. DOI: 10.3389/fvets.2022.1057079.

MULTIDISCIPLINARY APPROACH TO TREATMENT OF UNRESECTABLE LIVER METASTASES SEEDED BY LUMINAL BREAST CARCINOMA

Kolomiets KV ✉, Afashagova ZR, Erendzhenova DE, Bashirova AS, Falchari VV, Babayeva NE, Aliyeva AD, Kurmalieva RZ, Fedoseyev YB

Rostov State Medical University, Rostov-on-Don, Russia

Breast cancer (BC) remains the main oncological pathology in the female population. Liver metastases in such cases mean an extremely unfavorable prognosis of the course of the disease. The key predictor of clinical outcome of metastatic BC is the molecular biological subtype of the tumor. The main goals of treatment of metastatic BC are to increase life expectancy, alleviate tumor-related symptoms, and maintain or improve patients' quality of life. Transarterial chemoembolization (TACE) enables new ways of liver metastases control. This article presents a case of application of TACE in combination with hormone therapy and selective inhibitors of CDK4/6 in a patient with unresectable liver metastases seeded by hormone-receptor positive (ER^+/PR^-) breast carcinoma with an unknown Her2 status (2^+). The approach allowed achieving regression of the oncological process in the liver to the point of unclear CT visualizations of metastatic foci, and proper disease control in the course of 28 months.

Keywords: breast cancer, transarterial chemoembolization, hormone therapy, taxanes, selective inhibitors of cyclin-dependent kinases (CDK 4/6), liver metastases

Author contribution: Kolomiets KV — article authoring, editing; Afashagova ZR, Erendzhenova DE — literature review, article authoring, data analysis; Bashirova AS, Falchari VV — literature review, data collection, article authoring; Babayeva NE, Aliyeva AD — concept and design, literature review, article authoring; Kurmalieva RZ, Fedoseyev YuB — literature review, article authoring and editing.

Compliance with ethical standards: the patient signed a voluntary informed consent to publication of anonymized medical information.

✉ **Correspondence should be addressed:** Karina V. Kolomiets
Krasnoarmeyskaya st., 198, Novocherkassk, 346400, Russia; karina_kolomiets_99@mail.ru

Received: 19.02.2024 **Accepted:** 18.04.2024 **Published online:** 29.04.2024

DOI: 10.24075/brsmu.2024.014

МУЛЬТИДИСЦИПЛИНАРНЫЙ ПОДХОД К ЛЕЧЕНИЮ НЕРЕЗЕКТАБЕЛЬНОГО МЕТАСТАТИЧЕСКОГО ПОРАЖЕНИЯ ПЕЧЕНИ ПРИ ЛЮМИНАЛЬНОМ РАКЕ МОЛОЧНОЙ ЖЕЛЕЗЫ

К. В. Коломиец ✉, З. Р. Афашагова, Д. Э. Эрендженова, А. С. Баширова, В. В. Фалчари, Н. Э. Бабаева, А. Д. Алиева, Р. З. Курмалиева, Ю. Б. Федосеев

Ростовский государственный медицинский университет, Ростов-на-Дону, Россия

Рак молочной железы (РМЖ) остается основной онкологической патологией у женского населения. Наличие метастазов в печени при РМЖ определяет крайне неблагоприятный прогноз течения заболевания. Молекулярно-биологический подтип опухоли является главным предиктором клинического исхода при метастатическом РМЖ. Основной целью лечения метастатического РМЖ является увеличение продолжительности жизни, уменьшение симптомов, связанных с опухолью, поддержание или улучшение качества жизни пациентов. Внедрение трансартериальной химиоэмболизации (ТАХЭ) открыло новые возможности контроля над метастатическим поражением печени. В статье представлен клинический случай использования методики ТАХЭ в комбинации с гормонотерапией, а также селективными ингибиторами циклин-зависимых киназ CDK4/6 у пациентки при нерезектабельном метастатическом поражении печени карциномы молочной железы с положительным гормональным статусом (ER^+/PR^-) и неопределенным Her2-статусом (2^+). Подход позволил достигнуть регресса онкологического процесса в печени, вплоть до отсутствия четкой визуализации метастатических очагов в ней при компьютерной томографии органов брюшной полости, а также контролировать течение заболевания на протяжении 28 месяцев.

Ключевые слова: рак молочной железы, трансартериальная химиоэмболизация, гормонотерапия, таксаны, селективные ингибиторы циклин-зависимых киназ CDK 4/6, метастатическое поражение печени

Вклад авторов: К. В. Коломиец — написание статьи, редактирование; З. Р. Афашагова, Д. Э. Эрендженова — обзор литературы, написание статьи, анализ данных; А. С. Баширова, В. В. Фалчари — обзор литературы, сбор данных, написание статьи; Н. Э. Бабаева, А. Д. Алиева — концепция и дизайн, обзор литературы, написание статьи; Р. З. Курмалиева, Ю. Б. Федосеев — обзор литературы, написание и редактирование статьи.

Соблюдение этических стандартов: пациент подписал добровольное информированное согласие на публикацию персональной медицинской информации в обезличенной форме.

✉ **Для корреспонденции:** Карина Викторовна Коломиец
ул. Красноармейская, д. 198, г. Новочеркасск, 346400, Россия; karina_kolomiets_99@mail.ru

Статья получена: 19.02.2024 **Статья принята к печати:** 18.04.2024 **Опубликована онлайн:** 29.04.2024

DOI: 10.24075/vrgmu.2024.014

Breast cancer (BC) is the most common neoplasm that remains the main oncological pathology in the female population. In 2022, 2,296,840 new BC cases were registered in the world (first-time oncological diagnoses), and the disease was pronounced cause of death for 666,103 fatalities. As for the Russian Federation (RF), in 2020, there were 75,052 (12.7%) new cases of BC diagnosed there, and 23,130 lethal outcomes caused by it [1]. This is a very heterogeneous disease, with different molecular profiles, which are clinically divided into three main subtypes by the hormone receptors involved (estrogen receptors, ER; progesterone receptors, PR; human epidermal growth factor receptor 2, HER2 or ERBB2), and into luminal ER-positive and PR-positive, which are further subdivided into luminal A and B, HER2-positive and triple-negative BC. Nuclear protein Ki-67 encoded by the MK167 gene is also regarded as a marker of tumor's proliferation, since neoplasms of the least mature and differentiated cells are the most active in this respect [2]. The mandatory component of a BC treatment protocol is drug therapy: it can significantly increase life expectancy of patients with extensive or metastatic cancer, which prevent full recovery, and up the number of patients that recover from early stages of the disease [3].

The median overall survival (OS) after detection of BC-seeded liver metastases is 18–24 months; five- and ten-year survival

rates in such cases are 27% and 13%, respectively. Without effective treatment of metastatic liver damage, the prognosis is extremely unfavorable, with patients living a maximum of 4 through 8 months [4]. The best OS after detection of such damage is 38 months, peculiar to HER2-positive subtypes with mandatory anti-HER2 therapy in the background. In triple-negative BC cases, the median survival of patients with foci in the liver is only 9 months. For luminal A- and B-subtypes, OS fluctuates within a very large range and depends on the therapy regimen; the median before administration of iCDk is 21 months. These inhibitors significantly increase progression-free survival and OS in metastatic BC patients, even when there are liver metastases. In the placebo group, the median OS of patients without metastatic liver damage was 51.7 months, and metastases reduced this indicator to 36.1 months. Ribociclib allowed prolonging lives of such patients by 10 months, with median OS increasing to 46.5 months. Cyclin-dependent kinases (CDK4 and CDK6) are activated upon formation with D-cyclins; they play a major role in signaling pathways regulating cell cycle and cell proliferation. There are three CDK4/6 inhibitors — palbociclib, ribociclib, and abemaciclib — available for women with advanced or metastatic breast cancer, HR^+ as well as $HER2^-$. Three large-scale randomized trials PALOMA-2, MONALEESA-2, and MONARCH-3 have confirmed the efficacy of including palbociclib, ribociclib, and abemaciclib, respectively, to first-line therapy regimens for menopausal women in combination with aromatase inhibitors. Systemic therapy is the basis of treatment of metastatic BC [5, 6].

Adoption of radiographically controlled endovascular surgery methods, such as TACE, opened new ways to control liver metastases. This technique involves injection of a combination of chemotherapy drugs and microspheres, which slow down and stop supply of oxygen and nutrients to the tumor, into arteries that feed it. This minimally invasive method is applicable to both primary and metastatic cancers. It was developed and first applied in the late 1970s. Currently, the technique is used against tumors of various localizations; in particular, it is a common and effective choice in cases of unresectable liver metastases that originate from neoplasms in the colon, mammary glands, lungs, soft tissue sarcomas and melanomas. Depending on the extent of the lesion, TACE can be palliative treatment, or a procedure in the context of preparation of the patient to surgery, radiofrequency ablation, radiation therapy, etc. [7]. The preferred combinations include doxorubicin (or similar) and 5-fluorouracil, administered simultaneously with taxanes.

There is a systematic analysis of studies investigating application of TACE in cases of BC seeding liver metastases [8]. The researchers explored respective papers published from 2000 through 2017, and included only 10 of them into their work, with the total sample comprised of 519 patients. In that sample, only TACE was used in 78.0% of cases, TACE and systemic chemotherapy — in 9.9% of cases, and systemic chemotherapy alone in 12.1% of cases. The analysis has shown that the patients who underwent TACE had higher OS (median of 7.3–47.0 months) and disease-free survival (in the range from 2.9 through 17.0 months) [8].

This study aimed to evaluate the efficacy of a multidisciplinary approach to a case of liver metastases seeded by BC, the said approach involving TACE combined with taxanes (docetaxel), selective CDK4/6 inhibitors, and hormonal therapy.

Case description

A 57-year-old patient was diagnosed with right breast cancer in 2018 (C50), pT2N3M0, st IIIc, cl.gr. 2; the diagnosis was followed by radical mastectomy (RME) on the right side, remote gamma therapy (RGT), hormone therapy (tamoxifen).

Control examination results

Results of chest and abdominal CT, 22.12.2021: lungs without focal and infiltrative changes; density of liver parenchyma uneven, multiple metastatic foci up to 2.6 cm in both lobes (previously undiscovered) (Fig. 1A, B).

Despite multiple liver metastases, biliary tract was not compressed, and the patient's skin and mucous membranes had physiological color. She did not complain of itching, considered her condition satisfactory, and her biochemical indicators were within the reference ranges.

Results of US examination of mammary glands, 22.12.2021: no signs of recurrence and palpable abnormalities.

Results of immunohistochemical (IHC) examination of a liver metastasis sample (trephine biopsy), 29.12.2021: confirmed metastasis seeded by breast carcinoma, ER^+/PR^- and unknown Her2 status (2^+).

In view of the extent of the process and the results of IHC examination, the patient was recommended hormone therapy: letrozole 2.5 mg per day orally protractedly, ribociclib 600 mg per day orally from the 1st to the 21st days, interval of 7 days.

Diagnosis: (C50) right breast cancer, pT2N3M0, st IIIc, cl. gr. 2, complex treatment in 2018-2019 — RME on the right side, RGT, hormone therapy, December 2021 — progression (HER).

The patient self-referred to the clinic of Rostov State Medical University in December 2021; factoring in the volume of liver damage, the history of the disease and the results of

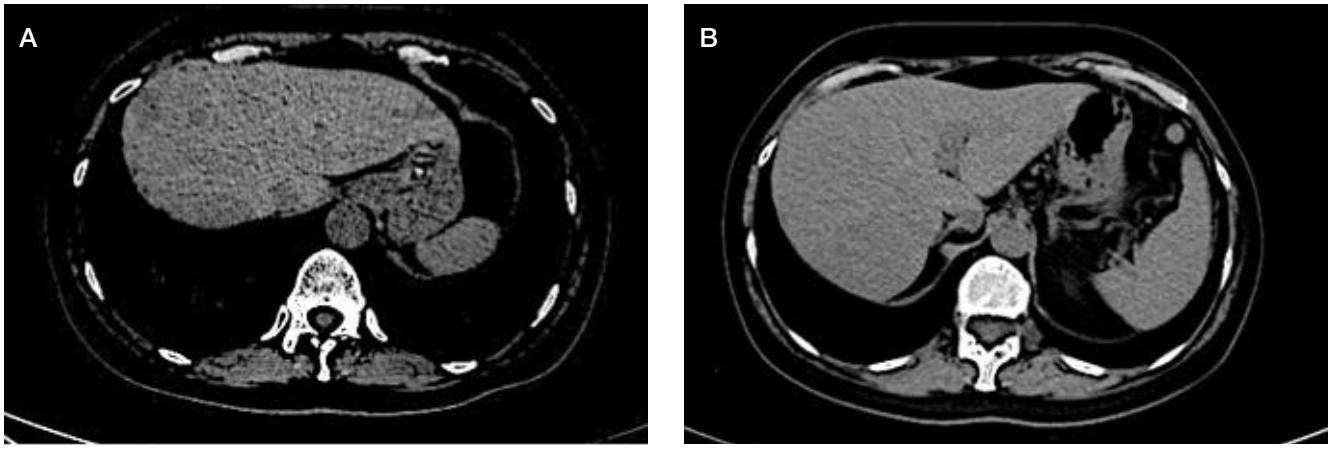

Fig. 1. A, **B**. Abdominal CT, 22.12.2021. multiple metastatic foci (size up to 2.6 cm) in both lobes

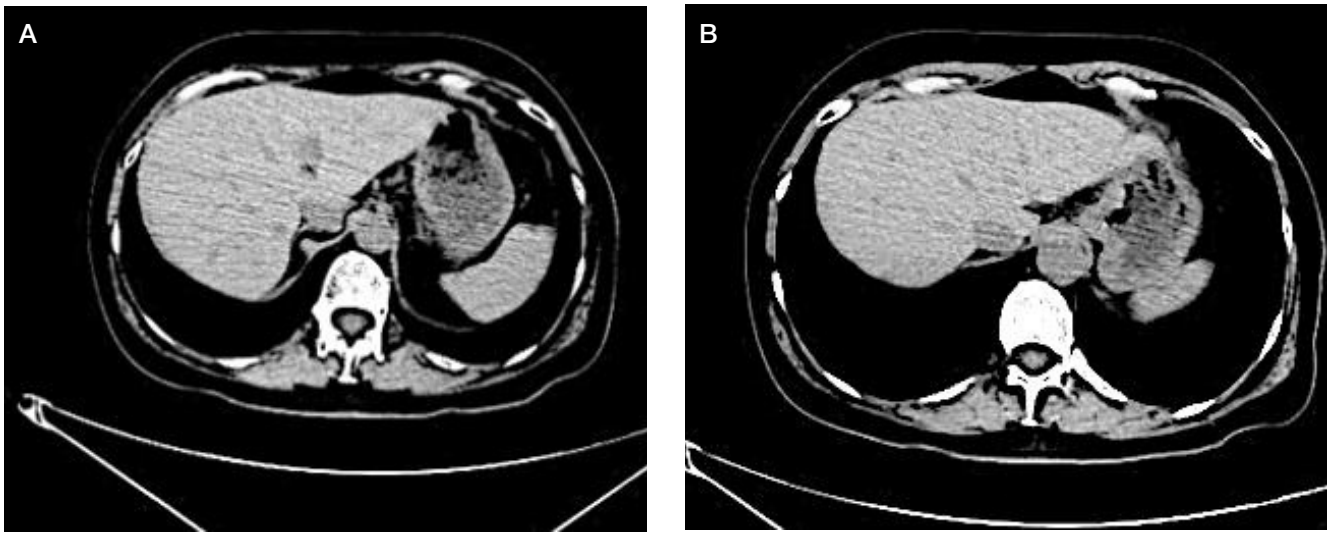

Fig. 2. A, **B**. Abdominal CT, 04.05.2022. Multiple metastatic foci (size up to 2.6 cm) in both lobes, uneven opacification; no changes since December 2021

instrumental examinations, as well as the extent of the process, the council decided it was expedient to include locoregional therapy (TACE) in the treatment regimen.

On 27.01.2022, the patient underwent TACE aimed at metastatic foci in the liver (docetaxel 150 mg + microspheres). When discharged, the patient assessed her condition as satisfactory, despite the volume of metastatic foci; her body temperature was slightly elevated during the first day after TACE. Further, as per recommendations of the chemotherapist, she received hormone therapy (anastrozole) and CDK4/6 inhibitors.

Description of the surgical intervention

Under aseptic conditions of the operating room with radiographic control equipment, following the required surgical field treatment, the patient, supine, had her left radial artery punctured in a typical location (angiographic needle 18G), using the Seldinger technique (introducer 5F 11 cm). Through a 035" 180 cm hydrophilic conductor, an H1 125 cm catheter was sequentially inserted into the left brachial, axillary, subclavian arteries, descending thoracic aorta. Removal of the conductor was followed by aortography, which established that the celiac trunk deviates at the L1 level. Celiac trunk's mouth was selectively catheterized: cranial position, splenic artery not dilated, convoluted, gastric branches (anastomoses) not found hypertrophied. The common hepatic artery could not be visualized; left hepatic artery branches from the celiac trunk, and in the middle section, the gastroduodenal artery branches off it. Selective catheterization of the superior mesenteric artery yielded visualization of the right hepatic artery extending from the proximal part of the superior mesenteric artery. The left and then the right hepatic arteries were selectively catheterized; angiography visualized hypervascular lumps in the projection of both lobes of the liver. Afferent tumor arteries were superselectively catheterized using a 1.98F microcatheter in a 014" 165 cm microconductor. Falciform ligament artery was embolized with a Concerto 5 × 15 cm spiral (protection against inappropriate embolization). Saturated with a chemotherapy drug (docetaxel 150 mg), 150–200 nm HepaSphere microspheres (Merit Medical; USA) were injected to achieve chemoembolization of arteries supplying blood to metastatic foci. Then microcatheter was removed. Control angiography revealed a significantly slower opacification in segmental branches of hepatic artery that deliver blood to multiple tumor foci. There were no signs of inappropriate embolization. The catheter was withdrawn into the aorta; control angiography revealed right and left hepatic, gastroduodenal, and superior mesenteric arteries to be uncompromised. The instruments were removed sequentially, with introducer pulled out last. Hemostasis by compression — 8 min (stable). The operative field was treated with alcohol and covered with an aseptic pressure bandage.

The postoperative pharmacotherapy included:

– analgesia: ketoprofen 100 mg IM twice a day for 5 days; drotaverine 40 mg IM twice a day for 5 days;

– prevention of thromboembolic complications: parnaparin sodium 0.3 ml SC once a day for 7 days;

– infusion therapy: for hepatoprotective purposes — remaxol 400 ml IV once a day for 3 days, for prevention of ulcerative complications — NaCl 0.9% 500 ml + 40 mg omeprazole IV once a day for 3 days.

Results of chest and abdominal CT, 04.05.2022: no focal and infiltrative changes in the lungs, liver parenchyma density uniform, multiple metastatic foci (size up to 2.6 cm) in both lobes accumulate contrast (Omnipak) unevenly, no changes since December 2021. Given the extent of damage to the liver, process dispersion and dynamics, in was decided to keep liver TACE in the treatment plan (Fig. 2A, B).

The decision to repeat TACE was made on 18.05.2022.

The patient underwent chemoembolization of metastatic foci in the liver and parenchymal chemoembolization of arteries supplying the foci (lipiodol 10 ml + docetaxel 150 mg). A hemostatic sponge suspension was used for arterial embolization. After surgery, the patient was prescribed pharmacotherapy as recommended earlier, after the first TACE of 27.01.2022, and subsequent therapy with hormones (anastrozole) and CDK4/6 inhibitors.

Control examination of 18.07.2022 included CT of the brain, chest and abdominal organs. Conclusion: no pathological changes discovered in the brain, neck, chest organs; multiple metastatic foci (size up to 2.1 cm) identified in both lobes of the liver (Fig. 3A, B).

Given the extent of damage to the liver, process dispersion and dynamics, in was decided to keep liver TACE in the treatment plan.

The decision to repeat TACE was made on 26.07.2022. Metastatic foci in the liver were chemoembolized. After superselective catheterization, right gastric artery was embolized (to prevent inappropriate embolization) using Amplatzer Vascular Plug II 9-AVP2-016 vascular occluder (Abbot; USA).

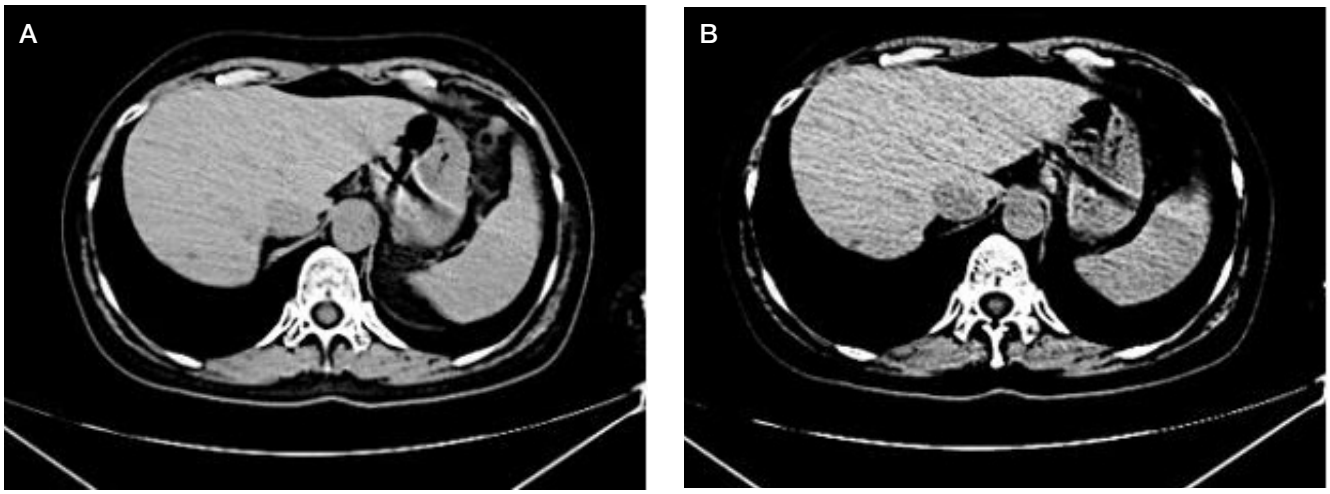

Fig. 3. A, **B**. Abdominal CT, 18.07.2022. Multiple metastatic foci (size up to 2.1 cm) in both lobes of the liver; positive dynamics compared to 04.05.2022

Chemoembolization (docetaxel 150 mg + hemostatic sponge suspension) was performed after superselective catheterization of afferent tumor arteries. After surgery, the patient was prescribed pharmacotherapy as recommended earlier, after the first TACE of 27.01.2022.

Following studies were conducted to verify the results achieved.

Abdominal CT, 26.09.2022: the contours of the liver are smooth, clear, the liver not enlarged, parenchyma's density uniform, multiple metastatic foci (size up to 2.1 cm) in both lobes of the liver (unchanged since 18.07.2022) (Fig. 4A, B).

Abdominal CT, 30.11.2022: parenchyma's density uniform, multiple metastatic foci (size up to 1.5 cm) in both lobes of the liver. Positive dynamics, size and number of foci reduced since 26.09.2022. The effectiveness of TACE was evaluated a month later using CT/MRI scans with intravenous contrasting, relying on RECIST 1.1 (Response evaluation criteria in solid tumours); the evaluation confirmed a partial response, regression: >30% of the sum of the largest sizes (long axes) of foci. Given the extent of damage to the liver, process dispersion and dynamics, in was decided to keep liver TACE in the treatment plan (Fig. 5A, B).

The decision to repeat TACE was made on 05.12.2022. The patient was hospitalized on 05.12.2022, and on 06.12.2022 she underwent 4th TACE procedure, aimed at liver metastases. Chemoembolization (docetaxel 150 mg + hemostatic sponge suspension) was performed after superselective catheterization of afferent tumor arteries.

After surgery, the patient was prescribed pharmacotherapy as recommended earlier, after the first TACE of 27.01.2022. Further, as per recommendations of the chemotherapist, she received hormone therapy (anastrozole) and CDK4/6 inhibitors.

On 01.03.2023, a control abdominal CT has shown the following: parenchyma's density uniform, single metastatic foci (size up to 0.9 cm) in both lobes, smaller compared to 30.11.2022; positive dynamics confirmed with RECIST 1.1 (Fig. 6A, B).

On 03.06.2023, the patient visited chemotherapist as scheduled; positive dynamics, satisfactory haematological parameters and absence of somatic contraindications allowed recommending continuation of hormone therapy: CDK4/6 inhibitors — ribociclib 600 mg or palbociclib 125 mg orally from day 1 to day 21, with an interval of 7 days, protractedly, a cycle of 28 days, plus aromatase inhibitors — letrozole 2.5 mg or anastrazole 1 mg daily, protractedly.

Results of chest and abdominal CT, 03.10.2023: metastatic foci in the liver not visualized clearly since 01.03.2023; parenchyma's density uniform, without localized condensation or rarefication spots (Fig. 7A, B).

Given the positive dynamics, satisfactory haematological parameters and absence of somatic contraindications, it was recommended to continue with the combined therapy: CDK4/6 inhibitors — ribociclib 600 mg or palbociclib 125 mg orally from day 1 to day 21, with an interval of 7 days, protractedly, a cycle of 28 days, plus aromatase inhibitors — letrozole 2.5 mg or anastrazole 1 mg daily, protractedly.

Results of CT, 15.01.2024: no pathological changes discovered in the brain, neck, chest organs; metastatic foci in the liver not visualized clearly since 03.10.2023;

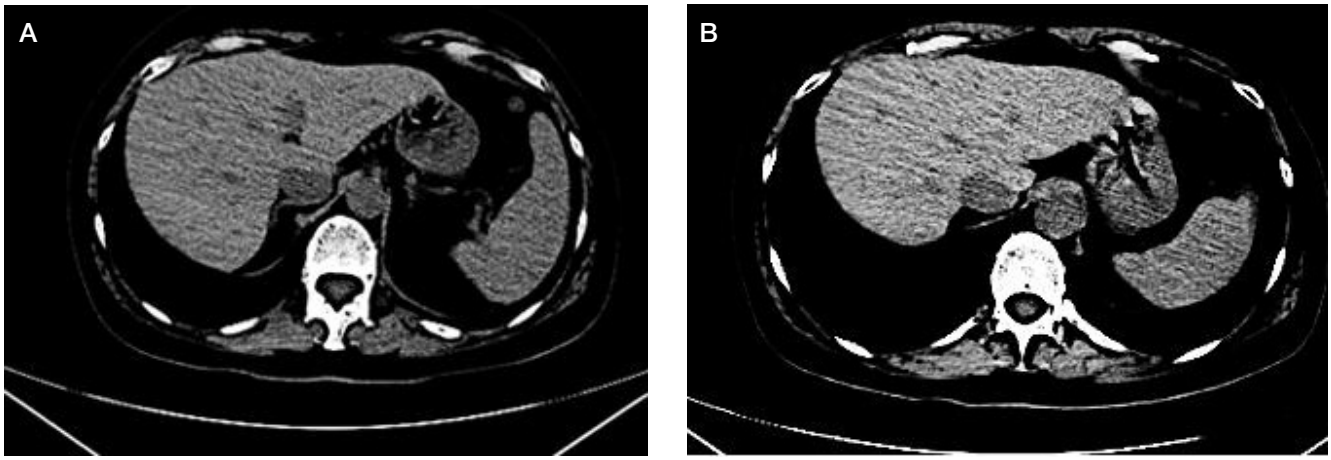

Fig. 4. A, **B**. Abdominal CT, 26.09.2022. Multiple metastatic foci (size up to 2.1 cm) in both lobes of the liver; no changes since 18.07.2022

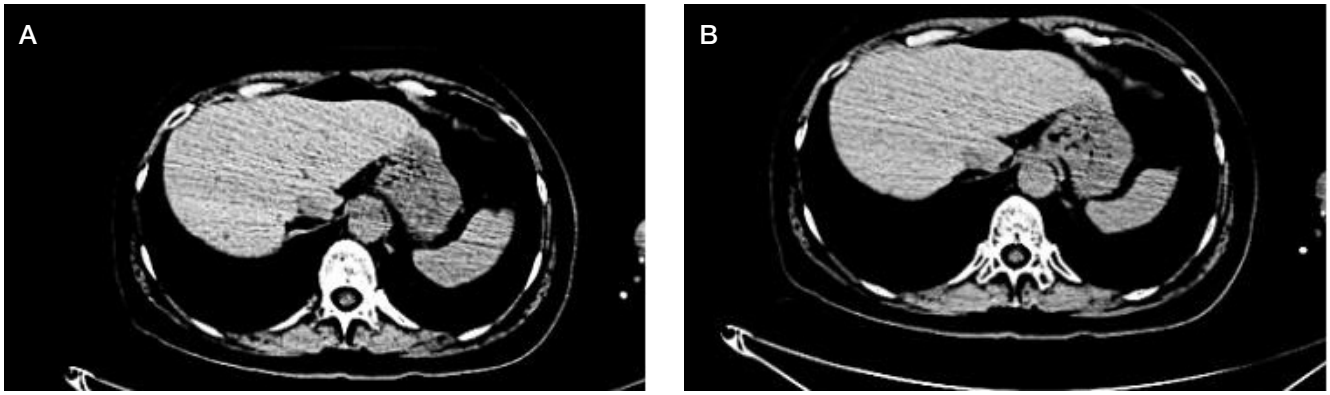

Fig. 5. A, **B**. Abdominal CT, 30.11.2022. Metastatic foci (size up to 1.5 cm) in both lobes of the liver; positive dynamics compared to 26.09.2022

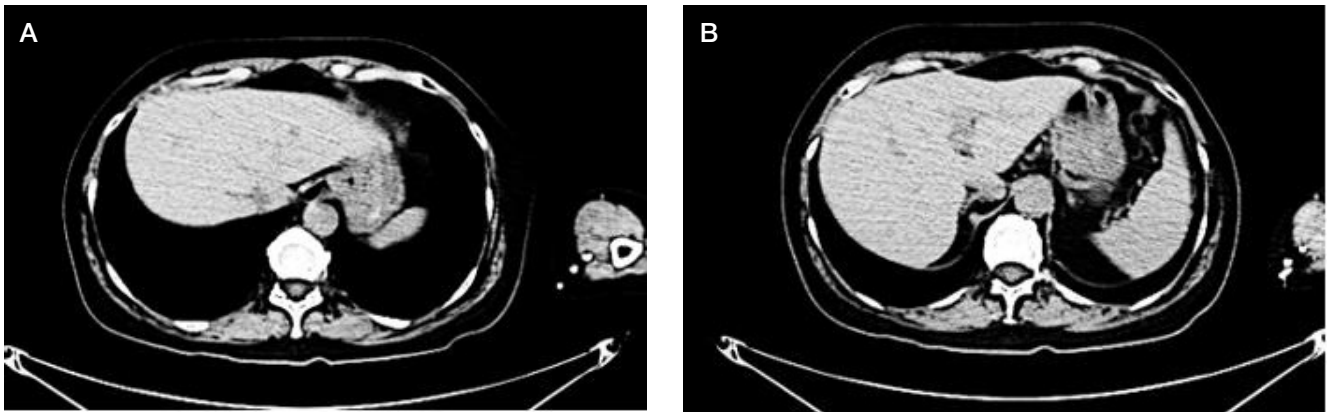

Fig. 6. A, **B**. Abdominal CT, 01.03.2023. Singular metastatic foci (size up to 0.9 cm) in both lobes of the liver; size of the foci decreased compared to 30.11.2022

Positive dynamics allowed suggesting continuation of the combined therapy; with the aim at preventing osteoporosis and mitigating the recurrence risk, the following was recommended:

– bisphosphonates (zoledronic acid 4 mg IV, once in 6 months);

– colecalciferol 400–800 IU/day orally, daily, plus calcium carbonate 500–1000 mg/day orally, daily, protractedly;

– densitometry (bone mineral density control) once a year.

Results of CT, 16.04.2024: no pathological changes discovered in the brain, neck, chest organs; metastatic foci in the liver not visualized clearly since 15.01.2024 (no negative dynamics).

It was recommended to continue combined therapy.

The therapy did not cause significant toxic effects, dose adjustment was not required; ALT and AST values spiked periodically. Currently, the patient follows the recommendations of the chemotherapist. She considers her condition to be satisfactory, has no active complaints. The treatment does not affect her quality of life.

Case discussion

Liver metastases shorten life expectancy of breast cancer patients significantly: the median OS, according to the SEER registries, is 20 months [9].

Surgery prescribed in connection with liver metastases seeded by hormone-receptor positive BC with unknown Her2 status (2^+) involved TACE and injection of microspheres, with two effects: firstly, prolonged ischemia caused by microspheres blocking arterial flow to the tumor, and secondly, gradual release of high-concentration docetaxel from those microspheres pre-saturated therewith, which occurred in the immediate vicinity of the metastases, thus minimizing systemic side effects.

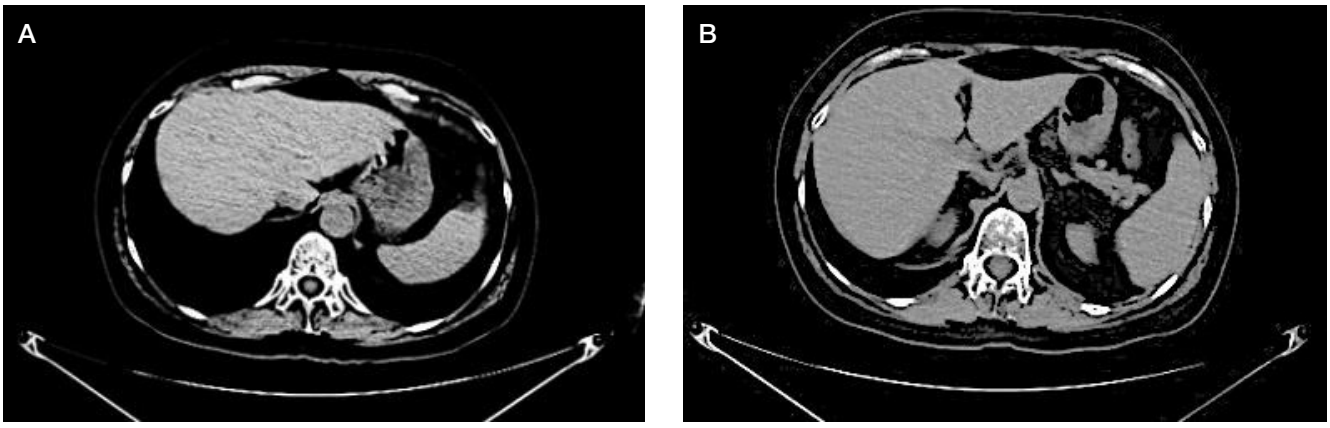

Fig. 7. A, **B**. Abdominal CT, 03.10.2023. Metastatic foci in the liver not visualized clearly since 01.01.2023 (positive dynamics)

Hormone therapy and selective CDK4/6 inhibitors (ribociclib) underpin significant achievements in the treatment of tumors and demonstrate encouraging results (as part of the first line regimens, they help overcome the five-year threshold), which significantly improves respective prognoses. In the context of MONALEESA-3randomized trial, tested both as a first and a second line regimen drug, ribociclib proved to be highly effective in the cohort of patients with metastatic liver damage (poorest prognoses), contributing to the increase of their life expectancy to 1 year, and in a heterogeneous population of patients, it enabled growth of OS to 36.1 months (median value).

CONCLUSION

The combination of contemporary methods of treatment, such as TACE, and classic approaches to BC-seeded liver metastases requires further investigation, since it helps to improve the patients' quality of life and increase disease-free and overall survival.

Effective multidisciplinary approach that involved TACE, selective CDK4/6 inhibitors (improved progression-free survival, increased life expectancy, preserved high quality of life), and hormone therapy, was practiced in treatment of a patient with unresectable liver metastases seeded by hormone-receptor positive BC (ER^+/PR^-) with unknown Her2 status (2^+), and yielded regression of the oncological process in the liver and rendered CT visualization of metastatic foci there unclear. When this report was prepared, the patient has been receiving therapy for metastatic breast cancer for 28 months. Absence of clearly visualized metastatic foci in her liver can be an important indicator of the effectiveness of combination therapy in this patient.

References

1. Bray F, Laversanne M, Sung H, et. al. Soerjomataram I, Jemal A. Global cancer statistics 2022: GLOBOCAN estimates of incidence and mortality worldwide for 36 cancers in 185 countries. CA Cancer J Clin. 2024; 4. DOI: 10.3322/caac.21834.
2. Loibl S, Poortmans P, Morrow M, et. al. Breast cancer. Lancet. 2021; 8; 397 (10286):1750–69. DOI: 10.1016/S0140-6736(20)32381-3.
3. Liberchuk AN, Deipolyi AR. Hepatic Metastasis from Breast Cancer. Semin Intervent Radiol. 2020; 37 (5): 518–26; DOI: 10.1055/s-0040-1720949.
4. Eng LG, Dawood S, Sopik V, et. al. Ten-year survival in women with primary stage IV breast cancer. Breast Cancer Res Treat. 2016; 160 (1): 145–52; DOI: 10.1007/s10549-016-3974-x.
5. Cersosimo RJ. Cyclin-dependent kinase 4/6 inhibitors for the management of advanced or metastatic breast cancer in women. Am J Health Syst Pharm. 2019; 76 (16): 1183–202. DOI: 10.1093/ajhp/zxz121.
6. Yardley DA, Chan A, Nusch A, et al. Abstract P6-18-07: Ribociclib+ endocrine therapy in patients with hormone receptor-positive, HER2-negative advanced breast cancer presenting with visceral metastases: Subgroup analysis of phase III MONALEESA trials. Canc Research. 2019; 79 (4): P6-18-07 — P6-18-07; DOI: 10.1158/1538-7445.SABCS18-P6-18-07.
7. Barakat E, Bibok A, Rishi A, et al. Transarterial Yttrium-90 glass microsphere radioembolization of chemotherapy-refractory breast cancer liver metastases: results of a single institution retrospective study. Adv Radiat Oncol. 2021; 7 (1): 100838; DOI: 10.1016/j.adro.2021.100838.
8. Wang L, Lin ZG, Ke Q, et. al. Adjuvant transarterial chemoembolization following radical resection for intrahepatic cholangiocarcinoma: A multi-center retrospective study. J Cancer. 2020; 11 (14): 4115–22; DOI:10.7150/jca.40358.
9. Surveillance, Epidemiology, and End Results Program, Research Data (1975–2016), National Cancer Institute (NCI), Division of Cancer Control and Population Sciences (DCCPS), Surveillance Research Program (SRP), released April 2019. Available from: https://seer.cancer.gov/.

Литература

1. Bray F, Laversanne M, Sung H, et. al. Soerjomataram I, Jemal A. Global cancer statistics 2022: GLOBOCAN estimates of incidence and mortality worldwide for 36 cancers in 185 countries. CA Cancer J Clin. 2024; 4. DOI: 10.3322/caac.21834.
2. Loibl S, Poortmans P, Morrow M, et. al. Breast cancer. Lancet. 2021; 8; 397 (10286):1750–69. DOI: 10.1016/S0140-6736(20)32381-3.
3. Liberchuk AN, Deipolyi AR. Hepatic Metastasis from Breast Cancer. Semin Intervent Radiol. 2020; 37 (5): 518–26; DOI: 10.1055/s-0040-1720949.
4. Eng LG, Dawood S, Sopik V, et. al. Ten-year survival in women with primary stage IV breast cancer. Breast Cancer Res Treat. 2016; 160 (1): 145–52; DOI: 10.1007/s10549-016-3974-x.
5. Cersosimo RJ. Cyclin-dependent kinase 4/6 inhibitors for the management of advanced or metastatic breast cancer in women. Am J Health Syst Pharm. 2019; 76 (16): 1183–202. DOI: 10.1093/ajhp/zxz121.
6. Yardley DA, Chan A, Nusch A, et al. Abstract P6-18-07: Ribociclib+ endocrine therapy in patients with hormone receptor-positive, HER2-negative advanced breast cancer presenting with visceral metastases: Subgroup analysis of phase III MONALEESA trials. Canc Research. 2019; 79 (4): P6-18-07 — P6-18-07; DOI: 10.1158/1538-7445.SABCS18-P6-18-07.
7. Barakat E, Bibok A, Rishi A, et al. Transarterial Yttrium-90 glass microsphere radioembolization of chemotherapy-refractory breast cancer liver metastases: results of a single institution retrospective study. Adv Radiat Oncol. 2021; 7 (1): 100838; DOI: 10.1016/j.adro.2021.100838.
8. Wang L, Lin ZG, Ke Q, et. al. Adjuvant transarterial chemoembolization following radical resection for intrahepatic cholangiocarcinoma: A multi-center retrospective study. J Cancer. 2020; 11 (14): 4115–22; DOI:10.7150/jca.40358.
9. Surveillance, Epidemiology, and End Results Program, Research Data (1975–2016), National Cancer Institute (NCI), Division of Cancer Control and Population Sciences (DCCPS), Surveillance Research Program (SRP), released April 2019. Available from: https://seer.cancer.gov/.

POTENTIALLY INAPPROPRIATE PRESCRIBING AMONG CRITICALLY ILL CHILDREN: POPI-CRITERIA IN RUSSIA

Vlasova AV[1,2,3] ✉, Kulichenko TV[4], Smirnova EV[2]

[1] Russian Medical Academy of Continuous Professional Education of the Ministry of Healthcare of the Russian Federation, Moscow, Russia
[2] Morozov Children's City Clinical Hospital, Moscow, Russia
[3] Research Institute for Healthcare Organization and Medical Management, Moscow, Russia
[4] Pirogov Russian National Research Medical University, Moscow, Russia

The POPI criteria (Pediatrics: Omission of Prescriptions and Inappropriate prescriptions) for assessment of treatment of comorbidities, complications and underlying conditions in children that are accepted as the only existing instrument for detection of potentially inappropriate prescriptions, make it possible to evaluate prescriptions in children at the inpatient and outpatients stages of care provision, similar to the Beers criteria for adults. The study was aimed to assess the structure and rate of potentially inappropriate prescribing in the pediatric anesthesiology and resuscitation department of the multidisciplinary children's hospital based on the adapted version of POPI criteria for non-antibiotic concomitant therapy of nosocomial infections. We analyzed 305 cases of non-antibiotic medication prescription per 100 patients included. The rate of potentially inappropriate prescribing was 31 cases (10.5%), among which potentially inappropriate medication was prescribed in 29 cases (9.5%), and potentially missed medication took place in three cases (1%). The highest rate of potentially inappropriate prescribing was reported for respiratory diseases. Assessment of concomitant therapy in the critically ill children with infections revealed no significant effects on the rate of adverse reactions to antibiotics in children. In the context of implementing medical information systems (MIS) and prescription sheets, integration of the adapted POPI criteria is topical in terms of maintaining the quality and safety of drug therapy for treatment of concomitant diseases, conditions, and complications in children.

Keywords: children, potentially inappropriate prescriptions, potentially missed medication, medication errors

Author contribution: Vlasova AV — study concept and design, data acquisition and processing, manuscript writing and editing; Smirnova EV — statistical data processing, manuscript editing; Kulichenko TV — manuscript editing.

Compliance with ethical standards: the study was approved by the Ethics Committee of the Morozov Children's City Clinical Hospital (the research protocol dated 24.10.2019 was published on ClinicalTrials.gov, ID: NCT04141657, Unique Protocol ID: 07819001, Brief Title: Safety Analysis of Antimicrobial Pharmacotherapy in Intensive Care Unit at Pediatric Hospital Official, Title: Observational Prospective Multidirectional Study on the Safety of Antimicrobial Pharmacotherapy in Intensive Care Unit (ICU) Children Aged 0-17).

✉ **Correspondence should be addressed:** Anna V. Vlasova
4th Dobryninsky pereulok, 1/9, Moscow,119049, Russia; annavlasova75@mail.ru

Received: 21.02.2024 **Accepted:** 27.04.2024 **Published online:** 30.04.2024

DOI: 10.24075/brsmu.2024.018

ПОТЕНЦИАЛЬНО НЕПРИЕМЛЕМЫЕ НАЗНАЧЕНИЯ ЛЕКАРСТВЕННЫХ ПРЕПАРАТОВ У ДЕТЕЙ В КРИТИЧЕСКИХ СОСТОЯНИЯХ: POPI-КРИТЕРИИ В РОССИИ

А. В. Власова[1,2,3] ✉, Т. В. Куличенко[4], Е. В. Смирнова[2]

[1] Российская медицинская академия непрерывного профессионального образования Минздрава России, Москва, Россия
[2] Морозовская детская городская клиническая больница, Москва, Россия
[3] Научно-исследовательский институт организации здравоохранения и медицинского менеджмента, Москва, Россия
[4] Российский национальный исследовательский медицинский университет имени Н. И. Пирогова, Москва, Россия

POPI-критерии (Pediatrics: Omission of Prescriptions and Inappropriate prescriptions) для оценки терапии сопутствующих заболеваний, осложнений и фоновых состояний у детей, по аналогии с критериями Бирса у взрослых, признаны единственным существующим инструментом выявления потенциально неприемлемых назначений, позволяют оценить назначения лекарственных препаратов у детей на стационарном и амбулаторном этапе оказания медицинской помощи. Целью исследования было изучить структуру и частоту потенциально неподходящих назначений лекарственных препаратов в детском отделении АиР детского многопрофильного стационара на основе адаптированной версии POPI-критериев для сопутствующей неантимикробной терапии при нозокомиальных инфекциях. Проводили анализ 305 случаев назначения неантимикробных лекарственных препаратов на 100 включенных пациентов. Частота потенциально неприемлемых назначений составила 31 (10,5%) случай, из них потенциально ненадлежащее лекарство назначено в 29 (9,5%) случаях и потенциально пропущено лекарство — в трех (1%) случаях. Самый высокий уровень потенциально неприемлемых назначений выявлен при респираторных заболеваниях. Оценка сопутствующей терапии у детей с инфекцией в критических состояниях не выявила статистически значимых влияний на частоту нежелательных реакций на антибиотики у детей. В условиях внедрения медицинских информационных систем (МИС) и листа назначений интеграция адаптированных POPI-критериев актуальна для поддержания качества и безопасности лекарственной терапии сопутствующих заболеваний, состояний и осложнений у детей.

Ключевые слова: дети, потенциально неприемлемые назначения, потенциально пропущенное лекарство, потенциально ненадежащее лекарство

Вклад авторов: А. В. Власова — концепция и дизайн исследования, сбор и обработка материала, написание и редактирование текста; Е. В. Смирнова — статистическая обработка данных, редактирование статьи; Т. В. Куличенко — редактирование статьи.

Соблюдение этических стандартов: исследование одобрено этическим комитетом ГБУЗ «Морозовская ДГКБ ДЗМ» (протокол исследования 24.10.2019 опубликован на платформе ClinicalTrials.gov ID: NCT04141657 Unique Protocol ID: 07819001 Brief Title: Safety Analysis of Antimicrobial Pharmacotherapy in Intensive Care Unit at Pediatric Hospital Official Title: Observational Prospective Multidirectional Study on the Safety of Antimicrobial Pharmacotherapy in Intensive Care Unit (ICU) Children Aged 0-17).

✉ **Для корреспонденции:** Анна Викторовна Власова
4-й Добрынинский переулок, дом 1/9, г. Москва,119049, Россия; annavlasova75@mail.ru

Статья получена: 21.02.2024 **Статья принята к печати:** 27.04.2024 **Опубликована онлайн:** 30.04.2024

DOI: 10.24075/vrgmu.2024.018

The incidence of adverse drug reactions (ADRs) in pediatric population reported for hospitalized patients is 9.53%, while that reported for ambulatory patients is 1.46%; the rate of ADRs resulting in hospitalization of children is 2.09% [1].

The incidence of ADRs among children is twice higher than among adults (it is four times higher among newborns); about 7000 children die annually due to medication errors, and the rate of irrational drug use reaches 12–32% [2, 3].

The limited data on the impact of drug therapy in pediatric patients with comorbidities on the ADR incidence make assessing safety of prescriptions at the anesthesiology and resuscitation departments a pressing issue. Studies of the procedure of using the Pediatrics: Omission of Prescriptions and Inappropriate Prescriptions (POPI) criteria for assessment of therapy for concomitant disorders, complications, and underlying conditions on children [2, 4–6], similar to the Beers criteria for adults [6], in the context of implementing medical information systems and prescription sheets require assessment of medication prescription practice existing in each medical institution aimed at reducing errors.

Many researchers believe that development of the criteria for prescription appropriateness evaluation in children is in its infancy; only three criteria sets were available for children [6–8]. The criteria for prescription evaluation in children were first developed by pediatric medical experts from France in 2011 [6], then POPI criteria were issued in the UK [7]. In 2022, the Chinese researchers, who were puzzled by the lack of instrument for prescription appropriateness evaluation in children after assessment of their own clinical practice, published a comprehensive systematic review of the existing instruments for determination of prescription appropriateness in children and fesibility of these prescriptions in clinical practice [2]. Prescription is considered to be appropriate when it is complicant with the indications, well-tolerated by the majority of patients, and economically justified. According to one of the proposed concepts [9], potentially inappropriate prescribing (PIP) is characterized by the presence of one component out of two: potentially inappropriate medication (PIM) and potentially omitted medication (POM). The judgment of PIM is based on the cases, when potential risks of ADRs outweight potential clinical benefits, especially when there is a more safe or effective alternative. PIM usually includes prescription errors: wrong choice, dose, duration, risk of potential interaction with other drugs or foods, etc., or overprescribing (polypharmacy). The judgment of POM is based on the identified cases of withholding showing significant benefits potentially imporoving the patients' life expectancy or quality of life provided that there are no contraindications, including cases of prescribing the drug approved by the national authorities or clinical guidelines [9].

The study was aimed to assess the structure and rate of potentially inappropriate mediation in the pediatric anesthesiology and resuscitation department based on the adapted version of POPI criteria.

METHODS

A prospective observational study conducted at the Morozov Children's City Clinical Hospital between 01 February 2020 and 01 September 2021 was focused on assessing concomitant therapy with the regularly used drugs in 100 critically ill children with nosocomial infections (44 boys, 56 girls) aged 0–17 years [10]. The average age of children was 5.36 ± 5.5 years, no significant differences in gender and age were reported. Inclusion of patients in the study was interrupted from 20 February 2020 to 30 November 2020 for the period, when the hospital accepted patients with novel coronavirus infection (COVID-19).

Inclusion criteria: infections with the risk factors of multidrug-resistant pathogens — types II–IV if stratified by AMS1; presence of symptom complex based on the criteria for compliance with the definite, probable or possible nosocomial infection based on the microbiological data [11] according to the definition of the US Centers for Disease Control and Prevention (CDC) [12] and the European Centre for Disease Prevention and Control (ECDC) [13]; positive results of the biomaterial microbiological testing involving isolation of the etiologically significant multidrug-resistant microorganism.

All the patients had indications for the use of antimicrobials in accordance with the established criteria for complicance with the standard case of determining the nosocomial infection caused by resistant microorganisms based on the CDC and ECDC criteria [11–13].

Exclusion criteria: novel coronavirus infection (COVID-19); cancer; community-acquired infections with no risk factors of multidrug-resistant pathogens — type I if stratified by AMS; end-stage organ and system failure as competing with the infection for primary diagnosis or condition. Other exclusion criteria: children under guardianship.Previous/concomitant therapy was of no importance for inclusion in the study.

Evaluation of concomitant therapy (non-antimicrobial) in critically ill children was performed using POPI criteria (2019 version, amended and supplemented) [5]. The method is similar to the Beers criteria for adults. The plan of evaluation procedures and personalized assessment of the use of POPI criteria are provided in Table 1.

In critically ill patients, systemic unflammation associated with infection was assessed based on the levels and dynamics of inflammatory markers: C-reactive protein and procalcitonin. The antimicrobial therapy efficacy was estimated based on the 2-fold decrease in the levels of procalcitonin and/or C-reactive protein. When estimating the dynamics, the imaging results for to the infection site were taken into account. When there were multiple infection sites, during assessment priority was given to the zone of interest showing the most prominent signs of involvement.

Statistical processing of the results was performed using the IBM SPSS Statistics v26 software package (IBM; USA). The odds ratio was used to compare the chances of obtaining the desired results in two groups of dichotomous variables.

Inclusion in the study took place at the time of infection: in 81 children, infection developed during their stay at the anesthesiology and resuscitation department agaist the background of underlying disorder or postoperative condition; in 19 patients, the infection caused by resistant pathogens resulted in admission to the anesthesiology and resuscitation department.

The characteristics of patients based on their underlying disorders are provided in Table 2. A total of 49 pediatric patients predominated in the structure of patients based on the primary diagnosis. Among them 19 children were initially admitted to the anesthesiology and resuscitation department due to devere pneumonia: 12 children with community-acquired pneumonia and 7 with aspiration pneumonia. Children with pneumonia had a comorbidity, epilepsy (regular use of low-to-medium doses of valproates at the prehospital stage of the use of these in combination with lamotrigine). Among them 30 children had multiple developmental defects: malformations of the kidney, GIT, CNS (regular use of proton pump inhibitors prescribed at the prehospital stage and resumed at the time of inclusion in the study). Postoperative surgical conditions ranked second

Table 1. Personalized assessment of non-antibiotic therapy based on POPI criteria for 100 patients of the anesthesiology and resuscitation department [5]

Assessment criterion	Present, 1 point (yes/no), number of patients assigned 1 point		
NSAIDs as antipyretics:			
Oral drug other than paracetamol as first-line treatment	1	yes	3
Rectal paracetamol as first-line treatment	1	no	0
Two antipyretics (paracetamol + ibuprofen) as first-line treatment	1	no	0
Oral ibuprofen 10 mg/kg 3 times/day	1	no	0
Combination of 2 NSAIDs is prescribed (except rectal paracetamol)	1	yes	14
Score ≥ 1 — therapy adjustment is required		total	17
Treatment of pain syndrome:			
The use of oral sugar or glucose solution 2 min before venipuncture in is not prescribed to newborns and infants under the age of 4 months	1	yes	9
Osmotic laxative is NOT prescribed for more than 48 h after prescription of morphine	1	yes	0
Score ≥ 1 — prescription adjustment is required		total	9
Vitamins [5]:			
Breastfeeding: vitamin D in a dose of 1000–1200 IU/day	1	yes	9
Bottle-feeding, age under 18 months, infant formula is enriched with vitamin D: 600–800 IU/day	1	no	0
Children aged between 18 months and 5 years and adolescents aged 10–18 years in witer: taking two doses of vitamin D per quarter (80 000–100 000 IU/day) [5]	1	no	0
Score ≥ 1 — no prescription adjustment is required		total	9
Nausea, vomiting, gastroesophageal reflux:			
Metoclopramide is prescribed	1	no	0
Domperidone is prescribed	1	yes	2
Oral administration of intravenous proton pump inhibitor or administration by nasogastric tube	1	no	0
Proton pump inhibitors or type H2 antihistamines are prescribed to individuals with the following disorders: gastroesophageal reflux, indigestion (nausea, vomiting)	1	no	0
Proton pump inhibitors are prescribed to patients with no risk factors, who are through the short course of NSAID, as a preventive measure	1	no	0
Type H2 antihistamines are used for long periods	1	no	0
Score ≥ 1 — prescription adjustment is required		total	2

in the structure of patients based on the primary diagnosis: 22 patients with multiple developmental defects who were through postoperative period: nine patients after gastrostomy feeding tube insertion and 13 patients after reconstructive surgery of the GIT; among them six children still needed pain relief (NSAIDs) during the postoperative period, and proton pump inhibitors were regularly used in 12 children. Congenital heart defects in the postoperative period without artificial circulation were reported in 20 children, among them three children needed pain relief (NSAIDs) for more than three days; regular use of spironolactone was reported in one child, and regular use of PPIs in three children. Neonatal diseases were reported in nine children (accompanying treatment with drugs for regular use is provided in Table 2); two vasopressors due to infectious disease were used in six children, and diuretics were used in eight children.

Patients were included in the observational study at the time of infection. Furthermore, in 81 children, manifestation of the infection occurred during their stay at the anesthesiology and resuscitation department against the background of the

Table 2. Characteristics of patients based on the underlying disease

Concomitant diseases (conditions)	Number of patients (n = 100)	Therapy for concomitant disease, number of children	Non-antimicrobial therapy at the time of enrollment in the anesthesiology and resuscitation department
Neonatal diseases	9 (9%)	No	Two vasopressors due to infectious disease — six children, diuretics — eight children
Congenital heart defects in the postoperative period without artificial circulation	20 (20%)	Of those: NSAIDs — 3, diuretics — 1, PPI — 3	Two vasopressors due to infectious disease — 12 children, diuretics — 20 children
Postoperative surgical conditions	22 (22%)	Of those: NSAIDs — 6, PPI — 12	Two vasopressors due to infectious disease — 8 children, diuretics — 8 children
Somatic perdiatric diseases (epilepsy, multiple developmental defects)	49 (49%)	Of those: anticonvulsants — 20, NSAIDs — 8, PPI — 29	Two vasopressors due to infectious disease — 18 children, diuretics — 20 children

underlying disorder or postoperative condition; in 19 cases, infections caused by resistant pathogens resulted in admission to the anesthesiology and resuscitation department. Children with ventilator-associated pneumonia (VAP) predominated among individuals included in the observational study — 41 (41%), along with children with catheter-associated bloodstream infections (CRBSI) — 30 (30%) and surgical site infections (SSI) — 19 (19%); nosocomial urinary tract infections (nosocomial UTI) reported in seven children (7%) and skin and soft tissue infections (SSTI) reported in three children (3%) were less frequent. *Predominance* of *Enterobacterales* associated with VAP in the anesthesiology and resuscitation department should be noted in 16 cases (40%), among which high levels of resistance took place in four cases (10%). *Acinetobacter complex* was often isolated from the trachea (11 patients (27%)), mostly having preserved susceptibility to the major classes of antimicrobials. However, a pan-drug resistant strain of *Acinetobacter complex* was isolated in two patients. Isolation of *P. aeruginosae* was reported in 9 patients (23%). Gram-negative bacteria with high levels of antibiotic resistance were most often plated in 30 children with c CRBSI. Thus, carbapenemase-producing bacteria were isolated in seven patients (34%): *Pseudomonas aeruginosa* in two cases and entherobacteria in five cases. The *Candida* pathogenic fungi were isolated from the blood cultures of 10 patients (33%); predominance of *C. parapsilosis* resistant to the azole antifungal agents was reported. Gram-positive bacteria were isolated from the blood cultures of nine patients (30%): coagulase-negative staphylococci in six patients and *Staphylococcus aureus* in three patients. *C. parapsilosis* was isolated from the intraoperaive material of 19 patients admitted to the anesthesiology and resuscitation department with SSI, members of the genus *Enterobacterales* and coagulase-negative staphylococci were reported in five patients (26.5%), respectively.

The length of children's stay at the anesthesiology and resuscitation department associated with various infections was on average 18–26 day. The longest patients' stay at the anesthesiology and resuscitation department was reported for VAP — about 26.46 days, CRBSI — 23.83 days, and complicated UTI — on average 23.43 days; the length of stay for SSI was 18.26 days and that for SSTI was 18.33 days. Thus, patients usually stayed in the ICU until their third week at the anesthesiology and resuscitation department.

RESULTS

Among all children enrolled, the initially prescribed antimicrobial therapy was effective in 85 children (85%). Timing of the antimicrobial de-escalation (ADE) was estimated. In 64 children (75.3%), treatment was changed on day 8.28 (14.51) as part of de-escalation, which was assessed as one course of antimicrobial therapy. In patients with severe systemic inflammation (high levels of CRP and procalcitonin), ADE was delayed or not performed throughout the patient's stay at the department. When de-escalation was performed in the line unit after transfer from the anesthesiology and resuscitation department, the fact of de-escalation was not considered in accordance with the protocol of our observational study. Among all the patients enrolled, de-escalation was not performed in 15 children (15%) due to inefficient antimicrobial therapy. Among them 12 children (12% of patients included in the study) needed prescribing the second course of antimicrobial therapy due to alternation of the clinically significant microorganism without alternation of the site of infection, the so-called "leading" causative agent of infection amidst "slipping away" of the applied therapy effect. Three children (3% of patients included in the study) needed prescribing the third course of antimicrobials due to "slipping away" of the effect against the background of antimicrobial drug therapy and alternation of the site of infection. In such cases there was CRBSI with subsequent VAP.

In our observational study, during three weeks of stay at the anesthesiology and resuscitation department each pediatric patient with infection experienced 1–2 changes in the course of antimicrobial therapy; combinations of antibacterial and antifungal drugs were used. According to Table 2, 40 children (40% of all patients included in the study) received concomitant treatment. The use of NSAIDs required adjustment in 17 patients (17%), treatment of pain syndrome had to be adjusted in 9 patients (9%), and adjustment of antireflux medication was required in 2 patients (2%).

In accordance with the aim of the study, we assessed the rate of potentially inappropriate prescribing in the anesthesiology and resuscitation department based on the adapted version of POPI for concomitant treatment. The number of concomitant prescriptions was 305 per 100 patients enrolled, which corresponded to 3.05 prescriptions per patient. Furthermore there were 31 cases (10.5%) of potentially inappropriate prescribing, among them potentially inappropriate medication was prescribed in 29 cases (9.5%) and potentially omitted medication took place in 3 cases (1%).

DISCUSSION

We have found several studies focused on assessing the rate of potentially inappropriate prescribing in pediatric hospitals; only one study was matched by the patient sample size for comparative analysis. In this study the rate of potentially inappropriate prescribing in the pediatric anesthesiology and resuscitation department reached 5.2% of cases, among which potentially inappropriate medication took place in 2.9% of cases and potentially omitted medication in 2.3% of cases; in contrast, the rate of potentially inappropriate prescribing in the pediatric emergency department was 18.4%, among which potentially inappropriate medication took place in 12.3% of cases and potentially omitted medication in 6.1% of cases. The highest rates of potentially inappropriate prescribing were reported for respiratory diseases and gastrointestinal tract disorders. The authors have shown that POPI criteria are currently the only available instrument for identification of potentially inappropriate prescriptions of concomitant therapy to children, which in practice has shown its effectiveness in an inpatient pediatric emergency department and turned out to be not entirely suitable for assessing concomitant therapy in children admitted to the anesthesiology and resuscitation department [2, 3].

The findings of our observational study focused on assessing concomitant therapy in children staying at the anesthesiology and resuscitation department show that the rate of potentially inappropriate prescribing is 10.5%, of that the rate of potentially inappropriate medication is 9.5% and the rate of potentially omitted medication is 1%. The highest rate of potentially inappropriate prescribing has been reported for treatment of respiratory diseases.

The identified differences between two studies of similar cohorts can, on one hand, be explained by different models of building a prescription sheet in the medical information system, but on the other hand these may point to the national specifics of the clinical decision-making support systems in China and Russia based on the clinical recommendations and guidelines supported in each country. Currently, POPI criteria are considered to be the only available instrument for identification of potentially inappropriate prescriptions that can be used for comparative assessment and improvement of pediatric clinical practice.

CONCLUSIONS

In this observational study, we analyzed potentially inappropriate prescribing of concomitant therapy to children with infections in the anesthesiology and resuscitation department: the number of concomitant therapy prescriptions was 305 cases per 100 patients included in the study, which corresponded to 3.05 prescriptions per patient; the rate of potentially inappropriate prescribing was 10.5% of cases, of that the rate of potentially inappropriate medication was 9.5% and the rate of potentially omitted medication was 1% of cases. The highest rate of potentially inappropriate prescribing was reported in patients with the primary diagnosis of "respiratory infection". The difficulties of selecting tools enabling assessment in real clinical practice has been shown. The findings can help develop the system for assessment of potentially inappropriate prescribing in the context of the electronic prescription sheet implementation and integration of the clinical decision-making support system based on the clinical guidelines.

References

1. Impicciatore P, Choonara I, Clarkson A, Provasi D, Pandolfini C, Bonati M. Incidence of adverse drug reactions in paediatric in/out-patients: a systematic review and meta-analysis of prospective studies. Br J Clin Pharmacol. 2001; 52 (1): 77–83.
2. Li S, Huang L, Zeng L, Yu D, Jia ZJ, Cheng G, et al. A tool for screening potentially inappropriate prescribing in Chinese children. Front Pharmacol. 2022; 13: 1019795.
3. Zhao Z, Shen J, Shen C, Zhu B, Sun J, Yu J,et al. An investigation of pharmacovigilance and reporting of adverse drug reactions in hospitals: a cross-sectional study in China. Curr Med Res Opin. 2021; 37 (11): 2001–6.
4. Balan S, Hassali MAA, Mak VS. Two decades of off-label prescribing in children: a literature review. World J Pediatr. 2018; 14: 528–40.
5. Berthe-Aucejo A, Nguyen PKH, Angoulvant F, Bellettre X, Albaret P, Weil T, et al. Retrospective study of irrational prescribing in French paediatric hospital: prevalence of inappropriate prescription detected by Pediatrics: Omission of Prescription and Inappropriate prescription (POPI) in the emergency unit and in the ambulatory setting. BMJ Open. 2019; 9 (3): e019186.
6. Prot-Labarthe S, Weil T, Angoulvant F, Boulkedid R, Alberti C, Bourdon O. POPI (Pediatrics: Omission of Prescriptions and Inappropriate prescriptions): development of a tool to identify inappropriate prescribing. PloS One. 2014; 9 (6): e101171.
7. Barry A, Olsson S, Minzi O, Bienvenu E, Makonnen E, Kamuhabwa A, et al. Comparative assessment of the national pharmacovigilance systems in East Africa: Ethiopia, Kenya, Rwanda and Tanzania. Drug Saf. 2020; 43: 339–50.
8. Corrick FJ. Paediatric rational prescribing: a study of paediatric rational prescribing tools and development of a novel tool for the UK. 2021.
9. Gallagher P, Ryan C, Byrne S, Kennedy J, O Mahony D. STOPP (screening tool of older person's prescriptions) and START (screening tool to alert doctors to right treatment). Consensus validation. Int J Clin Pharmacol Ther. 2008; 46 (2): 72.
10. Vlasova AV. Nezhelatel'nye reakcii detej na antimikrobnye preparaty: ogranichenija metoda spontannyh soobshhenij i vozmozhnosti metoda global'nyh triggerov lekarstvenno-inducirovannyh sostojanij. Farmateka. 2023 (1–2): 18–31. Russian.
11. Jakovlev SV, Briko NI, Sidorenko SV, Procenko DN. Programma SKAT (strategija kontrolja antimikrobnoj terapii) pri okazanii stacionarnoj medicinskoj pomoshhi: Rossijskie klinicheskie rekomendacii. M.: Pero, 2018; 156 s. Russian.
12. Centers for Disease Control and Prevention, CDC. Available from: https://www.cdc.gov/hai/vap/vap.html.
13. European Centre for Disease Prevention and Control, ECDC. Available from: https://www.cdc.gov/hai/vap/vap.html.

Литература

1. Impicciatore P, Choonara I, Clarkson A, Provasi D, Pandolfini C, Bonati M. Incidence of adverse drug reactions in paediatric in/out-patients: a systematic review and meta-analysis of prospective studies. Br J Clin Pharmacol. 2001; 52 (1): 77–83.
2. Li S, Huang L, Zeng L, Yu D, Jia ZJ, Cheng G, et al. A tool for screening potentially inappropriate prescribing in Chinese children. Front Pharmacol. 2022; 13: 1019795.
3. Zhao Z, Shen J, Shen C, Zhu B, Sun J, Yu J,et al. An investigation of pharmacovigilance and reporting of adverse drug reactions in hospitals: a cross-sectional study in China. Curr Med Res Opin. 2021; 37 (11): 2001–6.
4. Balan S, Hassali MAA, Mak VS. Two decades of off-label prescribing in children: a literature review. World J Pediatr. 2018; 14: 528–40.
5. Berthe-Aucejo A, Nguyen PKH, Angoulvant F, Bellettre X, Albaret P, Weil T, et al. Retrospective study of irrational prescribing in French paediatric hospital: prevalence of inappropriate prescription detected by Pediatrics: Omission of Prescription and Inappropriate prescription (POPI) in the emergency unit and in the ambulatory setting. BMJ Open. 2019; 9 (3): e019186.
6. Prot-Labarthe S, Weil T, Angoulvant F, Boulkedid R, Alberti C, Bourdon O. POPI (Pediatrics: Omission of Prescriptions and Inappropriate prescriptions): development of a tool to identify inappropriate prescribing. PloS One. 2014; 9 (6): e101171.
7. Barry A, Olsson S, Minzi O, Bienvenu E, Makonnen E, Kamuhabwa A, et al. Comparative assessment of the national pharmacovigilance systems in East Africa: Ethiopia, Kenya, Rwanda and Tanzania. Drug Saf. 2020; 43: 339–50.
8. Corrick FJ. Paediatric rational prescribing: a study of paediatric rational prescribing tools and development of a novel tool for the UK. 2021.
9. Gallagher P, Ryan C, Byrne S, Kennedy J, O Mahony D. STOPP (screening tool of older person's prescriptions) and START (screening tool to alert doctors to right treatment). Consensus validation. Int J Clin Pharmacol Ther. 2008; 46 (2): 72.
10. Власова А. В. Нежелательные реакции детей на антимикробные препараты: ограничения метода спонтанных сообщений и возможности метода глобальных триггеров лекарственно-индуцированных состояний. Фарматека. 2023 (1–2): 18–31.
11. Яковлев С. В., Брико Н. И., Сидоренко С. В., Проценко Д. Н. Программа СКАТ (стратегия контроля антимикробной терапии) при оказании стационарной медицинской помощи: Российские клинические рекомендации. М.: Перо, 2018; 156 с.
12. Centers for Disease Control and Prevention, CDC. Available from: https://www.cdc.gov/hai/vap/vap.html.
13. European Centre for Disease Prevention and Control, ECDC. Available from: https://www.cdc.gov/hai/vap/vap.html.

AMINO ACID PROFILE IN DIMINISHED OVARIAN RESERVE

Gavisova AA[1]✉, Shevtsova MA[1], Lvova PO[1], Biryukova DA[1], Ibragimova MH[1], Novoselova AV[1], Yushina MN[1], Chagovets VV[1], Frankevich VE[1,2]

[1] Kulakov National Medical Research Center for Obstetrics, Gynecology and Perinatology, Moscow, Russia

[2] Siberian State Medical University, Tomsk, Russia

Diminished ovarian reserve (DOR) represents a relevant issue of reproductive medicine that is often associated with infertility and reduced efficacy of IVF programs. The changes in amino acid metabolism can play a role in the DOR pathogenesis as manifestations of the folliculogenesis and oogenesis epigenetic alterations. The study was aimed to assess alterations of amino acid metabolic pathways in blood plasma and follicular fluid and estimate their clinical significance in DOR. A total of 115 infertile women aged 25–42 years were included in the study. Groups were formed based on the ovarian reserve and age. Amino acid levels in blood plasma and follicular fluid were assessed by high performance liquid chromatography–mass spectrometry (HPLC-MS); bioinformatics analysis of amino acid metabolic pathways was performed. We revealed significant changes in the phenylalanine, tyrosine and tryptophan biosynthesis (effect = 0.5; p = 0.026), alanine, aspartate and glutamate metabolism (effect = 0.114; p = 0.013), and arginine biosynthesis (effect = 0.289; p < 0.001) pathways playing a role in folliculogenesis, oogenesis, and embryogenesis. The detected differences in the amino acid levels in various body fluids made it possible to construct the logistic regression models confirming DOR with the 88% probability based on the amino acid levels in follicular fluid (sensitivity 88%, specificity 84%) and 82% probability based on plasma levels (sensitivity 65%, specificity 91%). The findings can be used for further research focused on the pathogenesis of infertility associated with DOR and for selection of the most optimal diagnostic and treatment tactics.

Keywords: amino acid profile, metabolism, metabolic pathway, childbearing age, infertility, diminished ovarian reserve, IVF, HPLC-MS

Author contribution: Gavisova AA — study design, data acquisition and processing, manuscript writing, editing; Shevtsova MA, Biryukova DA, Lvova PO — study design, data acquisition and processing, literature review, manuscript writing, editing; Novoselova AV, Yushina MN — developing the LC-MS method for analysis of amino acids in blood plasma and follicular fluid, experimental data processing; Ibragimova MH — data acquisition, editing; Chagovets VV, Frankevich VE — statistical data processing, editing.

Compliance with ethical standards: the study was approved by the Ethics Committee of the Kulakov National Medical Research Center for Obstetrics, Gynecology and Perinatology (protocol № 12 dated 25 November 2021).

✉ **Correspondence should be addressed:** Alla A. Gavisova
Akademika Oparina, 4, Moscow, 117997, Russia; gavialla@ya.ru

Received: 27.03.2024 **Accepted:** 22.04.2024 **Published online:** 30.04.2024

DOI: 10.24075/brsmu.2024.016

АМИНОКИСЛОТНЫЙ ПРОФИЛЬ ПРИ СНИЖЕННОМ ОВАРИАЛЬНОМ РЕЗЕРВЕ

А. А. Гависова[1]✉, М. А. Шевцова[1], П. О. Львова[1], Д. А. Бирюкова[1], М. Х. Ибрагимова[1], А. В. Новоселова[1], М. Н. Юшина[1], В. В. Чаговец[1], В. Е. Франкевич[1,2]

[1] Национальный медицинский исследовательский центр акушерства, гинекологии и перинатологии имени В. И. Кулакова, Москва, Россия

[2] ФГБОУ ВО «Сибирский государственный медицинский университет», Минздрава России, Томск, Россия

Сниженный овариальный резерв (СОР) является одной из актуальных проблем репродуктивной медицины и часто ассоциирован с бесплодием и уменьшением эффективности программ ЭКО. Изменение метаболизма аминокислот может играть роль в патогенезе СОР как проявление эпигенетических нарушений в процессах фолликуло- и оогенеза. Целью исследования было проанализировать изменения метаболических путей аминокислот в плазме крови и фолликулярной жидкости и оценить их клиническое значение при СОР. В исследование вошли 115 женщин в возрасте 25–42 лет с бесплодием. Группы были сформированы в зависимости от овариального резерва и возраста. Выполнено исследование уровней аминокислот в плазме крови и фолликулярной жидкости методом высокоэффективной жидкостной хроматографии с детектированием на масс-спектрометре (ВЭЖХ-МС) и проведен биоинформатический анализ их метаболических путей. Обнаружено статистически значимое изменение путей биосинтеза фенилаланина, тирозина и триптофана (влияние = 0,5; p = 0,026), метаболизма аланина, аспартата и глутамата (влияние = 0,114; p = 0,013) и биосинтеза аргинина (влияние = 0,289; p < 0,001), играющих роль в процессах фолликуло-, оогенеза и эмбриогенеза. Обнаруженные различия в содержании аминокислот в различных биологических жидкостях позволили разработать модели логистической регрессии, подтверждающие СОР с вероятностью 88% по уровням аминокислот в фолликулярной жидкости (чувствительность — 88%, специфичность — 84%) и 82% по уровням в плазме крови (чувствительность — 65%, специфичность — 91%). Эти результаты могут быть использованы для дальнейших исследований патогенеза бесплодия при СОР и выбора наиболее оптимальной тактики диагностики и лечения.

Ключевые слова: аминокислотный профиль, метаболизм, метаболический путь, репродуктивный возраст, бесплодие, сниженный овариальный резерв, ЭКО, ВЭЖХ-МС

Вклад авторов: А. А. Гависова — дизайн исследования, сбор и обработка материала, написание статьи, редактирование; М. А. Шевцова, Д. А. Бирюкова, П. О. Львова — дизайн исследования, сбор и обработка материала, обзор литературы, написание статьи, редактирование; А. В. Новоселова, М. Н. Юшина — разработка метода ЖХ-МС анализа аминокислот в плазме крови и фолликулярной жидкости, обработка экспериментальных данных; М. Х. Ибрагимова — сбор материала, редактирование; В. В. Чаговец, В. Е. Франкевич — статистическая обработка материала, редактирование.

Соблюдение этических стандартов: исследование одобрено этическим комитетом ФГБУ «НМИЦ АГП имени В. И. Кулакова» (протокол № 12 от 25 ноября 2021 г.).

✉ **Для корреспонденции:** Алла Анатольевна Гависова
ул. Академика Опарина, д. 4, г. Москва, 117997, Россия; gavialla@ya.ru

Статья получена: 27.03.2024 **Статья принята к печати:** 22.04.2024 **Опубликована онлайн:** 30.04.2024

DOI: 10.24075/vrgmu.2024.016

Diminished ovarian reserve (DOR) represents a relevant issue of reproductive medicine. The reduced antral follicle counts (AFC), decreased anti-mullerian hormone (AMH) levels and elevated basal follicle-stimulating hormone (FSH) levels in blood serum result in infertility, poor ovarian response, deterioration of oocyte quality, the decrease in fertilization and pregnancy rates in in vitro fertilization programs (IVF/ ICSI), and the increase in the rate of early pregnancy loss [1].

The hormone and amino acid metabolism that can reflect epigenetic alterations of the folliculogenesis and oogenesis processes [2] is characterized not only by changes in the levels of certain metabolites, but also in their interaction in the form of complex metabolic "networks" [3]. Considering the cumulative contribution of the endocrine and metabolomic alterations of blood and follicular fluid to the cell metabolism and their impact on the outcomes of IVF programs, we can uncover some pathogenetic mechanisms of DOR and determine metabolites that can serve as potential biomarkers for estimation of ovarian reserve [4, 5].

In our previously published study, a significant decrease in plasma levels of such amino acids, as sarcosine and tryptophan, decreased levels of phenylalanine, tryptophan, methionine, asparagine, arginine, and lysine in follicular fluid, and the correlation of those with the indicators of folliculogenesis, oogenesis, and early embryogenesis in the IVF program were found in women with infertility and diminished ovarian reserve [6].

The study was aimed to assess alterations of amino acid metabolic pathways in blood plasma and follicular fluid and their correlation with age, as well as to estimate their clinical significance for the DOR pathogenesis.

METHODS

The prospective observational study involved infertile women of childbearing age, who contacted the Kulakov National Medical Research Center for Obstetrics, Gynecology and Perinatology for IVF program.

The total sample consisted of 115 women, who were divided into groups with DOR (anti-mullerian hormone (AMH) < 1.2 ng/mL, antral follicle counts (AFC) < 5)) and normal ovarian reserve (AMH ≥ 1.2 ng/mL, AFC ≥ 5). To clarify the effect of age on the amino acid profiles of infertile women, the studied groups were further stratified by age: under the age of 35 years and over the age of 35 years. Inclusion criteria: childbearing age (25–42 years); not getting pregnant for at least one year of regular sexual activity without birth control; consent to study participation. Exclusion criteria: contraindications to ART; history of ovarian surgery; immunodeficiencies; systemic connective tissue disorders and rheumatic diseases; cancer of any etiology; chromosomal and genetic abnormalities; the use of donor oocytes or embryos, surrogacy.

All the patients underwent mandatory assessment prior to entering the assisted reproductive technology (ART) programs in accordance with the regulatory documents [7]. The levels of amino acids and their metabolites in blood plasma and follicular fluid were determined by high performance liquid chromatography–mass spectrometry (HPLC-MS) using the Agilent 1260 II liquid chromatography system (Agilent; USA) and the Agilent 6460 mass spectrometer (Agilent; USA). The parameters of mass spectrometry and chromatographic separation were set in accordance with the guidelines provided in the JASEM manual on amino acid analysis (JASEM; Türkiye).

Prior to statistical processing the HPLC-MS data were normalized to the composite signal of all analytes and converted into the standardized format using the following formula [9]:

$$z_i = \frac{x_i - \bar{x}}{\text{stddev}(x)}$$

where z_i — standardized parameter value, x_i — initial parameter value, $\bar{x}$ — average parameter value, stddev(x) — standard deviation for the population.

The search for metabolic pathways potentially involved in the DOR pathogenesis was performed using MetaboAnalyst via analysis of the involvement of amino acids, the levels of which differed significantly between the study groups. The metabolic pathway enrichment was assessed by the over-representation analysis (ORA) based on the hypergeometric test. Statistical significance of the metabolic pathway was determined using the hypergeometric test and the Benjamini-Hochberg procedure. Statistical significance of the pathway (p) corresponded to the probability of the experimental data random intersection with the metabolites of particular metabolic pathway (Fisher's exact test). The disease-associated pathways were considered to be significant at the false discovery rate (FDR) below 0.05.

The logistic regression models were developed to assess the possibility of classifying patients into groups based on the amino acid profiles of blood plasma and follicular fluid. For that all possible combinations of amino acids were considered as independent variables, while the patient's membership in one of the groups was considered as the dependent variable. The quality of models was estimated by ROC analysis and calculation of sensitivity and specificity. From all models, four with the largest area under the ROC curve (AUC) were selected. The Wald test, 95% confidence interval (CI), odds ratio (OR) and its confidence interval were calculated for each model.

The R scripts created using the Rstudio program were used for statistical processing of the HPLC-MS data [8]. The data distribution type was determined before conducting comparative metabolomic data analysis in the studied groups (Kolmogorov–Smirnov test, graphic data analysis).

When the data distribution was normal, the mean and standard deviation M (SD) were determined; Student's t-test was used to assess the differences in the groups. When the data distribution was non-normal, the data were presented as the median and interquartile range Me (Q_1; Q_3), the amino acid levels were compared using the nonparametric Wilcoxon–Mann–Whitney test. The threshold significance level (p) was considered to be 0.05.

RESULTS

The subjects' clinical, anamnestic, and endocrine characteristics are provided in Table. 1. All the patients were matched by age and anthropometric indices, had regular menstrual cycle; their average age was 37.2 ± 5.3 years. No significant differences in the rates of gynecological and somatic disorders were revealed. Patients with DOR had a significantly shorter menstrual cycle, lower antral follicle counts, and lower AMH levels. The endocrine profile analysis revealed an upward trend of FSH levels and a downward trend of androgen (androstenedione and DHEA-S) levels.

Assessment of amino acid profiles in the DOR group revealed a significant decrease in plasma levels of sarcosine and tryptophan and the decrease in the levels of phenylalanine, tryptophan, methionine, asparagine, arginine, and lysine in follicular fluid. The detailed analysis results have been published earlier [6]. The analysis of metabolic pathways involving amino acids with significantly lower levels was performed.

Alterations of the blood plasma and follicular fluid amino acid profiles associated with infertility and DOR have the most

Table 1. Clinical characteristics of women included in the study

Indicators	Group 1 DOR (*n* = 50)***	Group 2 NOR (*n* = 65)***	*p**
Age, years*	38.2 (6.18)	37.4 (4.6)	0.27
Age of menarche, years*	13.2 (1.2)	13.6 (1.4)	0.2
Length of menstrual cycle, days*	27.5 (1.99)	28.8 (1.7)	0.002
AFC*	4.6 (2.9)	13.0 (7.3)	< 0.001
AMH, ng/mL**	0.65 (0.32; 0.92)	2.7 (1.9; 4.6)	< 0.001
LH, mIU/mL**	5.8 (4.1-13.4)	4.1 (3.4-9.4)	0.2
FSH, mIU/mL**	8.3 (7.9-12.6)	6.5 (5.1-7.6)	0.1
DHEA-S, μmol/L**	3.8 (1.9; 5.4)	5.1 (4.1; 6.9)	0.14
Androstenedione, nmol/L**	4.5 (2.8; 7.8)	9.2 (7.9; 9.9)	0.09

Note: * — M (SD), *t*-test; ** — Mann–Whitney *U* test; *** — median (interquartile range).

prominent effect on the biosynthesis of phenylalanine, tyrosine, and tryptophan (effect = 0.5, p = 0.026). We also revealed significant impact on the arginine biosynthesis (effect = 0.289, p <0.001), aspartate metabolism (effect = 0.25, p = 0.027), alanine, aspartate, and glutamate metabolism (effect = 0.114, p = 0.013) (Fig. 1; Table 2).

The logistic regression models allowing one to distinguish the blood plasma an follicular fluid samples collected from patients with DOR and controls were constructed based on the amino acid profile analysis by HPLC-MS. All possible combinations of amino acids were used to construct the models. ROC analysis was performed for each model, and four models characterized by the largest area under the ROC curve (AUC) were selected.

The model constructed based on the age and the serine, tyrosine, and phenylalanine levels had the largest AUC (0.82). Specificity and sensitivity were 94 and 68%, respectively, and the threshold value was 0.69. All the models constructed included age and phenylalanine levels (Fig. 2; Table 3).

The logistic regression models similar to the earlier reported ones were also constructed for follicular fluid. All models had the same area under the curve (AUC = 0.88). Models 1 and 2 were characterized by higher sensitivity (84%), while models 3 and 4 had higher specificity (88%). All the models constructed included phenylalanine. This was clearly due to the fact that there were the largest differences in the levels of this amino acid between groups (Fig. 2; Table 3).

To clarify the effect of age on the amino acid profiles, patients of both groups were divided into two subgroups: under the age of 35 years and over the age of 35 years. In the late reproductive stage group (over the age of 35 years) with DOR, a significant decrease in plasma levels of lysine, glutamine, serine, glycine, threonine, tyrosine, leucine, tryptophan, glutamic and aspartic acids was revealed, along with the increase in proline levels (Fig. 3A). However, no age-related alterations of the follicular fluid amino acid profiles were revealed in women with infertility and DOR (Fig. 3B). Furthermore, women with normal ovarian reserve showed no significant age-related alterations of both blood plasma and follicular fluid amino acid profiles (Fig. 3C, D).

DISCUSSION

The findings suggest that amino acid metabolism alterations play an important role in the DOR pathogenesis. According to our results, DOR is characterized by alterations of the phenylalanine, tyrosine and tryptophan biosynthesis, i.e. biosynthesis of the aromatic amino acids representing precursors of neurotransmitters, serotonin and catecholamines (dopamine, norepinephrine and epinephrine), the deficiency of which can result in oxidative stress having a toxic effect on the folliculogenesis and oogenesis [10]. Phenylalanine plays an important role in the formation of protein tertiary structure and stabilization of protein structures [11]. The decrease in

Table 2. Involvement of the amino acids characterizing DOR in metabolic pathways

Pathway	Total	Markers	*p*	FDR	Effect
KEGG					
Biosynthesis of phenylalanine, tyrosine and tryptophan	4	1	0.026	0.0429	0.5
Phenylalanine metabolism	10	1	0.063	0.5866	0.357
Biosynthesis of arginine	14	3	< 0,001	0.0029	0.289
Tryptophan metabolism	41	1	0.236	1	0.143
Alanine, aspartate and glutamate metabolism	28	2	0.013	0.0272	0.114
Arginine and proline metabolism	38	1	0.22	1	0.111
Cysteine and methionine metabolism	33	1	0.194	1	0.104
Biosynthesis of aminoacyl-tRNA	48	8	< 0,001	1.68E-09	0
HMDB (Human Metabolome Database)					
Aspartate metabolism	34	2	0.027	1	0.25
Urea cycle	23	1	0.169	1	0.154
Arginine and proline metabolism	48	1	0.324	1	0.082
Ammonia metabolism	25	1	0.18	1	0.033
Biotin metabolism	7	1	0.054	1	0

Note: FDR — false discovery rate.

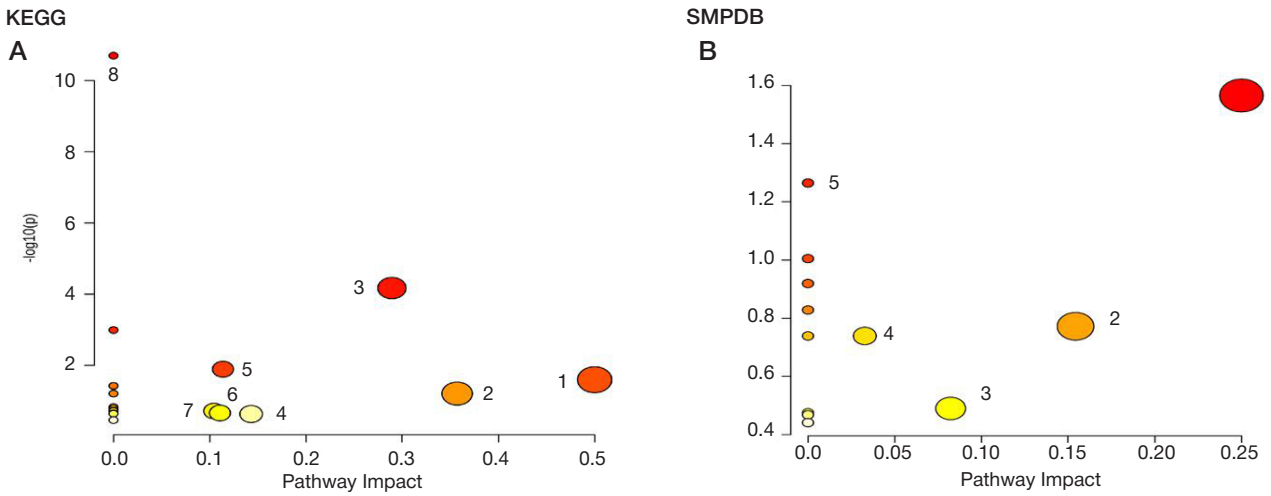

Fig. 1. Map of metabolic pathways involving amino acids showing significant differences in the blood plasma and follicular fluid levels between groups (Kyoto Encyclopedia of Genes and Genomes, KEGG): 1 — biosynthesis of phenylalanine, tyrosine and tryptophan; 2 — phenylalanine metabolism; 3 — biosynthesis of arginine; 4 — tryptophan metabolism; 5 — alanine, aspartate and glutamate metabolism; 6 — arginine and proline metabolism; 7 — cysteine and methionine metabolism; 8 — biosynthesis of aminoacyl-tRNA. Small Molecule Pathway Database (SMPDB): 1 — aspartate metabolism; 2 — urea cycle; 3 — arginine and proline metabolism; 4 — ammonia processing; 5 — biotin metabolism.). The Y-axis and the node color reflect statistical significance of the identified amino acids' involvement in appropriate metabolic pathways; the x-axis and the node radius reflect the studied metabolites' effect of the pathway

phenylalanine levels observed in women with DOR in our study is consistent with the results reported by other authors [12]. The role of phenylalanine in the DOR pathogenesis was been also confirmed by the fact that in our study phenylalanine was included in all logistic regression models with the greatest significance.

The decrease in the levels of phenylalanine being the main substrate for tyrosine synthesis in the body is associated with the

Table 3. Logistic regression models constructed based on the amino acid levels in blood plasma and follicular fluid

Blood plasma				
Model	AUC	Threshold value	Sensitivity	Specificity
Age, serine, tyrosine, phenylalanine	0.82	0.69	0.68 (0.48; 0.88)	0.94 (0.68; 1)
Age, serine, sarcosine, phenylalanine	0.81	0.75	0.65 (0.42; 0.85)	0.94 (0.71; 1)
Age, lysine, histidine, phenylalanine	0.81	0.5	0.8 (0.45; 0.98)	0.76 (0.5; 1)
Age, histidine, serine, phenylalanine	0.81	0.61	0.7 (0.48; 0.85)	0.88 (0.71; 1)
Follicular fluid				
Model	AUC	Threshold value	Sensitivity	Specificity
Methylhistidine, serine, alanine, phenylalanine	0.88	0.45	0.88 (0.62; 0.97)	0.84 (0.69; 1)
Age, ornithine, serine, phenylalanine	0.88	0.47	0.88 (0.59; 0.97)	0.84 (0.69; 1)
Ornithine, serine, alanine, phenylalanine	0.88	0.55	0.84 (0.69; 0.97)	0.88 (0.69; 0.97)
Ornithine, serine, valine, phenylalanine	0.88	0.57	0.84 (0.66; 0.97)	0.88 (0.66; 1)

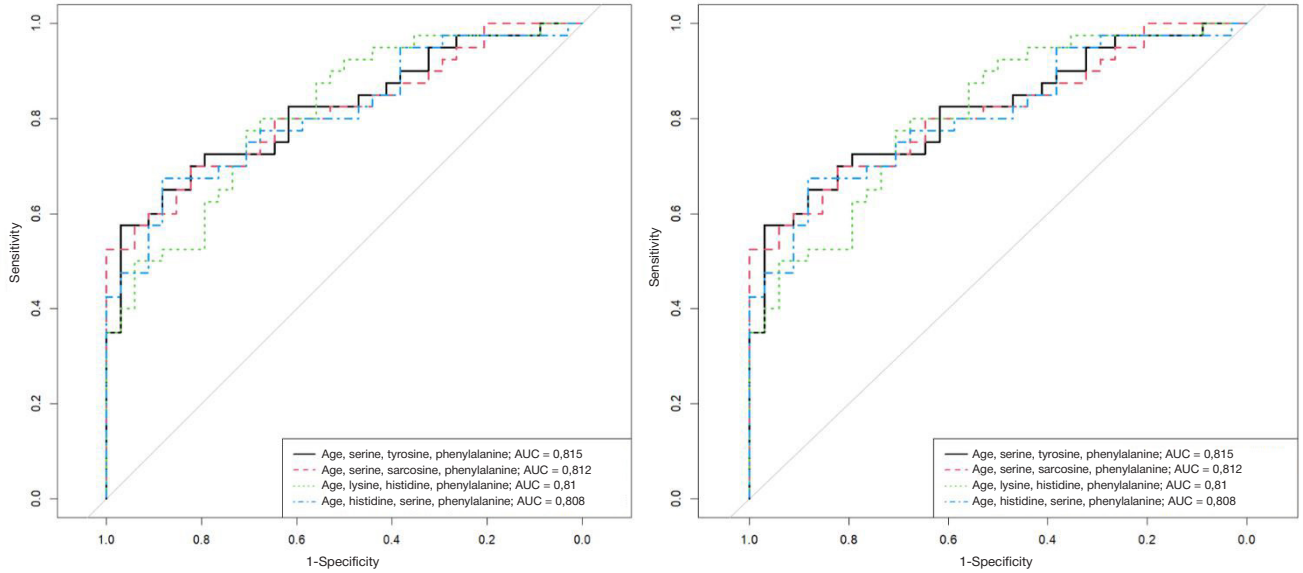

Fig. 2. ROC analysis of the logistic regression models for determination of DOR based on the blood plasma and follicular fluid amino acid composition

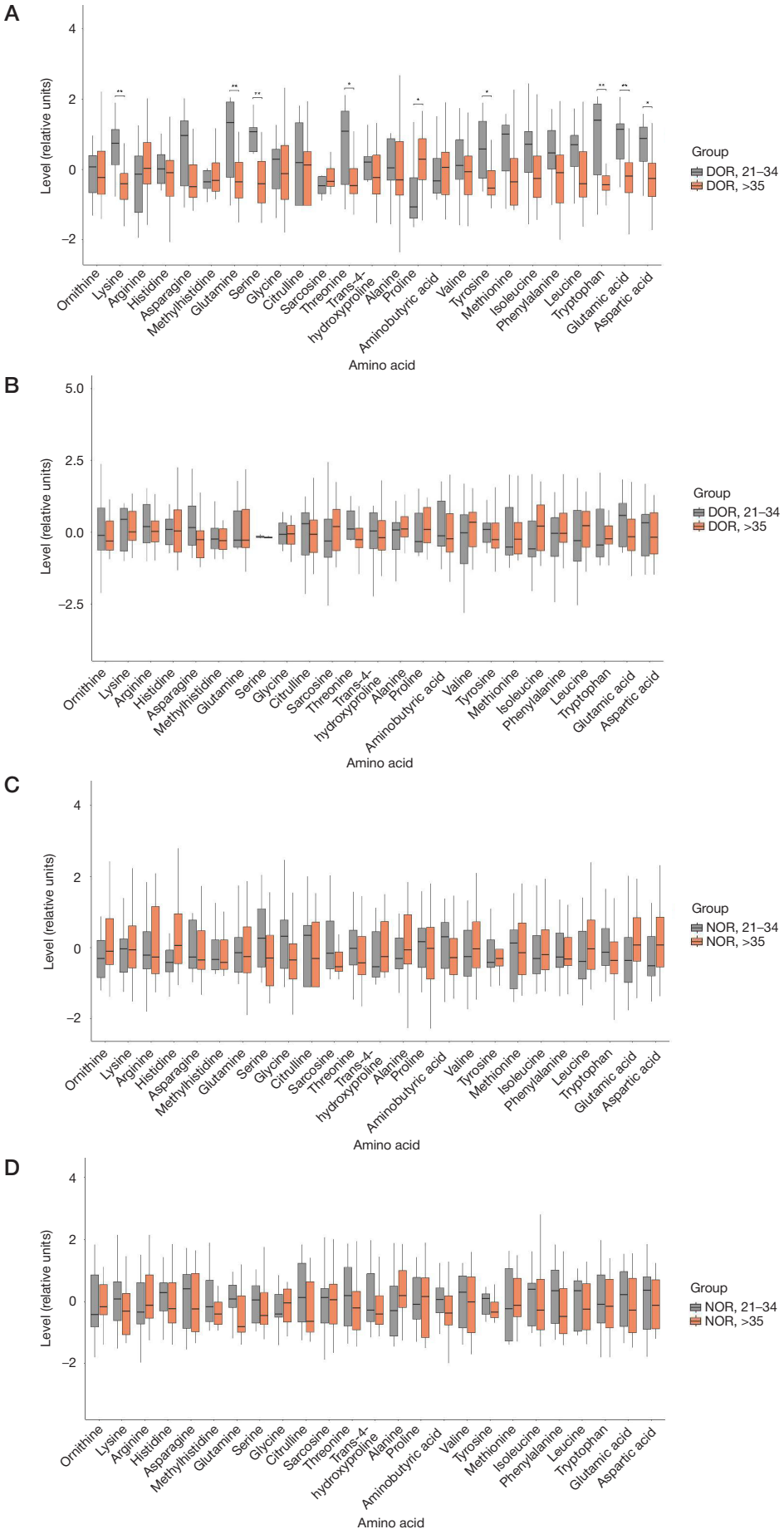

Fig. 3. Comparison of the amino acid profiles of blood plasma **(A, C)** and follicular fluid **(B, D)** in the groups DOR 21–34, DOR >35 **(A, B)**, NOR 21–34 and NOR >35 **(C, D)**

decrease in its availability for production of tyrosine [13] that serves as a basis for the synthesis of amine mediators and hormones: catecholamines, serotonin, melatonin. All tyrosine metabolites contribute to proper and consistent functioning of all body systems in order to ensure fertility. Tyrosine, like its precursor, is essential for synthesis of the benzoquinone structure which is part of the coenzyme Q10 representing an antioxidant capable of neutralizing free radicals, inhibiting lipid peroxidation in biological membranes, and protecting mitochondrial proteins and DNA against oxidative damage; coenzyme Q10 is also involved in ATP synthesis in mitochondria as an electron carrier [14]. The antioxidant effects of tyrosine have been also reported in the study of seminal plasma [15].

The role of tryptophan in many physiological processes, such as maintaining cell growth and regulation of the immune function, synthesis of serotonin and melatonin, the decrease in the levels of which results in disruption of early embryogenesis, is invaluable [16].

In our study, women with DOR of late reproductive age demonstrate the correlation between the decrease in the levels of tyrosine and tryptophan and worse outcomes of IVF programs, which confirms the role of tyrosine and tryptophan in the age-related alterations of oogenesis and early embryogenesis and is consistent with the data reported by foreign colleagues [17].

The arginine biosynthesis that turned out to be significantly altered in our study is of crucial importance for the synthesis of nitric oxide (NO). The latter is a factor of vasorelaxation ensuring optimization of blood flow to the tissues [18] and contributing to normal endometrial growth [19], steroidogenesis and folliculogenesis regulation [20]. Taking drugs with high arginine content by women with poor ovarian response, who are through IVF programs, results in elevation of the arginine, citrulline, and NO levels in blood plasma and follicular fluid and is associated with improved uterine and ovarian blood flow, increased fertilization and pregnancy rates, and reduced rate of pregnancy complications (early pregnancy loss, intrauterine growth restriction, and preeclampsia) [21].

The analysis of amino acid involvement in metabolic pathways has revealed significant changes in the alanine, aspartate and glutamate metabolism. Aspartate and glutamate are excitatory neurotransmitters of the CNS that are involved in the synthesis of purine and pyrimidine nucleotides. According to our research, is higher concentrations of aspartate are found in follicular fluid in women of early reproductive age compared to women of late reproductive age, which has been also confirmed by the positive correlation between the levels of D-aspartic acid in follicular fluid and the oocyte morphology, maturation, percentage of mature oocytes, fertilization rate in one of the studies [22]. Methionine is formed from aspartic acid that is involved in the synthesis of polyamines, post-translational modification of proteins, and regulation of the DNA reading processes. In the animal experiment, dietary methionine restriction decreased the levels of insulin-like growth factor 1, thyroid hormones in blood plasma and reduced fertility [23].

High prognostic potential of follicular fluid in women with DOR, along with blood plasma, was reported in our study, which was in line with the results of other studies confirming the role of amino acid metabolism in follicular fluid as a functional indicator of oocyte quality in women of late reproductive age, who were through the IVF/ICSI programs [24]. The probable decrease in the amino acid availability from follicular fluid can result in the increased amino acid uptake by oocytes in the culture medium in the IVF program.

The important role of antioxidant systems in oocytes and the age-related imbalance between prooxidant activity and the antioxidant defense systems in oocytes [25] trigger the development of mitochondrial dysfunction, contribute to higher rates of aneuploid oocytes/embryos and lower pregnancy rate [26]. Our data on the prominent amino acid profile alterations associated with DOR in women of late reproductive age confirm the overall decrease in amino acid metabolism with age that is also associated with reduction of their antioxidant activity. The data can be used for estimation of ovarian reserve. Further research focused on the use of amino acids in clinical practice for improvement of the outcomes of IVF/ICSI programs both in vitro, involving supplementation of the embryological media, and in vivo, involving taking drugs with high content of essential amino acids, is still relevant [27, 28].

CONCLUSIONS

Significant changes in the amino acid metabolism in blood plasma and follicular fluid associated with infertility and DOR, including metabolism of phenylalanine, tyrosine and tryptophan involved in realization of antioxidant defense in the ovarian tissues, as well as in the synthesis of neurotransmitters, catecholamines and hormones, directly affect the reproductive system by altering the cellular energy metabolism. The models allowing one to confirm DOR based on the amino acid profile of blood plasma with the 82% probability and amino acid profile of follicular fluid with the probability of 88% have been constructed based on the differences revealed using the targeted semi-quantitative metabolomics analysis methods. The data on the age-related alterations of amino acid levels associated with DOR confirm relevance of the studies focused on the use of preliminary treatment with the drugs containing amino acids aimed to improve the IVF program outcomes.

References

1. Hu S. Perinatal outcome in young patients with diminished ovarian reserve undergoing assisted reproductive technology / S. Hu, B. Xu, L. Jin // Fertility and Sterility. 2020; 114 (1): 118–124.e1.
2. Collado-Fernandez E, Picton HM, R. Dumollard Collado-Fernandez E. Metabolism throughout follicle and oocyte development in mammals. The International Journal of Developmental Biology.2012; 56 (10-11-12): 799–808.
3. Dillin A, Gottschling DE, T. Nyström Dillin A. The good and the bad of being connected: the integrons of aging. Current Opinion in Cell Biology. 2014; 26: 107–12.
4. Yang J, Feng T, Li S, et al. Human follicular fluid shows diverse metabolic profiles at different follicle developmental stages. Reproductive Biology and Endocrinology. 2020; 18 (1): 74.
5. Moslehi N, Mirmiran P, Marzbani R. et al. Serum metabolomics study of women with different annual decline rates of anti-Müllerian hormone: an untargeted gas chromatography–mass spectrometry-based study. Human Reproduction. 2021; 36 (3): 721–33.
6. Shevtsova SMA, Gavisova GAA, Krasnova KNA, et al. Amino acid profile of blood plasma and follicular fluid in women with infertility and diminished ovarian reserve. Akusherstvo i ginekologiia. 2024; 2 (2024): 79–88.
7. Клинические рекомендации «Женское бесплодие». 2021.
8. RStudio Team. RStudio: Integrated Development for R. RStudio, Inc., Boston, MA; 2016. Available from: http://www.rstudio.com/.
9. Misra BB. Data normalization strategies in metabolomics: Current

challenges, approaches, and tools. European Journal of Mass Spectrometry. 2020; 26 (3): 165–74.
10. Zhang X, Yoshihara K, Miyata N, et al. Dietary tryptophan, tyrosine, and phenylalanine depletion induce reduced food intake and behavioral alterations in mice. Physiology & Behavior. 2022; 244: 113653.
11. Deanfield JE, Halcox JP, Rabelink TJ. Endothelial Function and Dysfunction. Circulation. 2007; 115 (10): 1285–95.
12. Li J, Zhang Z, Wei Y, et al. Metabonomic analysis of follicular fluid in patients with diminished ovarian reserve. Frontiers in Endocrinology. 2023; 14. DOI: 10.3389/fendo.2023.1132621.
13. Ross AC, Caballero BH, Cousins RJ, et al. Modern nutrition in health and disease: Eleventh edition. Wolters Kluwer Health Adis (ESP). 2012; 1616 p.
14. Rasmussen DD, Ishizuka B, Quigley ME, Yen SSC. Effects of tyrosine and tryptophan ingestion on plasma catecholamine and 3,4-dihydroxyphenylacetic acid concentrations. The Journal of Clinical Endocrinology & Metabolism. 1983; 57 (4): 760–3.
15. van Overveld F. W. P. C/, Haenen. G. R. M. M., Rhemrev J, et al. Tyrosine as important contributor to the antioxidant capacity of seminal plasma. Chemico-Biological Interactions. 2000; 127 (2): 151–61.
16. Dubé F, Amireault P. Local serotonergic signaling in mammalian follicles, oocytes and early embryos. Life Sciences. 2007; 81 (25–26): 1627–37.
17. Liu A, Shen H, Li Q, et al. Determination of tryptophan and its indole metabolites in follicular fluid of women with diminished ovarian reserve. Scientific Reports. 2023; 13 (1): 17124.
18. DuPont JJ, Farquhar WB, Townsend RR, Edwards DG. Ascorbic acid or <scp>l</scp> -arginine improves cutaneous microvascular function in chronic kidney disease. Journal of Applied Physiology. 2011; 111 (6): 1561–7.
19. Takasaki A, Tamura H, Miwa I, et al. Endometrial growth and uterine blood flow: a pilot study for improving endometrial thickness in the patients with a thin endometrium. Fertility and Sterility. 2010; 93 (6): 1851–8.
20. Luo Y, Zhu Y, Basang W, et al. Roles of nitric oxide in the regulation of reproduction: a review. Frontiers in Endocrinology. 2021; 12.
21. Kopets R, Kuibida I, Chernyavska I, et al. Dietary supplementation with a novel <scp>l</scp> -carnitine multi-micronutrient in idiopathic male subfertility involving oligo-, astheno-, teratozoospermia: a randomized clinical study. Andrology. 2020; 8 (5): 1184–93.
22. D'Aniello G, Grieco N, Di Filippo MA, et al. Reproductive implication of D-aspartic acid in human pre-ovulatory follicular fluid. Human Reproduction. 2007; 22 (12): 3178–83.
23. Expansion of liver cancer stem cells during aging in methionine adenosyltransferase 1A-deficient mice. Rountree CB, Senadheera S, Mato JM, et al. Hepatology. 2007; 47 (4): 1288–97.
24. Akamine K, Mekaru K, Gibo K, et al. Impact of the one-carbon metabolism on oocyte maturation, fertilization, embryo quality, and subsequent pregnancy. Reproductive Medicine and Biology. 2021; 20 (1): 76–82.
25. Tatone C, Amicarelli F. The aging ovary — the poor granulosa cells. Fertility and Sterility. 2013; 99 (1): 12–17.
26. Chappel S. The role of mitochondria from mature oocyte to viable blastocyst. Obstetrics and Gynecology International. 2013; 2013: 1–10.
27. Youssef M. A. F. M., Abdelmoty HI, Elashmwi HA, et al. Oral antioxidants supplementation for women with unexplained infertility undergoing ICSI/IVF: Randomized controlled trial. Human Fertility. 2015; 18 (1): 38–42.
28. Anchordoquy JP, Lizarraga RM, Anchordoquy JM, et al. Effect of cysteine, glutamate and glycine supplementation to in vitro fertilization medium during bovine early embryo development. Reproductive Biology. 2019; 19 (4): 349–55.

Литература

1. Hu S. Perinatal outcome in young patients with diminished ovarian reserve undergoing assisted reproductive technology / S. Hu, B. Xu, L. Jin // Fertility and Sterility. 2020; 114 (1): 118–124.e1.
2. Collado-Fernandez E, Picton HM, R. Dumollard Collado-Fernandez E. Metabolism throughout follicle and oocyte development in mammals. The International Journal of Developmental Biology.2012; 56 (10-11-12): 799–808.
3. Dillin A, Gottschling DE, T. Nyström Dillin A. The good and the bad of being connected: the integrons of aging. Current Opinion in Cell Biology. 2014; 26: 107–12.
4. Yang J, Feng T, Li S, et al. Human follicular fluid shows diverse metabolic profiles at different follicle developmental stages. Reproductive Biology and Endocrinology. 2020; 18 (1): 74.
5. Moslehi N, Mirmiran P, Marzbani R. et al. Serum metabolomics study of women with different annual decline rates of anti-Müllerian hormone: an untargeted gas chromatography–mass spectrometry-based study. Human Reproduction. 2021; 36 (3): 721–33.
6. Shevtsova SMA, Gavisova GAA, Krasnova KNA, et al. Amino acid profile of blood plasma and follicular fluid in women with infertility and diminished ovarian reserve. Akusherstvo i ginekologiia. 2024; 2 (2024): 79–88.
7. Клинические рекомендации «Женское бесплодие». 2021.
8. RStudio Team. RStudio: Integrated Development for R. RStudio, Inc., Boston, MA; 2016. Available from: http://www.rstudio.com/.
9. Misra BB. Data normalization strategies in metabolomics: Current challenges, approaches, and tools. European Journal of Mass Spectrometry. 2020; 26 (3): 165–74.
10. Zhang X, Yoshihara K, Miyata N, et al. Dietary tryptophan, tyrosine, and phenylalanine depletion induce reduced food intake and behavioral alterations in mice. Physiology & Behavior. 2022; 244: 113653.
11. Deanfield JE, Halcox JP, Rabelink TJ. Endothelial Function and Dysfunction. Circulation. 2007; 115 (10): 1285–95.
12. Li J, Zhang Z, Wei Y, et al. Metabonomic analysis of follicular fluid in patients with diminished ovarian reserve. Frontiers in Endocrinology. 2023; 14. DOI: 10.3389/fendo.2023.1132621.
13. Ross AC, Caballero BH, Cousins RJ, et al. Modern nutrition in health and disease: Eleventh edition. Wolters Kluwer Health Adis (ESP). 2012; 1616 p.
14. Rasmussen DD, Ishizuka B, Quigley ME, Yen SSC. Effects of tyrosine and tryptophan ingestion on plasma catecholamine and 3,4-dihydroxyphenylacetic acid concentrations. The Journal of Clinical Endocrinology & Metabolism. 1983; 57 (4): 760–3.
15. van Overveld F. W. P. C/, Haenen. G. R. M. M., Rhemrev J, et al. Tyrosine as important contributor to the antioxidant capacity of seminal plasma. Chemico-Biological Interactions. 2000; 127 (2): 151–61.
16. Dubé F, Amireault P. Local serotonergic signaling in mammalian follicles, oocytes and early embryos. Life Sciences. 2007; 81 (25–26): 1627–37.
17. Liu A, Shen H, Li Q, et al. Determination of tryptophan and its indole metabolites in follicular fluid of women with diminished ovarian reserve. Scientific Reports. 2023; 13 (1): 17124.
18. DuPont JJ, Farquhar WB, Townsend RR, Edwards DG. Ascorbic acid or <scp>l</scp> -arginine improves cutaneous microvascular function in chronic kidney disease. Journal of Applied Physiology. 2011; 111 (6): 1561–7.
19. Takasaki A, Tamura H, Miwa I, et al. Endometrial growth and uterine blood flow: a pilot study for improving endometrial thickness in the patients with a thin endometrium. Fertility and Sterility. 2010; 93 (6): 1851–8.
20. Luo Y, Zhu Y, Basang W, et al. Roles of nitric oxide in the regulation of reproduction: a review. Frontiers in Endocrinology. 2021; 12.
21. Kopets R, Kuibida I, Chernyavska I, et al. Dietary supplementation with a novel <scp>l</scp> -carnitine multi-micronutrient in idiopathic male subfertility involving oligo-, astheno-, teratozoospermia: a randomized clinical study. Andrology. 2020; 8 (5): 1184–93.
22. D'Aniello G, Grieco N, Di Filippo MA, et al. Reproductive implication

of D-aspartic acid in human pre-ovulatory follicular fluid. Human Reproduction. 2007; 22 (12): 3178–83.
23. Expansion of liver cancer stem cells during aging in methionine adenosyltransferase 1A-deficient mice. Rountree CB, Senadheera S, Mato JM, et al. Hepatology. 2007; 47 (4): 1288–97.
24. Akamine K, Mekaru K, Gibo K, et al. Impact of the one-carbon metabolism on oocyte maturation, fertilization, embryo quality, and subsequent pregnancy. Reproductive Medicine and Biology. 2021; 20 (1): 76–82.
25. Tatone C, Amicarelli F. The aging ovary — the poor granulosa cells. Fertility and Sterility. 2013; 99 (1): 12–17.
26. Chappel S. The role of mitochondria from mature oocyte to viable blastocyst. Obstetrics and Gynecology International. 2013; 2013: 1–10.
27. Youssef M. A. F. M., Abdelmoty HI, Elashmwi HA, et al. Oral antioxidants supplementation for women with unexplained infertility undergoing ICSI/IVF: Randomized controlled trial. Human Fertility. 2015; 18 (1): 38–42.
28. Anchordoquy JP, Lizarraga RM, Anchordoquy JM, et al. Effect of cysteine, glutamate and glycine supplementation to in vitro fertilization medium during bovine early embryo development. Reproductive Biology. 2019; 19 (4): 349–55.